DEVELOPMENT OF NATURAL DYE-SENSITIZED SOLAR CELL GREENHOUSE FOR PLANT CULTIVATION

GLENNISE FAYE MEJICA

MASTER OF ENGINEERING IN RENEWABLE ENERGY ENGINEERING

MAEJO UNIVERSITY

2021

DEVELOPMENT OF NATURAL DYE-SENSITIZED SOLAR CELL GREENHOUSE FOR PLANT CULTIVATION

GLENNISE FAYE MEJICA

A THESIS SUBMITTED IN PARTIAL FULFILLMENT
OF THE REQUIREMENTS FOR THE DEGREE OF MASTER OF ENGINEERING
IN RENEWABLE ENERGY ENGINEERING
ACADEMIC ADMINISTRATION AND DEVELOPMENT MAEJO UNIVERSITY
2021

DEVELOPMENT OF NATURAL DYE-SENSITIZED SOLAR CELL GREENHOUSE FOR PLANT CULTIVATION

GLENNISE FAYE MEJICA

THIS THESIS HAS BEEN APPROVED IN PARTIAL FULFLLMENT
OF THE REQUIREMENTS FOR THE DEGREE OF MASTER OF ENGINEERING
IN RENEWABLE ENERGY ENGINEERING

APPROVED BY **Advisory Committee**

Chair ....
(Dr. Rameshprabu Ramaraj)
................../................../ ....

Committee ....
(Assistant Professor Dr. Natthawud Dussadee)
................../................../ ....

Committee ....
(Assistant Professor Dr. Yuwalee Unpaprom)
................../................../ ....

Committee ....
(Associate Professor Theerapol Thurakitseree)
................../................../ ....

Program Chair, Master of Engineering
in Renewable Energy Engineering ....
(Assistant Professor Dr. Rotjapun Nirunsin)
................../................../ ....

CERTIFIED BY ACADEMIC
ADMINISTRATION AND DEVELOPMENT ....

(Associate Professor Dr. Yanin Opatpatanakit)
Vice President for the Acting President of Maejo University
................../................../ ....

ชื่อเรื่อง การพัฒนาโรงเรือนกระจกโซล่าเซลล์แบบย้อมสีไวแสงธรรมชาติเพื่อการเพาะปลูกพืช
ชื่อผู้เขียน Miss Glennise Faye Mejica
ชื่อปริญญา วิศวกรรมศาสตรมหาบัณฑิต สาขาวิชาวิศวกรรมพลังงานทดแทน
อาจารย์ที่ปรึกษาหลัก Dr. Rameshprabu Ramaraj

บทคัดย่อ

การพัฒนาเซลล์แสงอาทิตย์ชนิดสีย้อมไวแสง (DSSC) ซึ่งเป็นเซลล์แสงอาทิตย์รุ่นที่สามได้มีการนำสีย้อมสังเคราะห์ใช้เป็นสารย้อมไวแสงกันอย่างแพร่หลาย สำหรับการผลิตสีย้อมดังกล่าวต้องผ่านกระบวนการที่ซับซ้อนซึ่งเกี่ยวข้องกับการใช้สารเคมีที่เป็นพิษและก่อให้เกิดความเสี่ยงต่อสุขภาพและเป็นอันตรายต่อสิ่งแวดล้อม เนื่องจากผลกระทบโดยรวมที่มีต่อมนุษย์และธรรมชาติดังกล่าวนี้ การสกัดสีย้อมธรรมชาติหรือเม็ดสีจากพืช เช่น คลอโรฟิลล์ แอนโธไซยานิน แคโรทีนอยด์ เป็นต้น จึงเป็นที่น่าสนใจของการทำวิจัยในฐานะสีย้อมทางเลือก อีกประการหนึ่ง เนื่องจากการแข่งขันระหว่างการนำพืชไปใช้ประโยชน์เพื่อเป็นอาหารและแหล่งพลังงาน เทคโนโลยีเซลล์แสงอาทิตย์ที่ใช้สีย้อมจากวัสดุที่ไม่กระทบกับห่วงโซ่อาหารจึงเข้ามามีส่วนสำคัญในกิจกรรมต่างๆ ที่เกี่ยวข้องกับการผลิตพลังงานไฟฟ้าที่แปลงมาจากพลังงานแสงอาทิตย์ ดังนั้น งานวิจัยนี้ได้ทำการประเมินศักยภาพองสีย้อมธรรมชาติ จากผลผักปลัง (*Basella alba*), ใบคราม (*Strobilanthes cusia Nees*), ใบลำไย (*Dimocarpus longan*) และใบอินทนิลบก (*Lagerstroemia macrocarpa*) (ใบสีแดง) ในกระบวนการเตรียมฟิล์มบาง TiO_2 ได้ใช้เทคนิคดอกเตอร์เบลด การสกัดสีย้อมธรรมชาติใช้วิธีการสกัดด้วยตัวทำละลาย และรายละเอียดขั้นตอนการทดลองได้นำเสนอในบทวิธีการ จากผลการทดลอง พบว่า ใบอินทนิลบกมีศักยภาพในการแปลงพลังงานสูงสุดที่ 1.134%, V_{oc}= 0.5426 V, I_{sc}= 0.2952 mA, I_{sc}= 0.2952 mA นอกจากนี้ ใบลำไยมีประสิทธิภาพรองลงมาคือ 0.158% โดยมีค่า V_{oc}= 0.5552 V และ I_{sc}=0.05332 mA ผลผักปลังมีค่าประสิทธิภาพ 0.1021%, V_{oc}= 0.4877 V, I_{sc}= 0.0682 mA และใบครามให้ประสิทธิภาพต่ำสุดคือ 0.0118%, V_{oc}=0.283 V และ I_{sc}=0.00943 mA

นอกจากนี้ ใบอินทนิลบกที่แสดงศักยภาพสูงสุด จึงถูกนำไปพัฒนาเรือนกระจก DSSC โดยให้แรงดันที่ 9.0 V และกระแสไฟฟ้าที่ 6.0 mA ตามลำดับ นอกจากนี้ *Solanum melongena* หรือที่รู้จักในชื่อมะเขือยาวได้ใช้เป็นพืชทดลองในการประเมินผลของหลังคา DSSC ต่อการปลูกพืช จากผลการวิจัยพบว่าความเข้มแสงผ่านเรือนกระจกเพียงประมาณ 50% เมื่อเทียบกับภายนอก เมื่อ

เพิ่มความเข้มแสงด้วยหลอดไฟแอลอีดีด้วยระบบ DSSC เป็น 55% ความเข้มของแสงภายในเรือนกระจกวัดได้จาก 5 ตำแหน่ง ได้แก่ ด้านหลังซ้าย (BL) ด้านหลังขวา (BR) ตรงกลาง (C) ด้านหน้าซ้าย (FL) และด้านหน้าขวา (FR) และการวัดที่สอดคล้องกันคือ 29,250 ± 657.65 Lux, 18,225 ± 521.42 Lux, 26,325 ± 491.81 Lux, 27,010 ± 468.29 Lux และ 26,080 ± 536.84 Lux อย่างไรก็ตาม จากการสังเกตทางกายภาพ (ความสูงและจำนวนใบใหม่) พบว่าพืชมีการเจริญเติบโตอย่างเป็นผลสำเร็จ ดังนั้นจึงสามารถสรุปได้ว่าแสงที่ส่องผ่านเรือนกระจกจาก DSSC และต่อด้วยหลอดไฟแอลอีดี นั้นเพียงพอสำหรับการเพาะปลูกพืช

คำสำคัญ : เซลล์แสงอาทิตย์ชนิดสีย้อมไวแสง, สีย้อมธรรมชาติ, โรงเรือนกระจก, สารไวแสง, การสกัดสีย้อม

Title	DEVELOPMENT OF NATURAL DYE-SENSITIZED SOLAR CELL GREENHOUSE FOR PLANT CULTIVATION
Author	Miss Glennise Faye Mejica
Degree	Master of Engineering in Renewable Energy Engineering
Advisory Committee Chairperson	Dr. Rameshprabu Ramaraj

ABSTRACT

For years, the synthetic dye has been a widely used dye sensitizer for the development of dye-sensitized solar cells (DSSC), the third generation of solar cells. However, producing such dyes undergoes complex processes that involve the use of toxic chemicals that pose a health risk and are harmful to the environment. Due to its overall impact on humans and nature, the extraction of natural dyes or pigments from plants such as chlorophyll, anthocyanin, carotenoid, etc., has attracted the interest of research as an alternative dye. Moreover, because of the competition between the use of plants as a food source and as an energy source, photovoltaic technology plays a part in helping the various activities related to food production and subsequent supply chains by providing electricity converted from solar energy. Hence, this study investigated the potential of natural dye from Malabar spinach (*Basella alba*) fruits, Indigo plant leaves (*Strobilanthes cusia* Nees), Longan leaves (*Dimocarpus longan*), and Inthanin bok leaves (*Lagerstroemia macrocarpa*) (red leaves) as photosensitizers, and also developed a DSSC greenhouse. In the preparation of the TiO_2 thin film, the doctor blade technique was used. In addition, the natural dyes were extracted using the solvent extraction method. Further experimental procedures were presented in the methodology chapter. Based on the evaluation of natural pigments, Inthanin bok had the highest energy conversion efficiency (η) of 1.134%, V_{oc}= 0.5426 V, I_{sc}= 0.2952 mA. , I_{sc}= 0.2952 mA. Furthermore, the longan leaves had a 0.158% efficiency with V_{oc}= 0.5552 V and

I_{sc}=0.05332 mA. The Malabar spinach produced η=0.1021% V_{oc}= 0.4877 V, I_{sc}= 0.0682 mA and. and lastly, the Indigo plant produced the lowest efficiency, with 0.0118%, V_{oc}=0.283 V, and I_{sc}=0.00943 mA.

In addition, Inthanin bok showed the highest potential and was further used in developing the DSSC roofed greenhouse. The voltage and current produced by the DSSC roof were found to be 9 V and 0.5 mA, respectively. *Solanum melongena*, also known as eggplant, was used as an experimental crop to evaluate the effect of DSSC canopy on crops. According to research results, the intensity of light passing through the greenhouse is only about 50% compared to outside. With the addition of the LED by DSSC, the light intensity was increased to 55%. The light intensity inside the greenhouse was measured in five (5) locations: back left (BL), back right (BR), center (C), front left. (FL) and front right (FR) and corresponding measurements are 29,250 ± 657.65 Lux, 18,225 ± 521.42 Lux, 26,325 ± 491.81 Lux, 27,010 ± 468.29 Lux and 26,080 ± 536.84 Lux. Based on the physical observations (height and number of new leaves) of the plants, it was found out to be growing successfully. Therefore, it can be concluded that the light transmitted through the greenhouse from DSSC and connected with LED lamps is sufficient for the cultivation of plants.

Keywords : Dye-sensitized solar cell, Natural pigment, Greenhouse, Photosensitizer, Dye extraction

ACKNOWLEDGEMENTS

The researcher would like to express her heartfelt gratitude to the following people for their utmost support, guidance, expertise, and inspiration in the completion of this paper:

To her adviser and committee, Dr. Rameshprabu Ramaraj, Asst. Prof. Dr. Natthawud Dussadee, Asst. Prof. Dr. Yuwalee Unpaprom, Assoc. Prof. Dr. Theerapol Thurakitseree, and Asst. Prof. Dr. Rattanachai Pairintra for their advice for making this work possible;

To the School of Renewable Energy and Faculty of Science for allowing the researcher to conduct her experiments in their laboratories;

To Ms. Sawitree Tudtou of the Faculty of Science for guiding and assisting her during the conduct of the study, as well as Asst Prof. Dr. Sermsuk Buochareon for helping in the construction of the greenhouse and sharing his knowledge;

To the School of Renewable Energy for giving her a full scholarship grant and financial support while studying; and

To her family, lab mates, friends, colleagues, and all the people who in one way or another shared their contributions morally, and with sympathetic understanding, that contributed immensely to the completion of this thesis. Also, thank you to Ms. Tabetha Velasco for her kindness and wisdom.

Most importantly, she would like to thank her parents, Mr. Joemarie G. Mejica and Mrs. Gwendolyn C. Mejica, as well as her siblings, Dr. Frenz Jansen C. Mejica, Mac Andrew C. Mejica, and Angel Marie C. Mejica, for inspiring, supporting, and trusting her to overcome all odds and challenges while writing this research work.

Above all, to the Almighty God, for all the spiritual guidance, grace, and strength.

Glennise Faye Mejica

TABLE OF CONTENTS

LIST OF TABLES

LIST OF FIGURES

CHAPTER 1
INTRODUCTION

1.1 Background of the study

According to the current US Census Bureau, the world population estimated in June 2019 shows that the global population is 7,577,130,400, which far exceeds the census conducted in 2015, with the world population of 7.2 billion. With this, as the earth's population increase, the demand and consumption of the energy escalate (World Population Review, 2019). Based on predictions by the US Energy Information Administration, by the year 2040, the total world energy consumption will rise to 25 TW. Hence, the continual rise of energy demand is catalyzed by an increase in the global population and the rapid industrialization undergone by large markets such as China and India (Lau and Soroush, 2019). In these countries and the rest of the world, carbon-based fossil fuels such as coal, oil and natural gas remain as main energy resources consumed and considered as a dominant energy provider. These fossil fuels generate approximately 90% of the world's electricity (Kabir et al., 2019; Lau and Soroush, 2019). Not only that, but it also provides thermal energy for industrial and domestic uses (Kabir et al., 2019).

However, fossil fuels are non-renewable energy resources. The problem with the production of energy from fossil fuel is it is not sustainable; moreover, the resources are depleting at a rapid rate. In addition, within 50-60 years, fossil fuels and natural gas reserves currently available will run out (Kabir et al., 2019; Lau and Soroush, 2019).

The consumption of fossil fuels have resulted to various environmental issues such as global climate change, ozone layer depletion, acid rain, water pollution, air pollution, land pollution, maritime pollution, etc. Furthermore, fossil fuels are the primary contributor to global warming (Kabir et al., 2019). Greenhouse gas emissions have been increasing rapidly, reaching a rate of 49 gigatons of CO_2-equivalents/year (GT CO_2eq/year) in 2010, with carbon dioxide gas emissions alone from fossil fuels and industrial processes accounting for 78% of total emissions. If present activities continue without any further mitigation efforts, atmospheric greenhouse gas concentrations could potentially increase from 430 ppm CO_2eq in 2011 to 1300 ppm by 2100, which could cause the global mean surface temperature to rise by up to 4.8℃ (Lau and Soroush, 2019).

To counter the effects of fossil fuels in the environment, this led to an exploration of finding new energy from renewable resources. Such sustainable energy resources are solar energy, wind power, hydropower, wave energy, tidal energy, biomass, biofuel, and geothermal energy. These are potential alternatives to conventional fossil fuel. Unlike fossil fuels, these renewable energy resources are not limited to a few countries but exist worldwide (Kabir et al., 2019). The research for the past few years aims to develop and commercialize renewable energy technologies that can suffice the energy demand globally (Lau and Soroush, 2019).

Among all the sustainable energy, the sun has the most noteworthy potential in providing cleaner, more carbon-neutral energy to fulfill the ever-growing energy demands of the future as its resource base is much larger than all the other renewables combined (Lau and Soroush, 2019) and are easily extractable by a photovoltaic (PV) system (Kabir et al., 2019). In the year 2000, the mean global energy consumption rate was 13 TW. By the year 2050, the global energy demand will increase approximately 28 TW (Hagfeldt et al., 2010). Solar energy, besides fusion, has the enormous potential to satisfy the future global need for renewable energy sources. From the 1.7×10^5 TW of energy from the sun that hits the earth’s surface, it is estimated that only 600 TW are practically harvested and solar farms are only 10% efficient, approximately 60 TW of power could be supplied, that can sufficiently provide the energy demands (Hagfeldt et al., 2010).

Even though a wide variety of solar technologies have been developed, there is still no definite solution that could eliminate our reliance on fossil fuels. The main challenge is to find a solar technology that is inexpensive, efficient, easily deployable, and versatilely adaptable, particularly to emerging and rapidly growing markets. As some of the countries can not house large-scale centralized energy grid systems, it is essential to look for ways that can aid the distribution of solar energy through a more localized, individualized approach using more efficient, durable, high-capacity, and easily installed energy systems (Lau and Soroush, 2019).

In comparison to the wide variety of solar technologies, the dye-sensitized solar cell (DSSC) shows remarkable potential in providing an efficient and low-cost solution that could lead us to a society free of fossil fuels. In addition, a study shows that the production of DSSC is inexpensive compared to traditional PV systems and offering a short payback period of less than one year (Lau and Soroush, 2019).

The photosynthesis and PV have a similar principle of harvesting the photons and converting it to energy, but they play different functions for bio-production and electricity production. Plants have provided humans not only for food but also been utilized as energy resources throughout the history of the human race. Hence, due to the rise of environmental problems caused by using fossil fuels and scarcity of its non-renewable resources, scientists are now utilizing plants to produce cleaner and renewable energy (Yano and Cossu, 2019).

Moreover, because of the competition between the uses of plants as a food and as an energy source, PV plays a part in helping the various activities related to food production and subsequent supply chains by providing electricity converted from solar energy (Yano and Cossu, 2019). Greenhouse plant production is a cultivation practice that controls the production environment, such as temperature and humidity, making it suitable for crop growth, development and production. Fuel and electricity are necessary to control the greenhouse interior environment, aiming to improve and maintain crop yields and quality, but because of the increasing prices of fuel and electricity, it reduces grower profits (Yano and Cossu, 2019). Hence, farmers struggle to increase crop production efficiency while minimizing the consumption of fuel and electricity. One of the possible solutions is to utilize actively in a greenhouse the renewable energy. These could aid in decreasing the consumption of fossil fuels and electricity (Yano and Cossu, 2019).

Currently, there are studies conducted about agrivoltaic. It is a system designed combining commercial agriculture and electricity within the same land unit area. However, the major problem manifested by agrivoltaics or photovoltaic greenhouse is the competition between PV roofs and plant to get incident solar radiation. Thus, dye-sensitized solar cell (DSSC); the third generation of solar PV gained the interest of this study due to their simple manufacturing process, low fabrication cost, low light level sensitivity, ease of use for bigger applications and flexibility in scaling characteristics. Which stirred the best candidates use as green energy buildings (Roslan et al., 2019). Moreover, the various color of DSSC (determined by the dye) can act as a plant growth regulator or can modify the solar spectrum which enters into the greenhouse. As a result, plant growth and photomorphogenesis can be optimized (Roslan et al., 2019).

The dye plays a major role in the absorption and conversion of the incident light ray to electricity. There are two types of dyes organic dyes such as natural dyes from leaves, fruits and flowers and inorganic dyes such as ruthenium (Ru), which provide greater efficiency. However, ruthenium-based dyes are quite expensive (Bagavathi and Clara Dhanemozhi, 2019). Due to the high cost and availability concern of the production of conventional photovoltaic cells, DSSC using natural dyes are considered a better alternative in recent years. The advantages of natural dyes over organic dyes are low cost, eco-friendly and natural abundancy (Kumar et al., 2016). Moreover, the process of producing synthetic dyes are more complex, complicated and costly. Alternatively, natural dyes can be used for the same purpose with an acceptable efficiency (Alhamed et al., 2012).

The objective of this research is to develop a multicolor natural dye-sensitized solar cell greenhouse, utilizing natural dye extracted from Malabar spinach (*Basella alba*), Indigo plant (*Strobilanthes cusia Nees*), Longan and Inthanin.

1.2 Research objectives

1. To develop a natural dye from Malabar spinach (*Basella alba*) fruits, Indigo plant *Strobilanthes cusia* (Nees), Longan (*Dimocarpus longan)* and Inthanin bok (*Lagerstroemia macrocarpa*) as photosensitizer.
2. To create a multicolor natural dye-sensitized solar cell.
3. To produce an agrivoltaic system for portable greenhouse integrated with natural dye based DSSC.

1.3 Scope of the research

1. Malabar spinach (*Basella alba*) fruits, Indigo plant *Strobilanthes cusia* (Nees), Longan (*Dimocarpus longan*) and Inthanin bok (*Lagerstroemia macrocarpa*) leaves extracted by organic solvent will be used as natural sensitizer.
2. Evaluation of Malabar spinach (*Basella alba*) fruits, Indigo plant *Strobilanthes cusia* (Nees), Longan (*Dimocarpus longan*) and Inthanin bok (*Lagerstroemia macrocarpa*).
3. Light intensity comparison of conventional greenhouse and natural DSSC greenhouse on plant growth.
4. The temperature and humidity outside and inside the mini greenhouse will be analyzed.

1.4 Significance of the study

1. The results of this study will contribute to the development of simple, economical and portable natural dye-sensitized solar cell greenhouse for plant cultivation.
2. This research could aid the growers increased their crop yield and plant quality while minimizing the cost of using fuels and electricity in maintaining the suitable environment of the greenhouse.
3. This study will also help the researchers and future researchers to expound and expand the research about the dye-sensitized solar cells and its practical applications.

CHAPTER 2
LITERATURE REVIEW

2.1 Agrivoltaic

Agrivoltaic is a system designed combining commercial agriculture and electricity within the same land unit area. However, the major problem manifested by agrivoltaics or photovoltaic greenhouse is the competition between PV roofs and plant to get incident solar radiation. Thus, dye-sensitized solar cell (DSSC); the third generation of solar PV is recently attracted due to their simple manufacturing process, low fabrication cost, low light level sensitivity, ease of use for bigger applications and flexibility in scaling characteristics which stirred the best candidates use as green energy buildings (Roslan et al., 2019).

Moreover, the various color of DSSC (determined by the dye) can act as a plant growth regulator or can modify the solar spectrum which enters into the greenhouse. As a result, plant growth and photomorphogenesis can be optimized. Hence, in this research a practical fieldwork is proposed by using integrated semi-transparent DSSC mini greenhouse to define DSSC module systems potential and performance nearby the tropical climate conditions (Roslan et al., 2019).

2.2 Dye-sensitized solar cells

The dye-sensitized solar cell or also known as DSSC belongs to the third generation solar cells. It is a low-cost solar cell due to the cost of materials and labor used during the construction. Aside from being affordable, DSSCs are also efficient, renewable and environmentally friendly. Same with the function of chlorophyll in plants, dye-sensitized solar cell harvested light from the sun and made it possible for the energy to transfers into an electron capture (Amadi et al., 2015).

Roslan et al., 2018 stated that DSSC is an electrochemical device that uses light-absorbing dye molecules adsorbed on semiconductor nanoparticles to generate electricity from sunlight. In DSSC, when the sunlight strikes on the surface of the cell, photons are absorbed by dye molecules, which then become excited.

2.2.1 Structure of dye-sensitized solar cells

Dissimilar with the typical solar cells, the DSSC at present shows as one of the ideal photovoltaic technologies alternative that can be used in replace of the conventional silicon-based solar cells (Carella et al., 2018). Carella and Borbone, 2018 stated that dye-sensitized solar cell is a multilayered device and all the layers undergo a systematic examination to assay it individually and the interaction of the components to other layers. The dye-sensitized solar cell is composed of a photo-anode and counter electrode (Amadi et al., 2015).

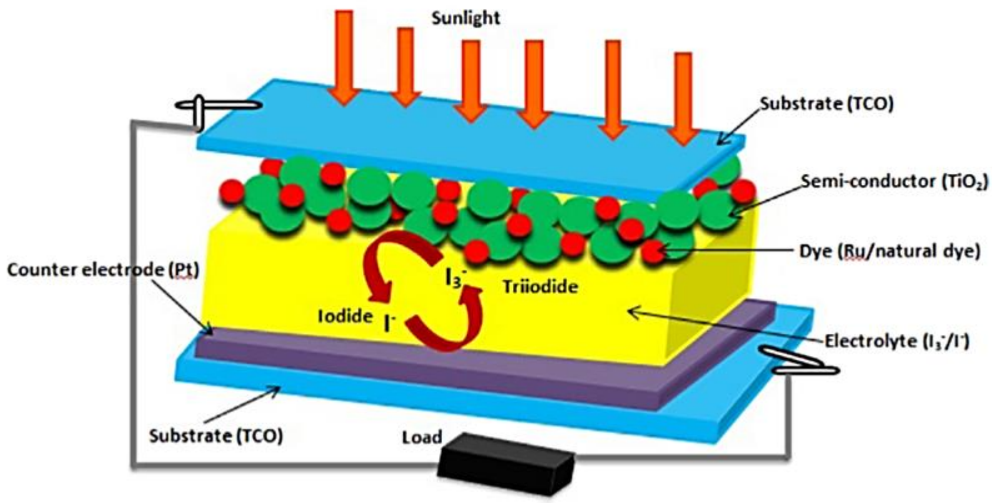

Figure 1 Structure of dye-sensitized solar cell (Roslan et al., 2018)

2.2.1.1 Photo-electrode

The oxidation process occurs in the photoanode. As illustrated in figure 2, the photo-electrode is composed of glass coated with transparent conducting oxide (TCO) material, usually, FTO or ITO, then followed by an electron capture materials commonly titanium dioxide and same with the purpose of CO_2 in the photosynthesis, TiO_2 accepts an electron, and lastly, the dye. The dye plays a vital role in the dye-sensitized solar cell because it serves as the light harvester. When the dye absorbed enough energy from the light, it produces excited electrons (Cherepy et al., 1997).

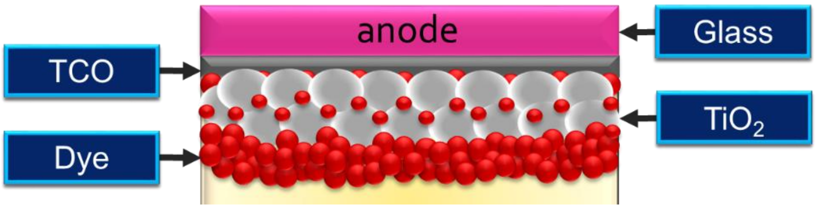

Figure 2 Composition of photo-electrode

2.2.1.1a Transparent conducting oxide (TCO)

According to (Dong et al., 2019), an electrode should be transparent because it is essential for solar cells as it allows incoming light to reach the photoactive layer. The transparent conducting oxides, also known as TCOs, are electrically conductive materials that exhibit low absorption of light. These materials are usually prepared with thin-film technologies and used in devices such as displays, circuities and solar cells. Commonly TCOs are semiconductors compound where oxygen composed the nonmetal part. Moreover, metal elements were used as compound materials or dopants with just a low percent content (Stadler, 2012).

- Indium tin oxide (ITO)

Indium tin oxide (ITO) is a colorless and transparent thin film. It is a compound of indium (III) oxide (In_2O_3) and tin (IV) oxide (SnO_2) and it is in solid-state. Technically, it has a chemical composition of 90%wt In_2O_3, 10%wt SnO_2. Indium tin oxide is the most widely used transparent conducting oxide because of its two key properties, its electrical conductivity and optical transparency (Stadler, 2012).

- Fluorine doped tin oxide (FTO)

In recent years, in making the organic solar cell (OSC), ITO has been favored compared to FTO as the transparent bottom electrode. However, due to the price of indium, which usually has a fraction of more than 70% in the ITO, is comparatively high compared to fluorine and tin (Dong et al., 2019). Studies revealed that the cost of the ITO coated substrate is the highest among the material costs for manufacturing organic photovoltaic modules. Notably, FTO also outperforms the ITO, in terms of the high-temperature processability and stability. It was concluded that FTO has higher thermal stability than ITO (Dong et al., 2019).

- Aluminum doped zinc oxide (ZnO: Al)

The aluminum-doped zinc oxide thin films ($Al_xZn_yO_z$, ZnO: Al) is composed of approximately 2%wt aluminum. Typically the ZnO: Al can be produced through spray pyrolysis, sol-gel technology, electrodeposition, vapor phase deposition and etc. (Stadler, 2012).

2.2.1.1b Titanium dioxide (TiO_2)

Titanium dioxide (TiO_2) is a white solid inorganic substance that is thermally stable, non-flammable, and almost insoluble (Titanium Dioxide Stewardship Council, 2012). TiO_2 is the preferred and suitable material for DSSC because its surface contains high resistant to the continued charge electron transfer molecule in sensitizers that have in dye molecules attached to the semiconductor surface (Gomesh et al., 2014)

2.2.1.1c The dye

García-Salinas and Ariza, 2019, mentioned that in the past, people used dyes from bioresources or natural dyes. Due to environmental issues and health concerns regarding synthetic dyes, this paved the way for natural dyes to be most preferable to use in different fields such as food industries, textile cosmetic, or pharmaceutical. Most natural dyes are found in the roots, barks, leaves, bracts, flowers, skins, and shells of plants. These plant pigments are classified into four major categories: 1.) tetrapyrroles, such as green chlorophylls; 2.) carotenoids, usually red, orange or yellow; 3.) flavonoids, of which red, purple or blue anthocyanins are an important subgroup; and 4.) betalains (yellow betaxanthins and red-purple betacyanins). Among the stated pigments, chlorophylls are the most abundant, followed by carotenoids. Carotenoids can coexist with other families, but betalains are incompatible with anthocyanins (García-Salinas and Ariza, 2019).

2.2.1.2 The counter-electrode

The counter-electrode (figure 3) is an electrode used to close the current circuit in the electrochemical cell and this is where the reduction process or the gain of electrons takes place. This electrode is composed of glass doped with FTO or ITO followed by an inert material also known as the catalyst layer (e.g., Pt, Au, graphite, glassy carbon) and usually, it does not participate in the electrochemical reaction (Patel et al., 2012).

Figure 3 Composition of counter electrode

2.2.1.3 The REDOX electrolyte

In between the photo-electrode and counter-electrode is the electrolyte. An electrolyte is a substance that contains free ions, which behaves as an electrically conductive medium. It is a good conductor and insulator for small voltages and open-circuit conditions, respectively. The electrolyte gives electrical contact and pathway for the ions to be injected into or ejected from the electrodes (Patel et al., 2012).

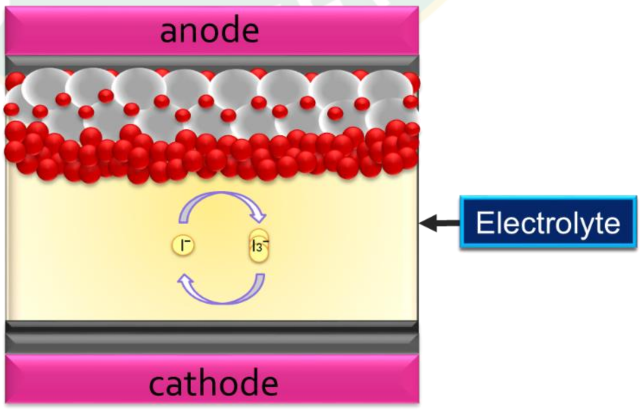

Figure 4 Electrolyte

According to (Lau and Soroush, 2019)), similar to the dyes, improving the redox electrolyte properties has been focused of researchers for the past few years. Ideally, the electrolyte should provide efficient charge transport in a noncorrosive environment without any appreciable light absorption. The original DSSC design involving the I^-/I_3^- redox shuttle remains a popular design choice given its favorable charge transfer characteristics, from the fast regeneration of the oxidized dye with the iodide to the extremely slow back electron recombination of the electrons in the TiO2 with the triiodide. The highest certified DSSC efficiency to date at 11.9% utilizes the I^-/I_3^- redox (Lau and Soroush, 2019).

2.2.2 Operating principle and charge transport mechanisms in DSSC

DSSCs are photoelectrochemical devices, which convert light energy into electrical energy by receiving photons from sunlight that excite the electrons of the dye molecule, followed by their injection into the conducting band of the adjacent mesoporous TiO_2 layer (Iftikhar et al., 2019). The dye-sensitized solar cells work differently from other types of solar cells because of its similarities to the natural process of photosynthesis. Hence, since the landmark publication by O'Regan and Gratzel, (1990), the system has repeatedly been described in terms of artificial photosynthesis (Lenzmann and Kroon, 2007). Like the chlorophyll in plants, a monolayer of dye molecules (sensitizers) absorbs the incident light, giving rise to the generation of positive and negative charge carriers.

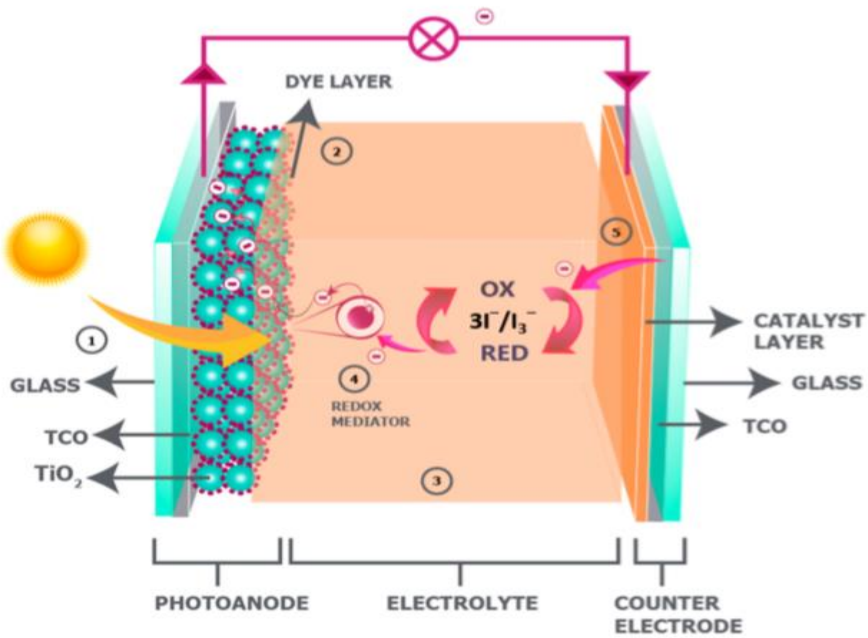

Figure 5 Schematic structure of DSSC (Iftikhar et al., 2019)

A traditional DSSC (as shown in figure 5) typically consists of the following components (Iftikhar et al., 2019):

1. A photoanode, which is traditionally, fabricated on a transparent conducting oxide (TCO) glass, such as a glass substrate that is coated with indium-doped tin oxide (ITO) or fluorine-doped tin oxide (FTO), by depositing the mesoporous electron transporting TiO_2 layer on this, via either doctor blading, screen-printing, or inkjet printing.
2. A monolayer of dye, which is usually based on ruthenium sensitizers, adsorbs over the mesoporous TiO_2 layer through its anchoring groups.
3. A liquid electrolyte containing a redox mediator, such as iodide/triiodide along with other additives, including an organic solvent to perform electron exchange during cell operation.
4. A CE (cathode), comprising a similar TCO-coated conducting glass substrate to that of the photoanode loaded with a catalyst layer, such as Pt or carbon, which receives electrons from external circuits and reduces the triiodide ion back to an iodide ion through an efficient charge transfer process.

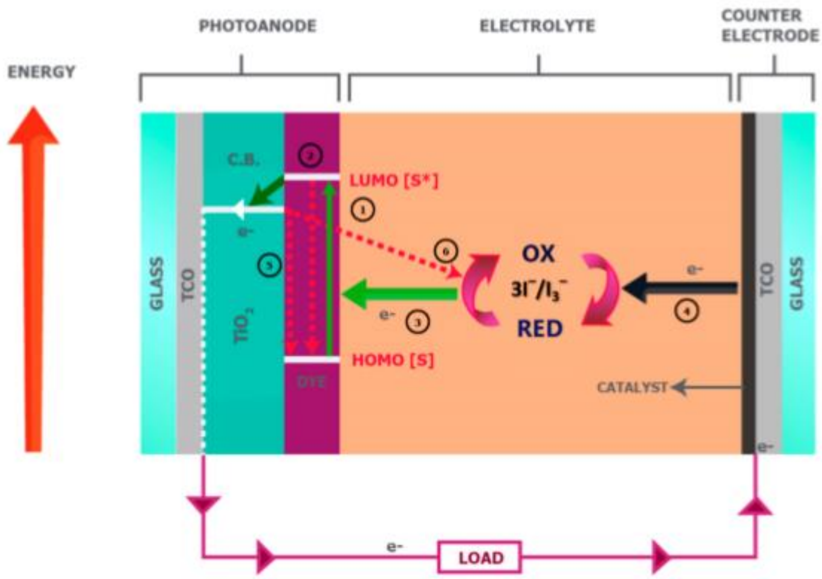

Figure 6 The operating mechanism of a typical dye-sensitized solar cell with iodine electrolyte

Overall process of dye-sensitized solar cell (figure 6) (Narayan, 2011):

1. Excitation of the dye. The light passes through the transparent photo-anode and inside the cell; a particle called photon hits the dye molecule and makes it electronically excited. The photon gives an electron enough energy to escape from the molecule. In results, the excited dye molecules inject (within femtoseconds) electrons into the TiO_2 layer that also acts as a semiconductor.
2. Injection of excited electron. The electrons are transported through the TiO_2 film by diffusion before reaching the anode of the cell.
3. Regeneration of the dye takes place as result of electrons accepted from the reduced state of the redox mediator, which in turn becomes oxidized itself in the process.
4. Regeneration of the electrolyte by accepting electrons from the counter electrode and returning to reduced state.

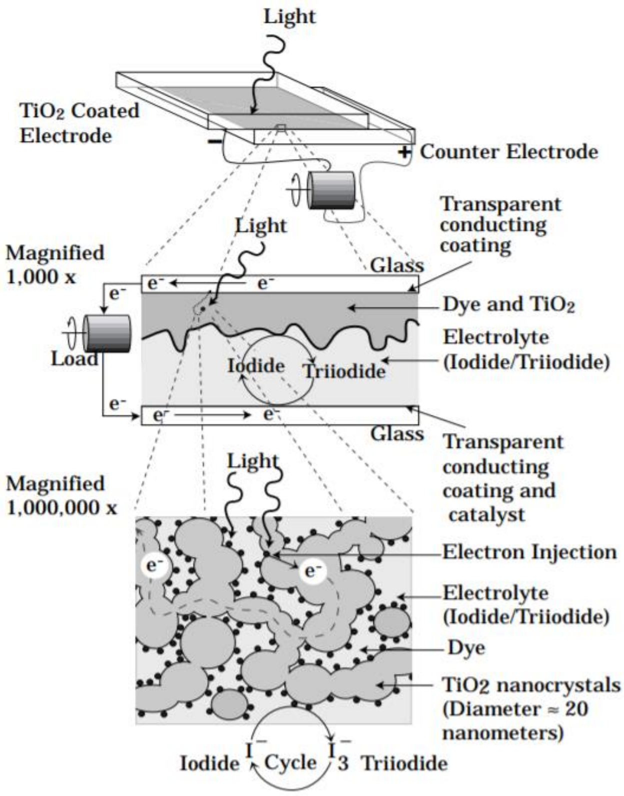

Figure 7 DSSC working principle

The photons from the light hit the dye molecules and make it electronically excited. The excited dye molecules then injected electrons to the TiO_2 layer. Moreover, within the electrolyte, the mediator (I^-/I_3^-) undergoes oxidation at the dye and regeneration at the catalyst-coated counter electrode as current flows through the electrical load (Smestad and Gratzel, 1998).

The overall chemical reactions operating the dye-sensitized solar cell are shown below (Iftikhar et al., 2019; Matthews et al., 1996; Narayan, 2011):

Dye excitation

$$S[TiO_2] + hv \rightarrow S^*[TiO_2] \quad (2.1)$$

Electron injection

$$S^*[TiO_2] \rightarrow S^+[TiO_2] + e^-[TiO_2] \quad (2.2)$$

Dye regeneration/ Mediator oxidation

$$S^+[TiO_2] + Red \rightarrow S[TiO_2] + Ox \quad (2.3)$$

Mediator regeneration

$$Ox + e^{-}[CE] \rightarrow Red + CE \quad (2.4)$$

Dye recombination

$$e^{-}[TiO_2] + S^{+}[TiO_2] \rightarrow S[TiO_2] \quad (2.5)$$

Recombination due to Ox

$$e^{-}[TiO_2] + Ox \rightarrow Red \quad (2.6)$$

2.3 Natural dye sensitizer

As the dye plays a vital role in solar energy to electricity conversion, several studies have conducted and focused on molecular engineering of several organic metal complexes and organic dyes. These natural colorants have been of interest in different fields and applications. Particularly interesting is the use of natural dyes as sensitizers in dye-sensitized solar cells (DSSCs) their main advantages being a simple extraction procedure, low cost, wide availability, and their environmentally friendly nature. For almost three decades, DSSCs are on the focus line of renewable energies, as a promising simple alternative power source. Points of interest of employing these natural dyes as photosensitizers in dye-sensitized solar cells are due to their large absorption coefficients in visible region, resource abundance, uncomplicated preparation and environment friendly. Significantly, the synthesis way for natural dye based DSSC is cost effective as it doesn’t involve costly materials and noble metals like Ru (Hemalatha et al., 2012; Ludin et al., 2014; Shalini et al., 2015).

These plant pigments exhibit either electronic structure that interacts with sunlight and alters the wavelengths that are transmitted or reflected by the plant tissue. This process leads to the occurrence of plant pigmentation and each pigment is described from the wavelength of maximum absorbance (λ_{max}) and the color perceived by humans. Chlorophyll, carotenoid, flavonoid and anthocyanin are the pigments for natural dyes that are relatively easy to extract from nature compared to synthetic dyes. Table 1 illustrates the most common pigment types found in flower and fruit colors in plants (Delgado-Vargas et al., 2000).

Table 1 Most common pigment types found in flower and fruit colors in plants

Name	Specific pigment type	Examples
Cream	Flavonols or flavones	Most cream flowers
Pink to red	Pelargonidin and/or cyanidin	Tomato, Lisianthus flowers, apple fruit
	Anthocyanin and carotenoid	Tulipa flowers
	Betacyanin	Bougainvillea flowers
Orange	Carotenoid	Marigold flowers
	Pelargonidin alone	Pelargonium flowers
	Anthocyanin and aurone mix	Snapdragon flowers
	Anthocyanin and chalcone mix	Carnation flowers
	Betacyanin	Purslane flowers
Yellow	Carotenoid	Most yellow flowers and fruit
	Aurone	Antirrhinum majus flowers
	Chalcone	Dianthus flowers
	Flavonol	Cotton flowers
	Betaxanthin	Portulaca flowers
Green	Chlorophyll	All green flowers and fruit
	Delphinidin	Most blue flowers and fruit
	Cyanidin	Morning glory flowers
Purple	Carotenoid	Pepper fruit
	Cyanidin and/or delphinidin	Eggplant
	Cyanidin and/or Delphinidin	Cymbidium orchids
Black	Delphinidin	Few black flowers, e.g. Viola (pansy)

2.3.1 Chlorophyll

Chlorophyll belongs to natural photosynthetic pigments that give plants green color. There are two major types of chlorophyll namely: chlorophyll-a and chlorophyll-b. This pigment and its derivatives are used as photosensitizers in DSSC because of their ability to absorb blue and red lights. The most efficient is the derivative of chlorophyll-a (methyl trans-32-carboxy-pyropheophorbide). The absorbance spectrum of chlorophyll-b shows a characteristic blue tinge and has a red shift when compared with chlorophyll-a. Chemical structure of chlorophyll-a and chlorophyll-b ` is shown in figure 8 (Shalini et al., 2016).

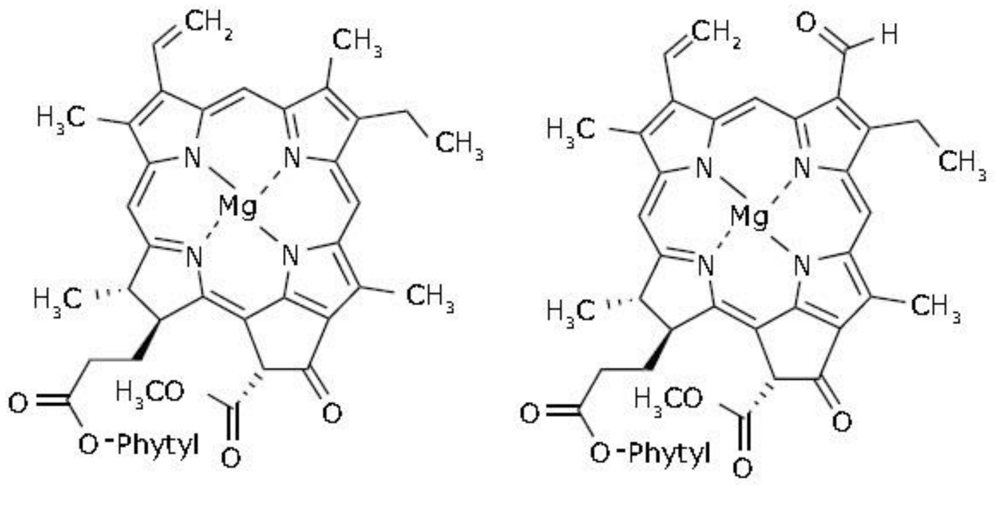

Chlorophyll a 00538 **Chlorophyll b 00538**

Figure 8 Chemical structure of Chlorophyll

2.3.2 Anthocyanin

Next to chlorophyll, anthocyanins are the most important group of pigments that are visible to human eye that are found in plants (Shalini et al., 2015). Anthocyanins are responsible for many of the attractive colors like blue, red, or purple pigments found in fruits and plants (Delgado-Vargas et al., 2000), and they have light absorbance in the wavelength range of 520–550 nm (Kumara et al., 2013).

The appearance of these pigments depends on the environment it lives, generally in acidic condition, anthocyanin appears as red pigment while blue pigment anthocyanin exists in alkaline conditions. Figure 9 shows the general molecular structure of anthocyanin. They are considered as one of the flavonoids although it has a positive charge at the oxygen atom of the C-ring of basic flavonoid structure. The stability of anthocyanin is dependent on pH, light, temperature, and structure. Moreover, many natural food colorants are anthocyanin derived from grape-skin, red-cabbage, purple-carrot extract and etc. (Giusti and Wrolstad, 2001).

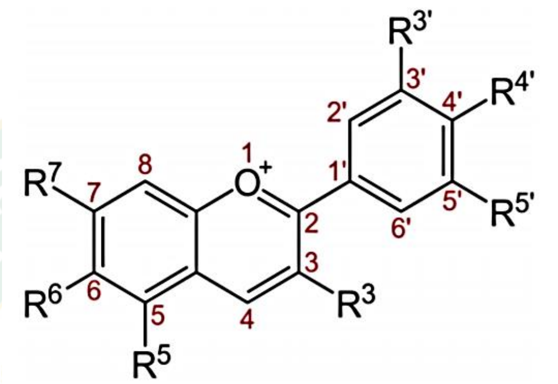

Figure 9 Basic structure of anthocyanin (Khoo et al., 2017).

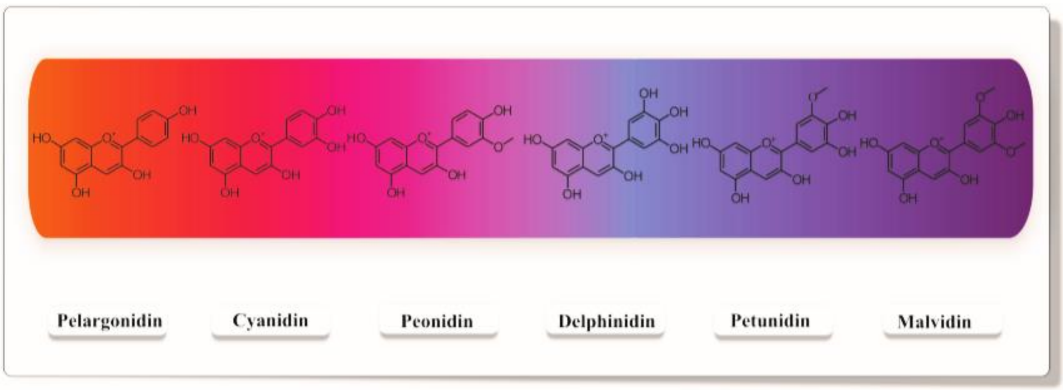

Figure 10 Visible color range of common anthocyanidins (Sladonja, 2013)

Table 2 Anthocyanidins found in nature

Name	Color produced
Pelargonidin	Orange, salmon
Cyanidin	Magenta and Crimson
Peonidin	Magenta
Delphinidin	Purple, mauve and blue
Petunidin	Purple
Malvidin	Purple
Apigeninidin	Orange
Aurantinidin	Orange
6-Hydroxycyanidin	Red
Luteolinidin	Orange
Triacetidin	Red

Furthermore, anthocyanin molecules have carbonyl and hydroxyl groups bound to the surface of TiO_2 semiconductor, which helps in excitation and transfer of electrons from the anthocyanin molecules to the conduction band of porous TiO_2 film (Shalini et al., 2015). Table 3 summarizes photoelectrochemical parameters of the dye-sensitize solar cells utilizing flavonoid anthocyanin dyes extracted from leaves, seeds, flowers, fruits, vegetables and tree barks (Shalini et al., 2015).

Table 3 Photoelectrochemical parameters of the with anthocyanin dyes extracted from leaves, seeds, flowers, fruits, vegetables and tree barks (Shalini et al., 2015)

Dye	Photos	λ_{max} (nm)	J_{sc} (mA/cm^2)	V_{OC} (V)	FF	η (%)
Begonia		540	0.63	0.537	72.2	0.24

Rhododendron		540	1.61	0.585	60.9	0.57
Violet		546	1.02	0.498	64.5	0.33
Hibiscus rosa-sinensis		534	4.04	0.40	0.63	1.02
Hylocereus costaricensis (Dragon fruit)		535	0.20	0.22	0.30	0.22
Brassica oleracea (Redcabbage)		537	0.50	0.37	0.54	0.13
Allium cepa (Red onion)		532	0.51	0.44	0.48	0.14
Sesbania grandiflora		544	4.40	0.41	0.57	1.02
Bauhinia tree		665	0.95	0.572	66.0	0.36

2.3.3 Flavonoids

Flavonoids are the most widespread and physiologically active group of natural constituents with a basic C_6-C_3-C_6 carbon framework. Flavone consists of two benzene rings, joined together by a γ ring that distinguishes one flavonoid compound from the other. Figure 11 shows the basic chemical structure of commonly occurring flavonoid. In case of flavonoids, the charge transfer transitions from HOMO (highest occupied molecule orbital) to LUMO (lowest un-occupied molecular orbital) require lesser energy, energizing the pigment molecules by visible light, leading to a broad absorption band in the visible region. This flavonoid is rapidly adsorbed to the surface of TiO_2 by displacing an OH^- counter ion from the Ti (IV) site that combines with a proton that is donated by the flavonoid.

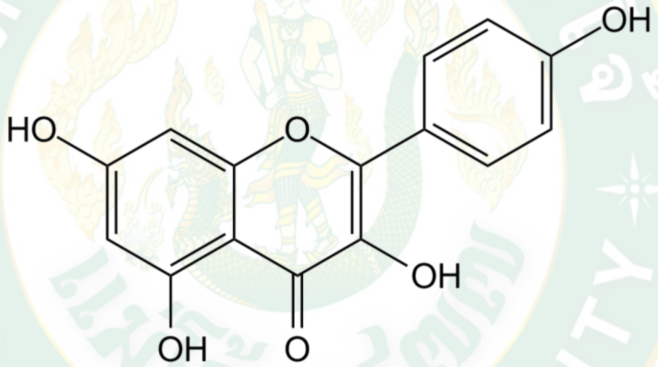

Figure 11 Basic structure of flavonoids

2.3.4 Carotenoids

Carotenoids are a large family (over 600 members) of isoprenoids that provide many fruits and flowers with distinctive red, orange, and yellow colors. These are organic molecules comprising of a C_{40} polyene backbone that is often cyclized to generate terminal ionone rings. This structure allows carotenoids to absorb short-wave visible light. These pigments occur in many flowers, fruits as well as in certain microorganisms. It contributes to red, orange and yellow colors and the pigments can play an important role in photosynthesis protection. Carotenoids can be categorized into two major classes known as xanthophylls (contains oxygen), and carotenes (purely hydrocarbons and has no oxygen).

2.4 Plant materials

2.4.1 Malabar spinach fruit

Even though natural dye based solar cells have lower light to electricity conversion efficiency compared to cells employing synthetic dyes, natural dyes are inexpensive, ecologically friendly, non-toxic, and are easily extractable. Thus, low conversion efficiencies of these natural sensitizers can boost research interest and provide opportunities to explore new natural dyes rendering good stability and higher efficiencies (Kabir et al., 2019; Shalini et al., 2015). Hence, it paved the way to research and develop natural dye from Malabar spinach fruits and Indigo plant.

Malabar spinach (figure 12) is a perennial plant that can grow easily under proper soil and climate condition as it prefers a warm climate. It can grow in an optimum temperature of 32°C and when the temperature drops to 26°C, the development is depressed. Specifically, this plant prefers soils that are warm, rich in minerals, moist and well-drained. The roots grow sufficiently in soils with a pH of 6.5-6.8 (Acikgoz and Adiloglu, 2018). The Malabar spinach can grow from the seeds and stems. The plant is suitable for continuous harvesting. In addition, during harvesting season, the stem, branches, leaves and young flower sprouts can be harvested (Acikgoz and Adiloglu, 2018).

Figure 12 Malabar Spinach (*Basella alba*)

Rank Scientific classification

Kingdom:	Plantae
Clade:	Tracheophytes
Clade:	Angiosperms
Clade:	Eudicots
Order:	Caryophyllales
Family:	Basellaceae
Genus:	*Basella*
Species:	*B. alba*
Binomial name:	*Basella alba*

Furthermore, Malabar spinach is rich in kaempferol, which is a flavonoid that is protective against cardiovascular diseases and cancer (Acikgoz and Adiloglu, 2018; Ray-Yu Yang et al., 2008). This plant also has antioxidant and phenolic compounds. The Anthocyanin that is a natural color pigment is present in stem, leaves and flowers (Acikgoz and Adiloglu, 2018).

2.4.2 Indigo plant

Probably one of the oldest and most famous dye is indigo, which has an intense dark blue color. Historically, the word "indigo" is derived from the Greek word "indikon" which means "Indian". From Asian civilization, at that time, dyes were imported from the Indian subcontinent as a highly expensive commodity. The main source of the Indigo dyes is from plants such as *Polygonum tinctorium*, *Isatis indigotica,* and *Strobilanthes cusia* (Nees) (Stasiak et al., 2014).

Figure 13 *Strobilanthes cusia* (Nees)

Rank Scientific classification

Scientific name: *Strobilanthes cusia (Nees) O.Kuntze*

Family name: Acanthaceae

Strobilanthes cusia (Nees) is a perennial plant with a height that can reach up to 60 cm. It grows in clay and wet soils and is tolerant of different soil pH levels. The species blooms well in either partial or complete shade and has oval-shaped leaves and hermaphrodite flowers (Stasiak et al., 2014).

2.4.3 Longan leaves

Figure 14 Longan tree

Rank Scientific classification

Kingdom:	Plantae
Clade:	Tracheophytes
Clade:	Angiosperms
Clade:	Eudicots
Clade:	Rosids
Order:	Sapindales
Family name:	Sapindaceae
Genus:	*Dimocarpus*
Species:	*D. longan*
Binomial name:	*Dimocarpus longan*

Dimocarpus longan, also known as Longan is as perennial subtropical tree that produces edible fruits. This tree is commonly found in tropical countries such as Thailand. It is the well known member of the Sapindaceae family. In spite of the fact that longan flowering can dependably be actuated through the application of potassium chlorate and hence generation is possible all year round, directly almost

80% of longan natural product is created amid the 'on-season', which starts with blooming in February and with natural products basically collected in July (Wiriya-Alongkorn et al., 2013).

2.4.4 Inthanin bok

Figure 15 Inthanin bok (*Lagerstroemia macrocarpa*) red leaves

Rank Scientific classification

Kingdom:	Plantae
Clade:	Tracheophytes
Clade:	Angiosperms
Clade:	Eudicots
Clade:	Rosids
Order:	Myrtales
Family name:	Lythraceae
Genus:	*Lagerstroemia*

Inthanin bok (*Lagerstroemia macrocarpa*) could be a medium-sized tree eight to 20 meters tall. It features a circular canopy with long, dainty stems clearing down to cover more than half of the tree's trunk. The leaves are usually 12-17cm wide and 20-30cm long, dark green and shiny. In addition, it has big flowers, 10-12cm wide, with cup-shaped sepal secured by thin hair. The Petals are purple, which turn to white before they fall from the tree. Leaves begin to fall in February and the color changes from dark green to red-orange-brown (Figure 15). While from the month of March to May new leaves grow.

2.6 Greenhouse

Many greenhouse types are used for plant protection worldwide. Some may be better than others may for particular applications, but there is no best greenhouse (Aldrich and Bartok, 1992). Commonly, the major crops produced through greenhouse systems are vegetables, fruits, and flowers. Greenhouse are usually made of transparent glass or plastic, enabling cultivation even when low temperatures restrict open field crop growth. This purpose is particularly useful in temperate zones. In addition, the greenhouse extends the cultivation season and broadens the choices of crop species. Actually, greenhouses can shorten the cultivation duration, increase the number of crop cycles, and thereby greatly enhance annual crop yields (Yano and Cossu, 2019).

The crop's quality can be improved by keeping up a suitable environment in greenhouses. The time for the greenhouse crop harvest can be adjusted to meet market demands until it becomes profitable for growers. If a greenhouse is designed as a closed system, including the ground area, then the use of water and fertilizers can be saved with optimum plant growth. Thus, the use of pesticides can be avoided because the cover materials protect the crops against insect infestations (Yano and Cossu, 2019).

Figure 16 Greenhouse

2.6.1 Considerations for greenhouse (interior environment control)

2.6.1a Temperature

Sunlight penetrates easily into a greenhouse because of roof and wall transparency. The cover materials block thermal leakage. Consequently, the internal temperature becomes higher than that outside. By exploiting this thermal property, various technologies related to nighttime heating have been applied. Mainly, such applications are based on the principle of thermal energy storage in walls, soil, or water tanks during the daytime, with the energy released into the greenhouse during nighttime (Yano and Cossu, 2019).

By contrast, greenhouse internal temperatures increase excessively during summer in high-insolation regions. Transitory or constantly high temperatures cause arrange of morpho-anatomical, physiological, and biochemical changes in plants. They affect plant growth and development and might engender a drastic reduction in their economic yield. Roof whitening is a simple and inexpensive cooling method. Plastic nets and thermal screens are also exploited to reduce sunlight energy penetration into greenhouses. To prioritize ventilation for cooling purposes, the roof and walls are replaced with mesh in some cases. Natural or forced ventilation, pad and fans, fogging, and heat pumps are often used for greenhouse cooling (Yano and Cossu, 2019).

2.6.1b Light

Sunlight is the original energy source of plant growth. Chlorophyll molecules in photosystems capture photons from the sunlight, where the photonic energy is converted into chemical energy to be stored in plants. Therefore, the number of photons colliding with the plant surfaces is necessary information when one considers plant growth. Greenhouse internal irradiance is usually less than the exterior irradiance because cover materials reflect or scatter partial sunlight to outside areas. Lighting during nighttime is also applied to regulate flowering for the timely delivery of produce to markets (Yano and Cossu, 2019).

2.6.1c Carbon dioxide

The greenhouse interior CO_2 concentration fluctuates according to the respiration and photosynthesis of the greenhouse crops. The CO_2 concentration in the greenhouse often falls to less than that of the exterior as plant photosynthesis proceeds in the daytime with limited greenhouse ventilation (Yano and Cossu, 2019). Crop photosynthesis is limited under lower CO_2 concentration conditions even if sufficient sunlight is available, and vice versa. Ventilation control plays a crucially important role for managing the CO_2 concentration, temperature, and humidity of the greenhouse interior air. To provide sufficient CO_2 to plants, CO_2 supply systems are often used. Continuing interest in closed and semi-closed greenhouses abounds because they can increase CO_2 levels inside the greenhouse, reduce pesticide application, and conserve energy and water. (Yano and Cossu, 2019).

2.6.1d Water and humidity

A greenhouse roof blocks Rainwater. Protecting leaves, flowers, and fruits from raindrop contact are desirable to prevent and suppress diseases. The greenhouse structure also contributes to the prevention of runoff of soils and crops during heavy rains. However, those benefits block the natural water supply that plants receive from rain. Therefore, irrigation is necessary for greenhouse cultivation. Irrigation and water circulation of hydroponics can be automated using electric pumps. The control of water and nutrient supplies for optimum plant growth and retrieval of nutrient-filled water that is not absorbed by crops are possible with greenhouse cultivation (Yano and Cossu, 2019).

Greenhouse interior humidity affects plant transpiration and disease infections. Stomata close to prevent extra transpiration when the surrounding air is dry. Consequently, CO_2 exchange between leaves and air is suppressed. Thereby, the net photosynthetic rate is decreased. For these reasons, humidity control is necessary to provide an adequate crop growth environment. Water vapor as a heat energy medium also affects the thermal greenhouse environment (Yano and Cossu, 2019).

CHAPTER 3

METHODOLOGY

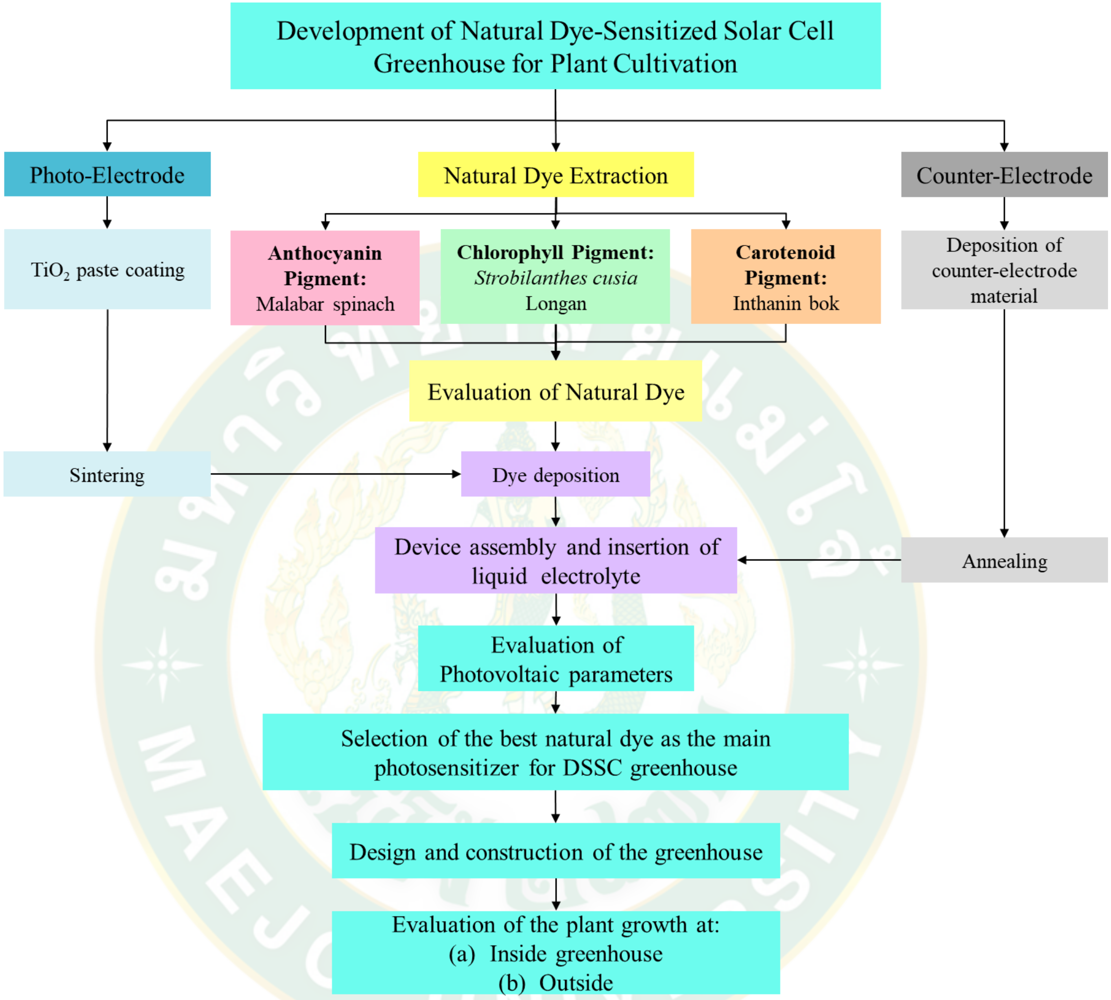

Figure 17 Experimental procedure of the study

3.1 Material and chemicals

The Malabar spinach fruits (*Basella alba*), Indigo plant leaves (*Strobilanthes cusia* (Nees)), Longan leaves (*Dimocarpus longan*) and Inthanin bok red leaves (*Lagerstroemia macrocarpa*) were collected from Rong Wua Daeng, San Kamphaeng District, Chiang Mai, Thailand and in the Maejo University. Moreover, in conducting this research work, various chemicals and materials are needed in order to proceed with the experiment. For the dye extractions, the chemicals needed are acetic acid-sodium acetate buffer pH 4.5, HCl acid-KCl buffer pH 1.0, NaOH and HCl. And for the fabrication of DSSC fabrication: FTO conductive glass (fluorine-doped SnO_2, sheet resistance: 40 Ω / sq), TiO_2 nanoparticles powder with particle size in the range of 15–20 nm, liquid electrolyte, platinum or activated carbon nanoparticles powder, sealer, acetic acid and soap solution

3.2 Dye extraction

3.2.1 Malabar spinach extraction

Malabar spinach fruits used in this research were collected from San Kamphaeng District, Chiang Mai, Thailand. HCl and acetic acid were purchased from Union Science. The buffers: (0.4M) Acetic acid-sodium acetate buffer pH 1.0 and (0.1M) HCl acid-KCl buffer pH 4.5, as well as the 50% methanol solvent and 50% methanol & 1% HCl, were prepared in the lab.

The Malabar spinach fruits were separated from its stalk and then were washed with water and dried at room temperature. The fruit samples were measured by following the ratio of 10 g of sample per 50 mL of solvent. For this study, three different methods were conducted: extraction of anthocyanin pigments from Malabar spinach fruits: a.) using pure methanol solvent, b.) using 50% methanol solvent, and c.) using 50% methanol & 1% HCl solvent. After the Malabar spinach fruits were measured, mortar and pestle were used to pound it and break it down into smaller pieces. The crashed samples were then put into a beaker covered with aluminum foil to avoid light exposure of the sample. Moreover the solvent: a.) using pure methanol solvent, b.) using 50% methanol solvent, and c.) using 50% methanol & 1% HCl solvent is then added and mixed in the beaker and then set aside for 10 mins, to give enough contact time for the solvent to extract the pigments. After 10 mins, the samples were then filtered using a vacuum pump. Lastly the filtrate were then kept in a covered glass bottle to avoid light exposure.

Figure 18 Raw materials are washed, dried at room temperature then weighed (left), then crushed with mortar and pestle (middle), mix with solvent (right)

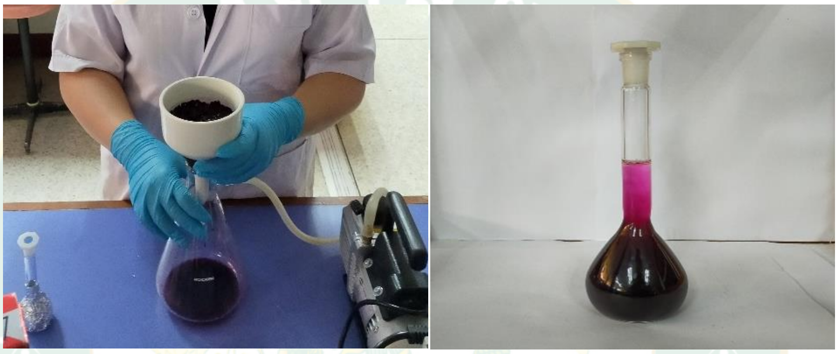

Figure 19 Solutions are filtered (left), transferred to the volumetric flask (right)

Furthermore, after the extraction, the dye is examined under the spectrophotometer for anthocyanin content analysis. During this process, the dye extract is diluted with two different buffers (Acetic acid-sodium acetate buffer pH 4.5 and HCl acid-KCL buffer pH 1.0). The samples were diluted, at a different dilution ratio as shown in Figure 20. Then measured the absorbance with the wavelength ranges from 510nm-540nm and 700nm.

Anthocyanin pigment concentration (APC) was calculated using the modified pH-differential method:

$$APC(mg/L) = \left(\frac{A * MW * Df * 10^3}{\varepsilon * L} \right) \tag{3.1}$$

where $A = (A_{\omega} - A_{700nm})_{pH1,0} - (A_{\omega} - A_{700nm})_{pH4.5}$, MW (molecular weight)= 449.2 g/mol, Df is dilution factor, $\varepsilon = 26{,}900$ L/cm mol, 10^{3} is the converting factor for g to mg, and L is the path length in cm.

The filtrate sample of Malabar spinach fruit extract undergoes light absorbance analysis using the spectrophotometer. Its absorbance was checked at different wavelengths (510 nm, 520 nm, 530 nm, 540 nm, & 700 nm). Moreover, the anthocyanin content was calculated using the pH-differential method; in this case, the filtrates were diluted at two different buffers: (0.4M) Acetic acid-sodium acetate buffer pH 1.0 and (0.1M) HCl acid-KCl buffer pH 4.5).

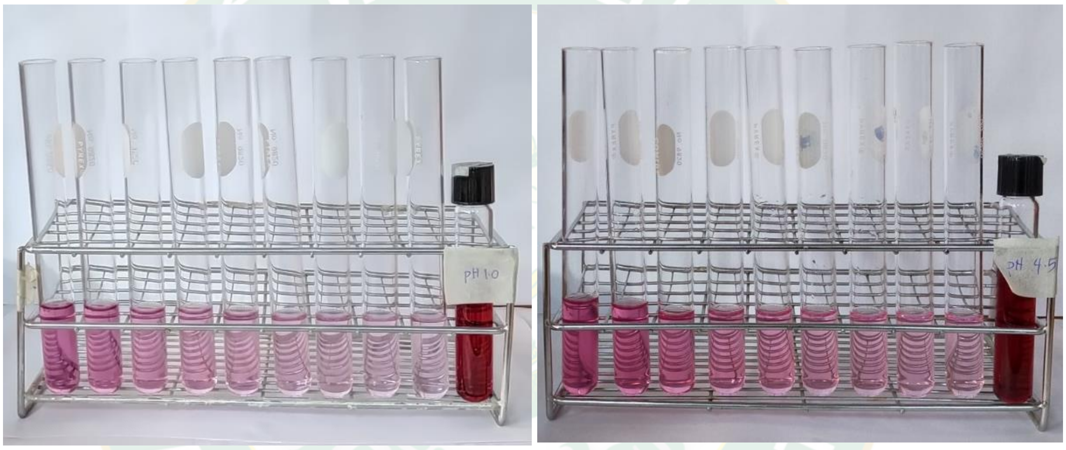

Figure 20 Diluted with HCl acid-KCL buffer pH 1.0 (left), Acetic acid-sodium acetate buffer pH 4.5 (right)

In addition, for comparison of anthocyanin content, the red cabbage (RC) dye was used. The vegetable was chopped into smaller pieces and then put in the blender together with the solvent. After it was blended, the solution was kept in a beaker and set aside for 10 mins at room temperature. Lastly, the solid residues were filtered out while the dye extract was stored in a container covered with aluminum foil. Both the Malabar spinach dye and red cabbage dye were kept in dark storage to avoid light exposure. The combination of 50% malabar spinach (MS) with 50% red cabbage (RC) was prepared by mixing 50 mL of dye from malabar spinach and 50 mL of red cabbage dye. Figure 21c shows the extracted dye from the experiment.

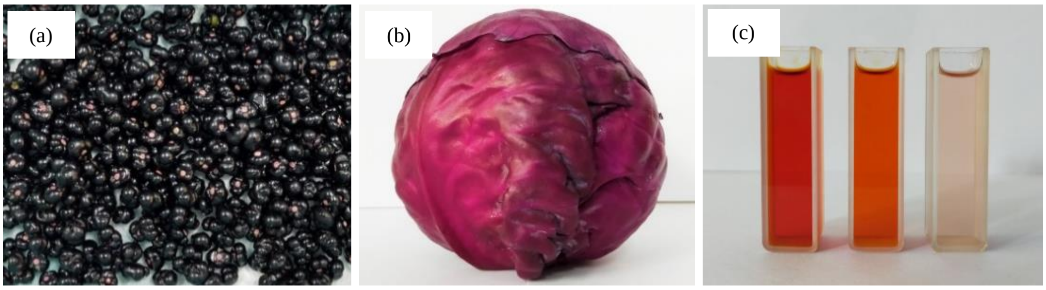

Figure 21 a.) Malabar spinach fruits, b.) Red cabbage c.) Natural dye (left to right): malabar spinach, 50% (MS) + 50% (RC), and red cabbage.

3.2.2 Indigo plant dye extraction

The extraction process used was adopted and modified from Sumanta et al. (2014). The *Strobilanthes cusia* (SC), commonly known as the Indigo plant, was collected from Chiang Mai Province, Thailand. The plant sample was thoroughly rinsed with water; subsequently, air-dried at room temperature until free from moisture, then cut into smaller size by using a blender together with the organic solvent. After it was blended, the solution was kept in a beaker and set aside for 10 mins at room temperature. Lastly, the solid residues were filtered out using Whatman filter paper, while the dye extract was stored in a container.

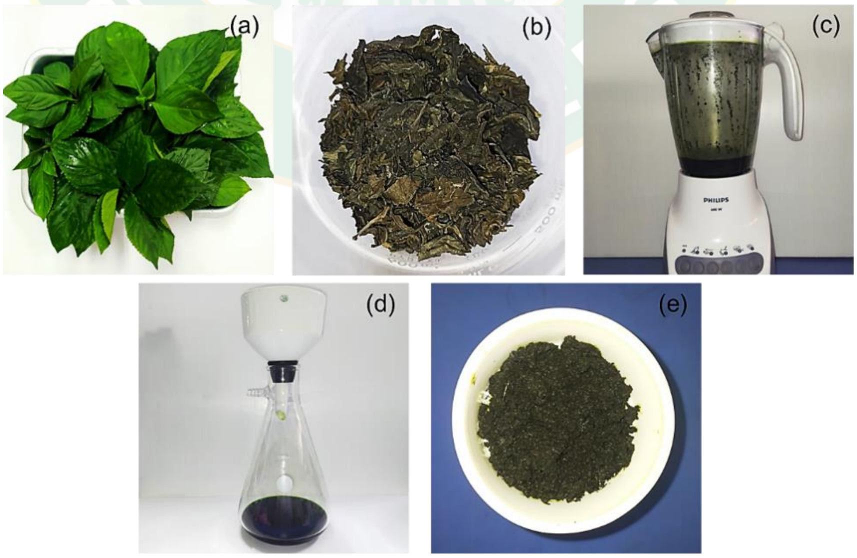

Figure 22 Strobilanthes cusia sample preparation & dye extraction process (a-d), residue (e)

3.2.3 Longan and Inthanin leaves extraction

For Longan and Inthanin extraction, the extraction method was used. The fresh leaves were washed and dried at room temperature. The samples were then weighed and break down into smaller pieces using the blender. Then followed by the addition of solvent (methanol) to the extract. The solution was set aside for 10 minutes for the better extraction of the solvent to the dye. Lastly, solutions were filtered and transferred to the volumetric flask.

Figure 23 Longan extract (left), Inthanin bok extract (right)

Absorbance is measured using spectrophotometer (figure 24). For the determination of Chlorophyll A, Chlorophyll B and Carotenoid content the following equation are used:

$$\text{Chlorophyll A } (C_a) = (12.25 \times A_{663} - 2.79 \times A_{645}) \times DF \quad (3.2)$$

$$\text{Chlorophyll B } (C_b) = (21.50 \times A_{645} - 5.10 \times A_{663}) \times DF \quad (3.3)$$

$$\text{Carotenoid content} = \frac{(1000 \times A_{470} - 1.43 \times C_a - 35.87 \times C_b) \times Df}{205} \quad (3.4)$$

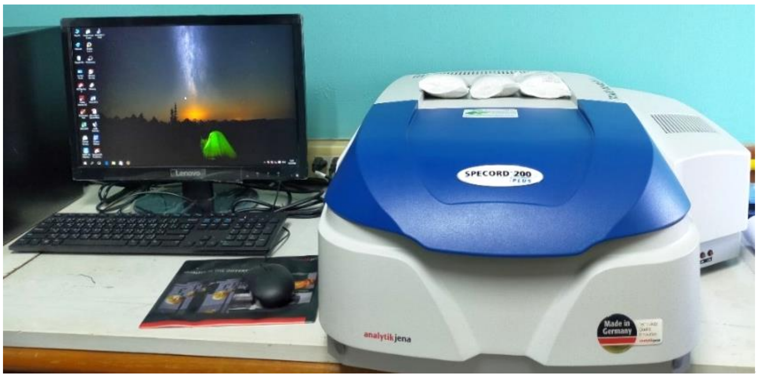

Figure 24 Spectrophotometer

3.3 Preparation of FTO substrates

The preparation of photo-electrode started with cleaning the FTO glass. The FTO glass was cleaned with soap solution, distilled water and methanol (Figure 25) for 15 mins in an ultrasonic bath, then dried at room temperature, and measured the resistance by multimeter as shown in figure 26.

Figure 25 Soap solution (left), distilled water (middle) and methanol (right)

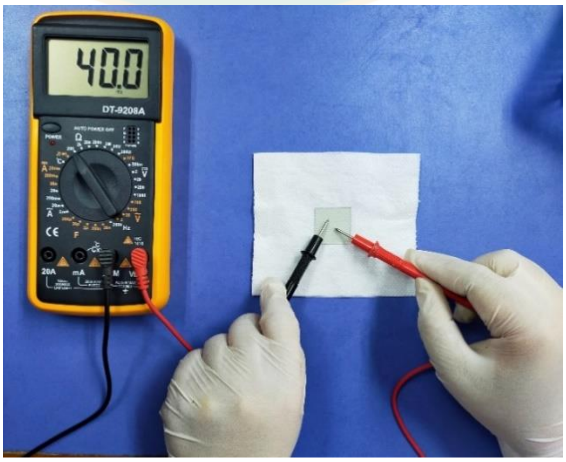

Figure 26 Measurement of the resistance of FTO glass (40 Ω / sq) by multimeter.

3.4 Preparation of TiO_2 paste

Different processes prepared the photoanode, also known as the working electrode. First, the FTO glass was cleaned by ultrasonic under three different solutions (soap, distilled H_2O, & methanol) for 10 min each, consecutively. Afterward, the FTO glass was air-dried, then was checked for the conductive side by measuring its resistance, and then the four corner sides were taped to get the desired surface area. Simultaneously, the TiO_2 paste was prepared by reducing the particle size of the TiO_2 powder by setting it to a magnetic mixer for 1hr. Hence, a ratio of 5g of TiO_2 powder, 10 ml of 5% acetic acid & 0.5 surfactants (Tween 20) was thoroughly mixed using a magnetic stirrer for 1hr then kept in a sealed container to avoid evaporation of the paste.

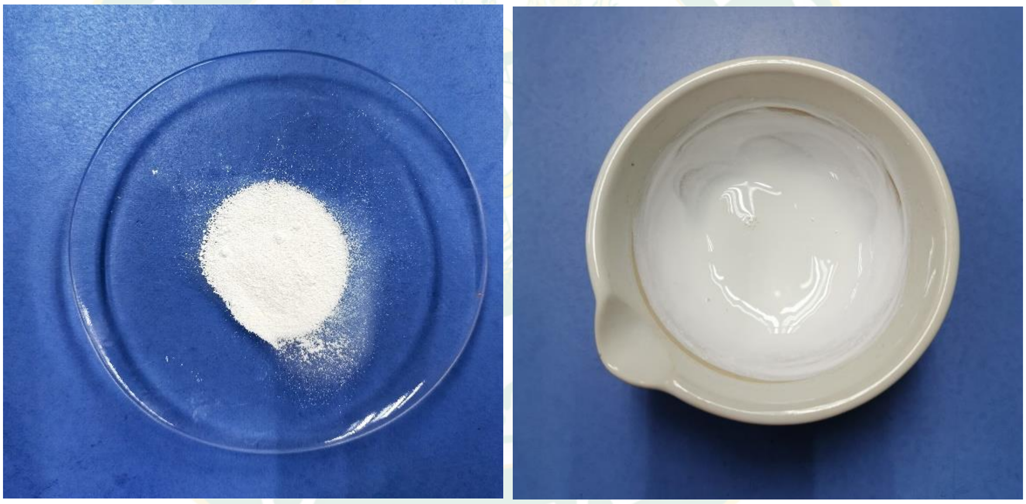

Figure 27 Preparation of TiO_2 paste: TiO_2 nanoparticles powder (left) and mixture of TiO_2 powder and 5% acetic acid (right)

3.5 Preparation of TiO_2 photo-electrode

Lastly, the TiO_2 paste was deposited on the glass substrate using the doctor blade technique. Subsequently, the annealing process was done by heating it at a temperature of 300°C for 1hr and then letting it cool down. Furthermore As shown in figure 28 , SC photosensitizer was loaded into the TiO_2 by slowly putting 10 drops of the dye then letting it dry for 5 mins. Subsequently, repeat the process two more times. After the dye loading, remove the excess dye from the FTO glass. The same dye loading process was used for Malabar spinach, longan, and inthanin bok

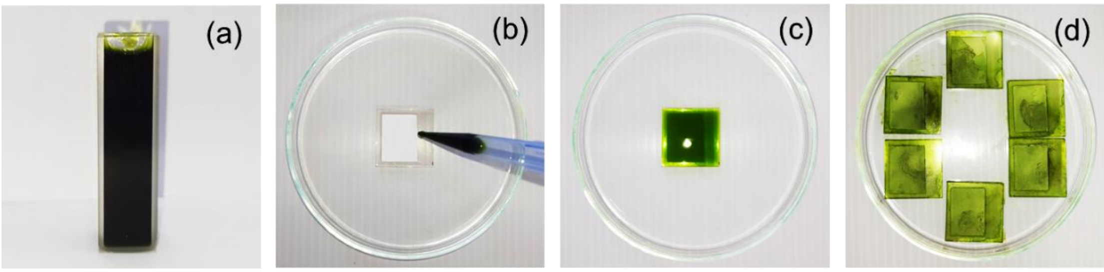

Figure 28 *Strobilanthes cusia* photosensitizer (a), dye loading to TiO_2 (b-d)

3.6 Preparation of counter electrode

To prepare the counter electrodes, a tape was fixed on the four sides of the cleaned FTO conductive glass. For the counter electrode material, several materials were examined (Platinum paste, pencil graphite and activated carbon powder). Then counter electrode material was coated on the FTO glass and let it dry at room temperature for 10 min. After the tape removed, the film was gradually sintered at 300 °C for 30 mins. Lastly, the counter electrode film was cooled at room temperature.

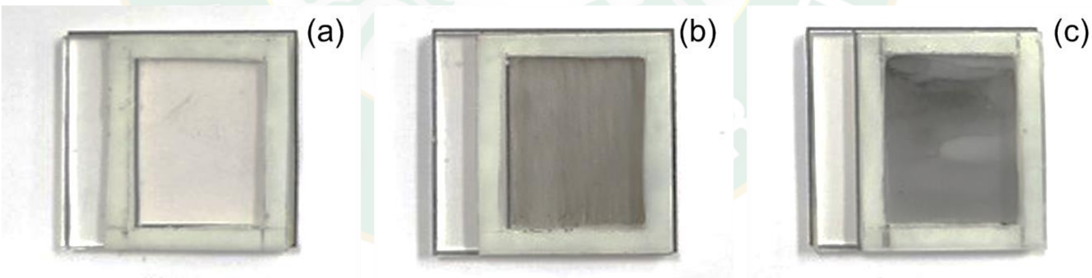

Figure 29 Counter electrodes: FTO glass (a), FTO glass with graphite (b), FTO glass coated with platinum (c)

3.7 Assembly of DSSC

Dye-sensitized solar cells were assembled by sandwiching the prepared photo-anode and counter electrode, and sealed with a hot-melt gasket. In addition, for the DSSC roof, silicon sealant was used to secure the cell. Figures 30 and 31 show the assembly and overall view of DSSC respectively. Then the electrolyte was injected between the two electrodes. Furthermore, after the preparation of the DSSC, all the parameters were measured instantly using a multimeter (figure 32) to avoid any changes in the dye and photoelectric properties caused by ageing.

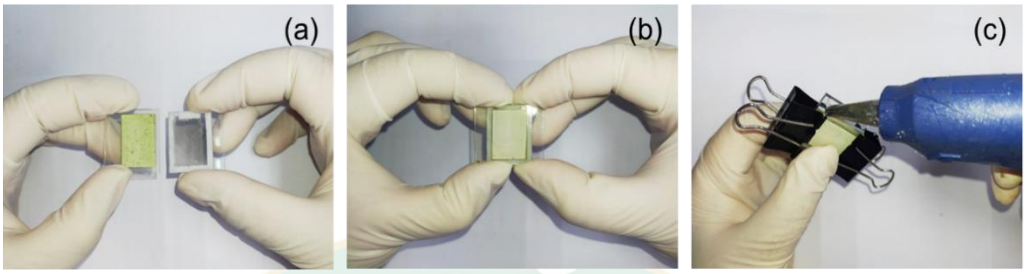

Figure 30 Photoanode and counter electrode (a) cell assembly (b), sealing (c)

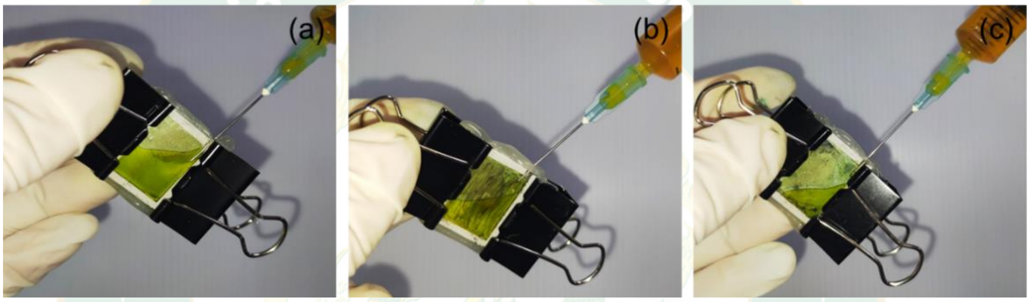

Figure 31 Injection of electrolyte to different counter electrodes: FTO glass (a), FTO glass with graphite (b), FTO glass coated with platinum (c)

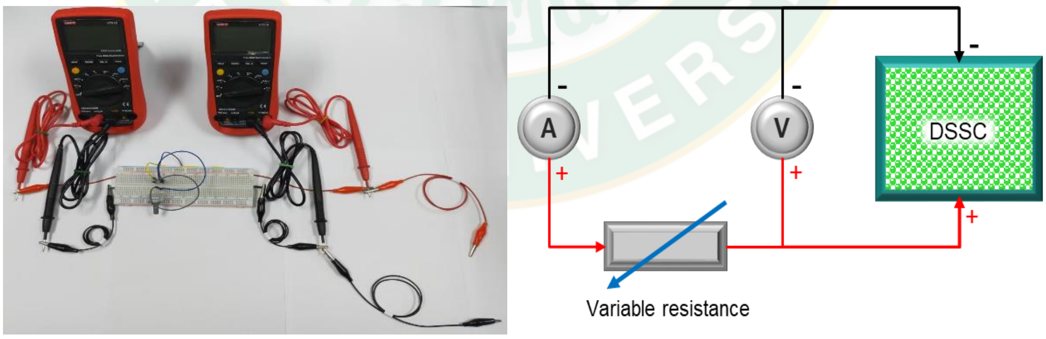

Figure 32 Schematic circuit diagram of the experimental setup used for measuring the current–voltage characteristics of DSSC with voltmeter (V), ammeter (A), and potentiometer variable resistance (10k Ω).

3.8 Performance parameter of dye-sensitized solar cells

In evaluating the performance of the DSSC, specific parameters are necessary in order to get the result for the evaluation. The primary parameters of the cell are obtained from current-voltage (J-V) measurements, as shown in Figure 33 (Dawoud, 2016).

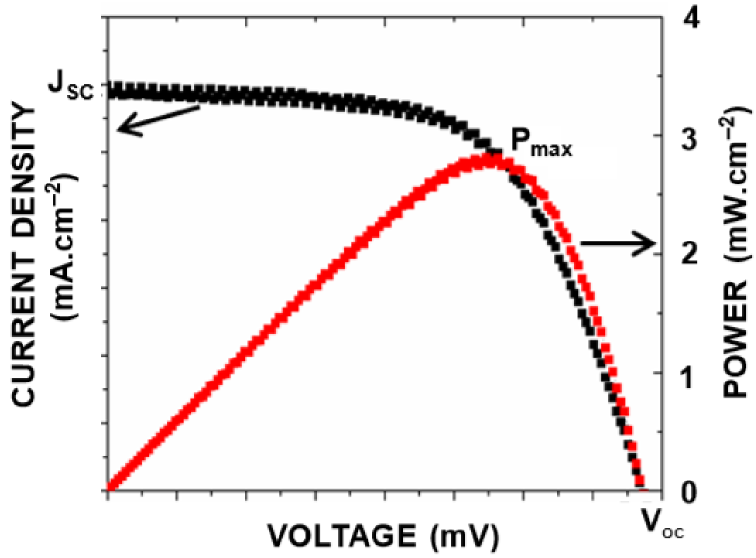

Figure 33 Illustration of current density-voltage characteristics of DSSC (Jena et al., 2012)

3.8.1 Short circuit current density

The short-circuit current (J_{SC}) is the current through the solar cell per unit area when the voltage across the solar cell is zero. The short-circuit current depends on several factors:

- The number of photons: (i.e., the intensity of the incident light source); Jsc from a solar cell is directly dependant on the light intensity.
- The spectrum of the incident light: For most solar cell measurements, the spectrum is standardized to the AM1.5 spectrum.
- The optical properties of the solar cell
- The collection probability of the solar cell: which depends chiefly on the surface passivation and the minority carrier lifetime in the base.

3.8.2 Open circuit voltage

The open-circuit voltage (V_{oc}) is the maximum voltage available from a solar cell, and this occurs at zero current. The open-circuit voltage corresponds to the amount of forwarding bias on the solar cell due to the bias of the solar cell junction with the light-generated current. The theoretical maximum V_{oc} of the cell is determined by the difference between the Fermi level of the semiconductor and the redox potential of the hole-conductor (Dawoud, 2016).

3.8.3 Fill factor

The fill factor, more commonly known by its abbreviation "FF", is basically a measure of the quality of the solar cell. The FF is determined by comparing the maximum power (P_{MAX}) to the theoretical power (P_T) that would be output obtained at the open-circuit voltage and the short circuit current.
The FF is typically calculated as:

$$FF = \frac{J_m \times V_m}{J_{sc} \times V_{oc}} \tag{3.5}$$

where J_m and V_m are the maximum current and voltage, respectively. The fill factor (FF) is a measure of the maximum power output from a solar cell, and it reflects the extent of electrical and electrochemical losses during cell operation. To obtain higher fill factor, improvement of the shunt resistance and decrement of the series resistance, with reduction of the overvoltage for diffusion and charge transfer, is required (Dawoud, 2016).

3.8.4 Power conversion efficiency

The efficiency is the most commonly used parameter to compare the performance of one solar cell to another and it is defined as the ratio of maximum electrical energy output to the energy input from the sun.
Power conversion efficiency under sunlight irradiation (e.g., AM 1.5) can be obtained using:

$$\eta = \frac{J_{sc} \times V_{oc} \times FF}{P_{in}} \qquad (3.6)$$

where P_{in} is the power per unit area of the incident light. Besides the solar cell performance itself, it depends on the incident light spectrum and intensity as well as operating temperature (Dawoud, 2016).

3.9 Construction of DSSC greenhouse

3.8 Prepation of DSSC roof

In the construction of the DSSC cells for the greenhouse, the natural pigment (Inthanin) that showed the highest photovoltaic efficiency was chosen as the main photosensitizer for the solar cell. In this part of the study, the glass used was 10 cm by 10 cm, and the sealant used was silicon. Figure 34a, displays the TiO_2 photoanode after sintering process and letting it cool. Figure 34b, shows the dye loading process of the natural pigment. Lastly, figure 34c, is the product of photo-electrode and counter-electrode fabrication, and ready to be assembled.

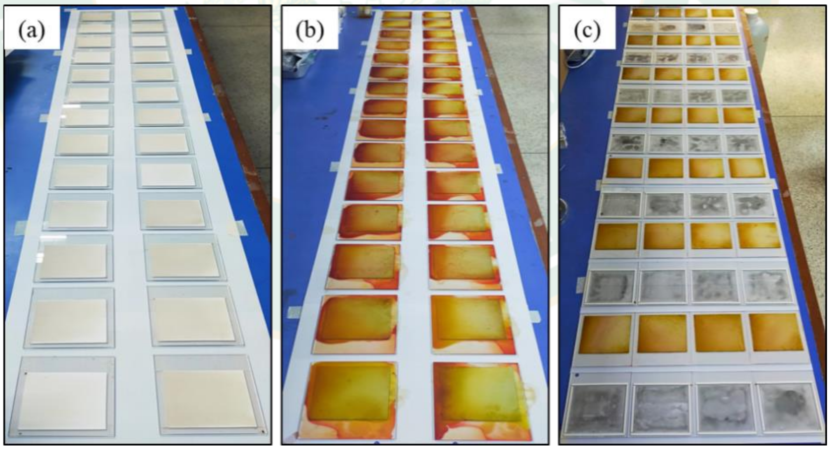

Figure 34 Fabrication of DSSC cells for greenhouse

Overall, 36 solar cells were fabricated. After the electodes were assembled, the liquid electrolyte was then injected using a syringe and the it was completely sealed. Figure 35(a&b), shows the top view and bottom view of the resulting product. Moreover, for the final process, electrical wires were attached in each negative and positive sides of the dye-sensitized solar cells. Subsequently, all the cells were connected with each other (figure 35c). Furthermore, the DSSCs were set up according to the schematic circuit diagram, as shown in figure 36. To summarize the electrical circuit includes 2 series connections (each composed of 18 cells). Following that, the series connections were then attached to each other in a parallel way.

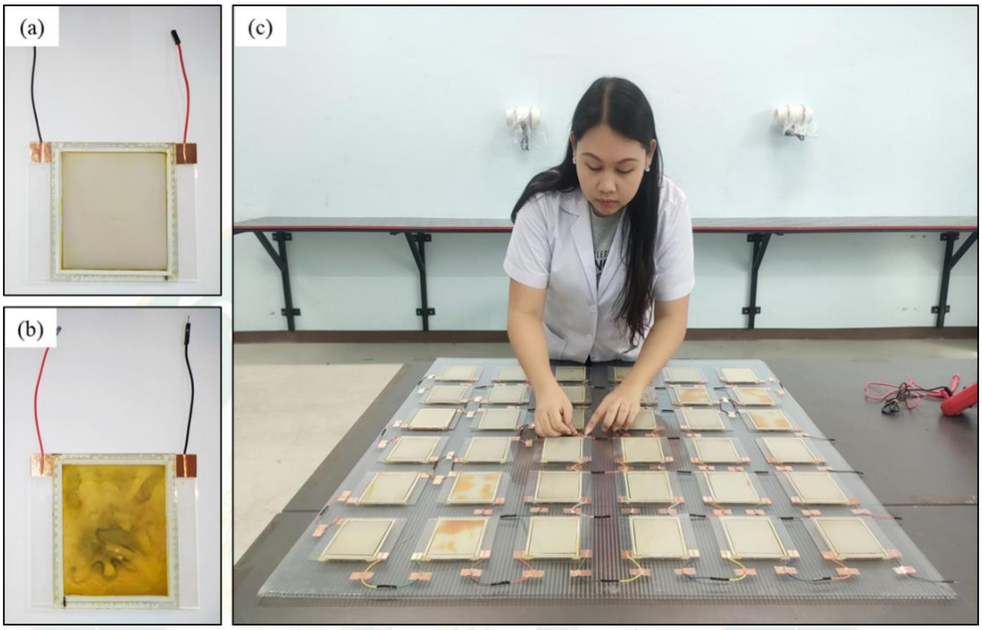

Figure 35 DSSCs for the greenhouse

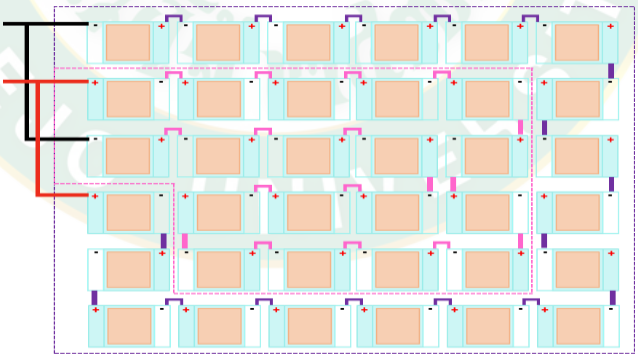

Figure 36 Schematic circuit diagram of the DSSC roof

Agrivoltaic is a system designed combining commercial agriculture and electricity within the same land unit area. However, the major problem manifested by agrivoltaics or photovoltaic greenhouse is the competition between PV roofs and plant to get incident solar radiation. Thus, dye-sensitized solar cell (DSSC); the third generation of solar PV is recently attracted due to their simple manufacturing process, low fabrication cost, low light level sensitivity, ease of use for bigger applications and flexibility in scaling characteristics which stirred the best candidates use as green energy buildings (Roslan et al., 2019).

Moreover, the various color of DSSC (determined by the dye) can act as a plant growth regulator or can modify the solar spectrum which enters into the greenhouse. As a result, plant growth and photomorphogenesis can be optimized. Hence, in this research a practical fieldwork is proposed by using integrated semi-transparent DSSC mini greenhouse to define DSSC module systems potential and performance nearby the tropical climate conditions (Roslan et al., 2019). The proposed design and materials used in the construction of the portable natural dye-sensitized solar cell greenhouse is shown in figure 37.

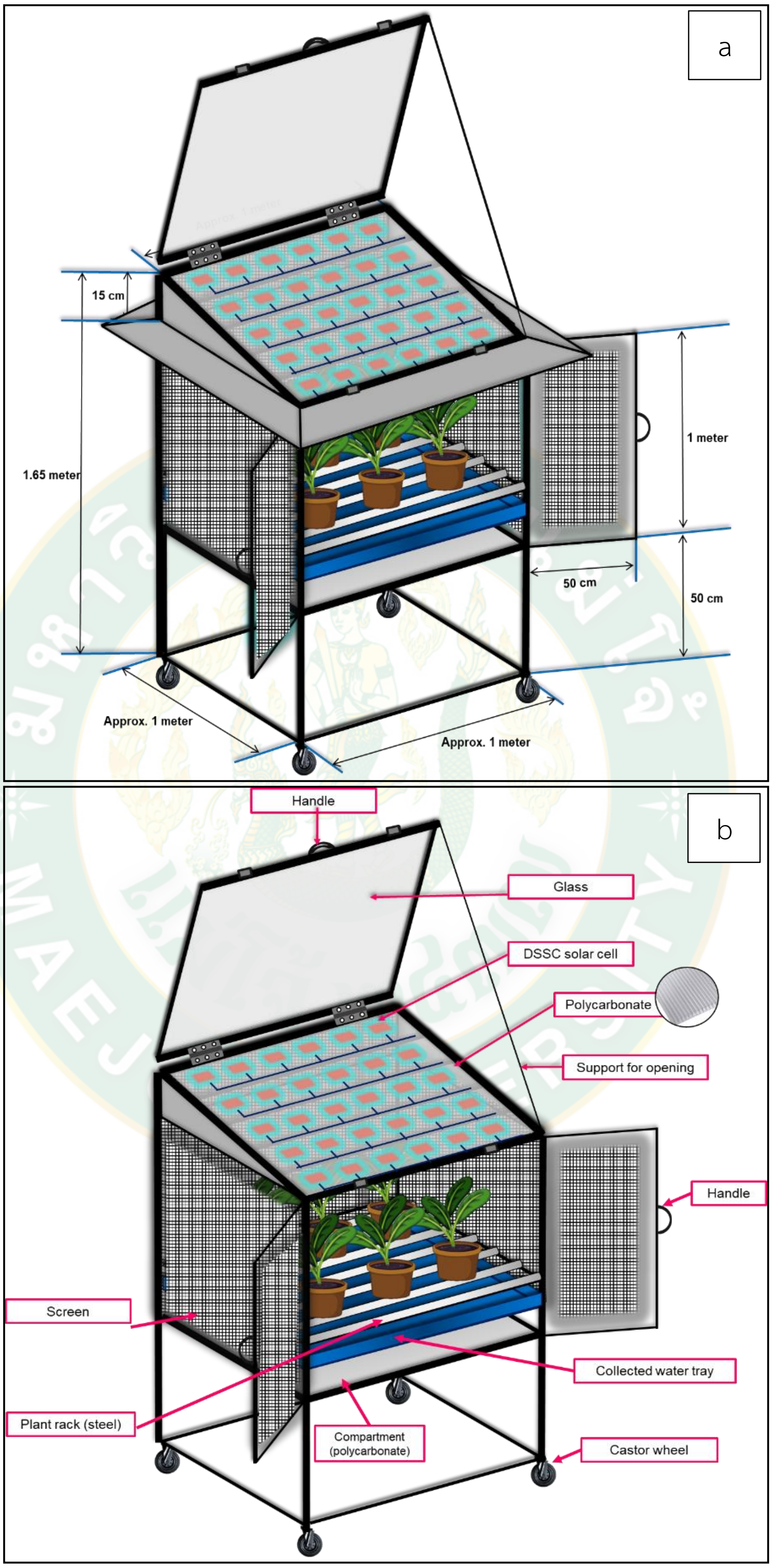

Figure 37 Experimental DSSC roofed greenhouse: Dimension (a), and materials (b)

CHAPTER 4
RESULTS AND DISCUSSION

4.1 Analysis of *Strobilanthes cusia* dye

4.1.1 Evaluation of chlorophyll pigment content of *Strobilanthes cusia*

In this research, methanol was used to extract the chlorophyll lpigment from *Strobilanthes cusia*. Methanol is an excellent chlorophyll extractant, particularly for algae and recalcitrantbvascular plants (Ritchie 2006). During the experiment, three replicates of the SC dye were prepared to ensure reliable data. Chlorophyll is a type of cyclic tetrapyrrole, similar to porphyrin and phthalocyanines. Calogero et al. (2014) mentioned that Caventou and Pelletier discovered chlorophyll as a chlorin ring with a magnesium ion at its center. These green pigments contain reduced pyrrole rings and a phytol group. Among the chlorophyll chemical structures, chlorophyll a ($C_{55}H_{72}O_5N_4Mg$, blue-green) and chlorophyll b ($C_{55}H_{70}O_6N_4Mg$, yellow-green) are distinguished as common chlorophyll pigments (Calogero et al. 2014).

The result of the chlorophyll estimation of the natural dye showed that the amount of CPC from SC was primarily composed of Chl-a with 64.5345 ± 0.4226 µg/m followed by Chl-b with 41.4341 ± 0.2636 µg/ml. According to Zielewicz et al. (2020), the typical ratio of Chl-a:Chl-b is 3:1 since Chl-a is the primary pigment of photosynthesis that absorbs light from the sun. At the same time, Chl-b is considered an accessory pigment because it is not needed during photosynthesis. Furthermore, the key structural distinction between chlorophyll a and chlorophyll b is the composition of a single side chain of the cyclic tetrapyrrole, which in Chl-a is a $-CH_3$ and in Chl-b is a –CHO. Chlorophylls have a highly stable polycyclic network of alternating single- and doublebond- (polyenes) conjugated structure that allows the orbitals to delocalize, making them suitable for photosensitizers (Kay et al. 1994; Calogero et al. 2014).

4.1.2 Surface morphologic analysis of TiO_2 film and SC dye/TiO_2 composite film

The assessment of the surface morphology of a dyesensitized solar cell is part of the study of its properties. According to Khammee et al. (2020a, b, 2021), the hydroxyl groups on nanostructured TiO_2 allow for natural dyes' chemical adsorption. For establishing the chemical bonding of the carbonyl and hydroxyl groups, it is essential to analyze the morphological surface of TiO_2/FTO film TiO_2/FTO film's morphological surface after dye loading of *Strobilanthes cusia* extract (SC dye/TiO_2/FTO composite film). The morphology of the TiO_2/FTO film and SC dye/TiO_2/FTO composite film was evaluated using a scanning electron microscope (SEM). Moreover, figure 38a1 displays the assessment of the morphology of a TiO_2 film. Herewith, the substrate was assayed at a total magnification of 1000 ×. A heterogeneous nanoparticle made of mesoporous TiO_2 and a porous surface was shown. The highlighted factor of TiO_2 film is its porous configuration, which secures the adsorbing dye molecules and the diffusion path of electrolyte in the DSSCs (Wei et al. 2011).

Moreover, the pores could increase the contact area between dye molecules and the electrolyte contributing to the oxidized dye reduced immediately by I_3^- in the electrolyte. The DSSC is a rather complicated system that includes light absorption, charge injection, charge collection, and electrolyte diffusion (Ni et al. 2008). In addition, figure 38b1 shows the SEM picture of SC dye/TiO_2/FTO composite film at a magnification of 1000×. The composite film's surface was observed to be less porous, indicating dye molecules penetrating between the gap/pores in the TiO_2 substrate.

For further assessment, the SEM samples (TiO_2/FTO film and SC dye/TiO_2/FTO composite film) were examined for energy-dispersive X-ray spectroscopy (EDX), an elemental technique to distinguish the chemical elements present in the composite. Figure 38a2 displays that the elemental composition of TiO_2 film consists solely of titanium and oxygen, supported by the results shown in table 4, where the film consists of 20.99 atomic% titanium (Ti) and 79.01 atomic% oxygen (O). TiO_2 usually exhibits a characteristic spectrum of fundamental Ti–O bond absorption in the UV region between 320 and 400 nm, with a characteristic peak of about 350 nm (band edge) for TiO_2. These rely on the production of highly reactive free radicals like the hydroxyl radical, which aid in the degradation of organic pollutants. These hydroxyl radicals can be made using several methods, including photocatalysis with semiconductors and light (Pawar et al. 2019; Khammee et al. 2020a, b, 2021). In comparison, figure 38b2 and table 4 display the presence of carbon in SC dye/TiO_2/FTO composite film. Thus, this shows the sensitization of the dye molecules on the TiO_2 film. It is known that generally, plant composition consists of 45% C and 45% O; as mentioned by Calogero et al. (2014). Chlorophyll chemical structures contain chlorophyll a (*Chl-a*) ($C_{55}H_{72}O_5N_4Mg$) and chlorophyll b (*Chl-b*) ($C_{55}H_{70}O_6N_4Mg$,), alternating conjugated structures of the C=O (carbonyl) and C–O. Chlorophylls have strong absorption bands in the blue and red regions of the visible spectrum (λmax, ≈ 430 and 665 nm in Chl-a, and 425 and 655 nm in Chl-b). Hence, it is a feasible compound for photosensitizer application in the dye-sensitized solar cell.

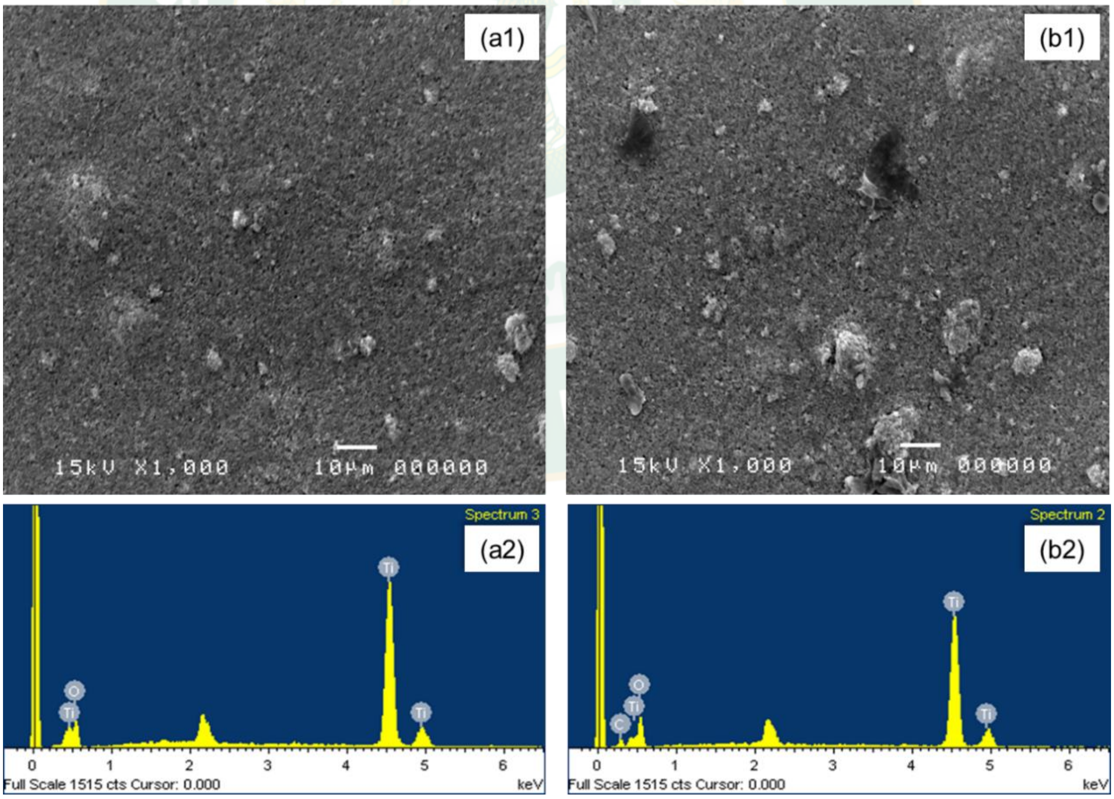

Figure 38 SEM and EDX image of TiO_2 film (a1 and a2), and TiO_2 film loaded with *Strobilanthes cusia* dye (b1 and b2).

Table 4 EDX weight ratio of TiO_2 film and TiO_2 photoanode loaded with *Strobilanthes cusia* dye.

Photoanode	Titanium (Ti)		Oxygen (O)		Carbon (C)	
	Weight (%)	Atomic (%)	Weight (%)	Atomic (%)	Weight (%)	Atomic (%)
TiO_2 film	44.30	20.99	55.70	79.01	-	-
TiO_2 loaded with SC dye	33.25	13.50	53.49	65.03	13.26	21.47

4.1.3 Characterization and performance analysis of fabricated DSSC

The chemical reactions operating the chlorophyll-based DSSC begin during the light exposure of the cell. The photons from the light hit the dye molecules and make them electronically excited. The excited dye molecules then injected electrons into the TiO_2 layer. Moreover, within the electrolyte, the mediator (I^-/I_3^-) undergoes oxidation at the dye and regeneration at the catalyst-coated counter electrode as current flows through the electrical load (Smestad et al. 1998).

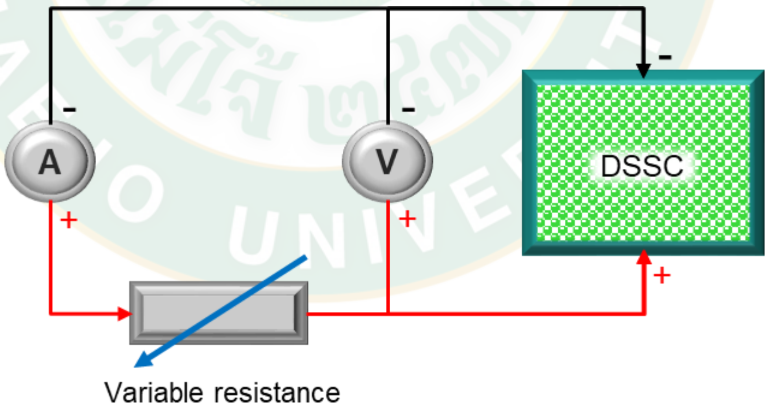

Figure 39 Schematic circuit diagram of the experimental setup used for measuring the current–voltage characteristics of DSSC with voltmeter (V), ammeter (A), and potentiometer variable resistance (10k Ω).

Kumara et al. (2017) reported that the performances of DSSC are evaluated using the current–voltage (*I–V*) characteristic curve and the power density–voltage curve (*Pρ–V*). In this study, the photovoltaic performance of the fabricated DSSCs was carried out under irradiation of white LED light at 13,000 lx (0.001903367 W/cm^2) in the ambient atmosphere using an experimental setup. Moreover, the schematic circuit diagram for measuring the photovoltaic parameters is shown in figure 39, and the circuit is composed of a voltmeter (*V*) for measuring the voltage, ammeter (*A*) for current, and potentiometer variable resistance (10 k Ω). According to Dinesh et al. (2019), an important factor on the *I*–*V* curve is the point at which maximum power (*P*MAX) is supplied (also referred to as the 'knee of the curve'), the short circuit current (I_{sc}) when V = 0; the knee point is (I_{max}, V_{max}) which is the point of maximum power, and V_{OC} the opencircuit voltage, when I = 0.

Figure 40 displays the *I*–*V* and power density–voltage curve recorded from this experiment wherein SC dye based DSSCs were examined under three different counter electrodes: FTO CE, graphite/FTO CE, and pt/FTO CE, respectively. Figure 40a shows the point at which the FTO CE obtained its maximum power of 0.0000128 mW/cm^2, V_{oc} = 0.19262 V, I_{sc} = 0.00294 mA, and ff = 0.203. Moreover, Fig. 40b displays the higher photoelectric output of graphite/FTO CE having V_{oc}=0.30635 V, I_{sc} = 0.01555 mA, ff = 0.462, and P_{max} = 0.000734 mW/cm^2. And the pt/FTO CE (Fig. 40c) obtained V_{oc} = 0.28339 V, I_{sc} = 0.00943 mA, ff = 0.252, and P_{max} = 0.000225 mW/cm^2.

The data parameters from the *I*–*V* and power density–voltage were then used to quantify the performance of the assembled DSSC. The efficiency was calculated by using the following equation (Dawoud 2016):

$$\eta = \frac{P_{max}}{P_{in}} = \frac{J_{sc} \times V_{oc} \times FF}{P_{in}} \tag{4.1}$$

where P_{max} is the maximum power output of the solar cell, P_{in} is the solar irradiation of the light source, J_{sc} = short circuit density, and FF = fill factor.

One of the most critical components in DSSCs is the counter electrode (CE). The CE's primary function is to either (a) catalyze by reducing redox species, which are charge mediators for regenerating the sensitizer (dye) after electron insertion into TiO_2 semiconductor film (Thomas et al. 2014). Thus, the DSSC without counter electrode material limits the cycle of the electron flow within the device. This corresponds to the efficiency output of 0.00067% of not employing counter electrode material (FTO glass only) to the DSSC. The absence of counter electrode material restricts the movement of the electron, which slows down the recharge of electrolyte mediator (I^-/I_3^-), hence, resulting in low values of short-circuit current (I_{SC}) = 2.94 μA and open-circuit voltage (V_{OC}) = 192.62 mV.

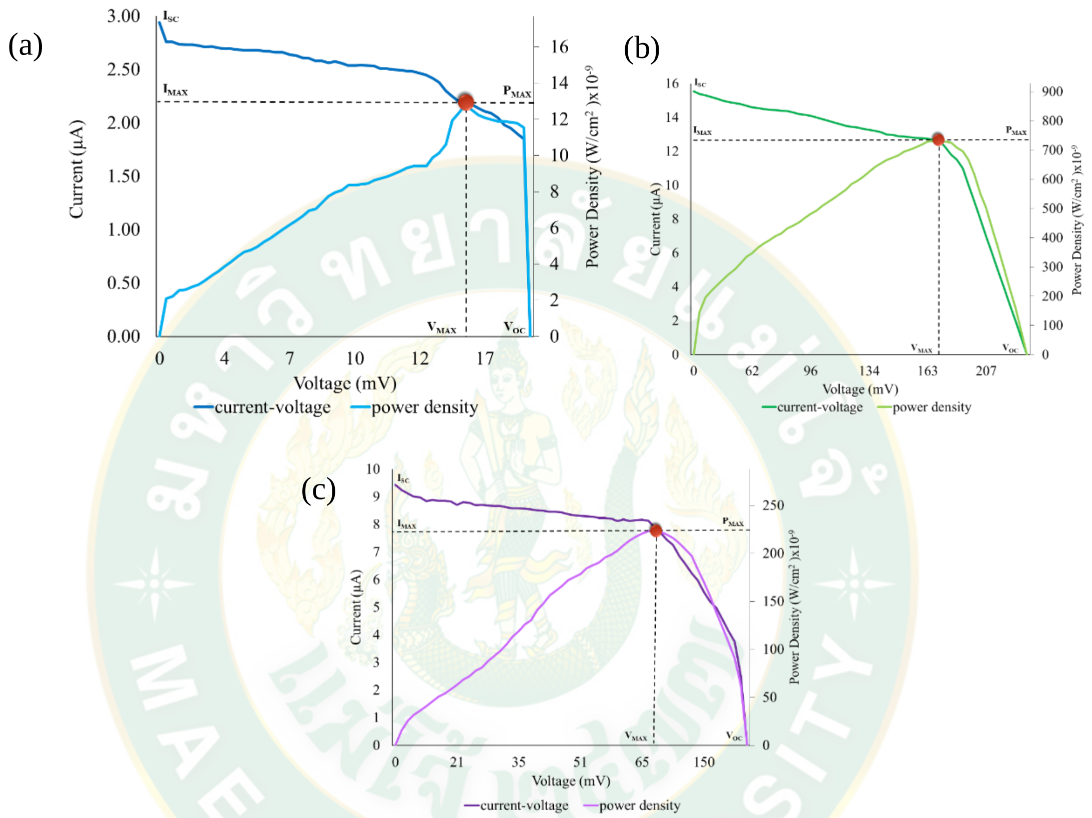

Figure 40 I-V and power density curve of DSSC using different counter electrode: FTO glass (a) graphite/FTO glass (b), and pt/FTO glass (c).

The majority of DSSC research focuses on improving performance by increasing the short-circuit current (I_{SC}), and open-circuit voltage (V_{OC}). As a CE, a Pt coated FTO is usually used. The experiment results show the improvement of the cell's photovoltaic output integrating pt/FTO CE compared to FTO CE, having an efficiency of 0.0118%. The fill factor (FF) of the cell increases as the CE material improves, which is primarily influenced by the cell's series resistance (Rs) related to the tangent line's slope to the *I–V* curve at V_{OC}. The Warburg impedance concerning the Nernst diffusion of the I_3^- species in the electrolyte is used to calculate the series resistance (Zn), which is the electrical hindrance of charge-transfer at the CE and the regeneration of dye and electrolyte, resistance at the fluorine-doped tin oxide glass, and charge-transfer resistance at the CE, and the electrolyte interface (Thomas et al. 2014). Platinum deposited on transparent conducting oxide, with a thickness of 0.2–2 micron, acts as a catalyst (O'Regan and Grätzel 1991) to improve the flow of electrons from dye molecules to the electrolyte(regeneration of dye molecules and electrolyte). These CE films have excellent electrical conductivity, catalytic behavior against I_3^-, and reflectivity. However, pt is expensive due to its small global reserves. Additionally, according to (Koo et al. 2006), when in contact with the I_3^-/I^- liquid electrolyte, pt continues to degrade over time, decreasing the efficiency of DSSC.

Considering the cost of platinum, a low-cost dye-sensitized solar cell, the use of an alternative, a cheap and plentiful material found in the Earth's crust as the counter electrode, which can replace Pt in DSSC, is being investigated. The graphite counter electrode is a cheaper alternative to platinum, which is commonly used in these cells. The use of a graphite pencil as a source of graphite for graphite/FTO CE was tested. Among the three conditions evaluated (FTO CE, graphite/FTO CE, and pt/FTO CE), graphite exemplifies significant DSSC performance, in which the efficiency obtained was 0.0385%. The difference in graphite counter electrodes' performance is primarily due to the high degree of mechanical stability (Wang and Hu, 2012) and wide surface area (Marques et al. 2020; Smestad and Gratzel 1998). Table 5 shows some of the available photovoltaic performances of chlorophyll dye-based dye sensitized solar cells. It can be concluded that the results from this scientific research are within the range of the developed DSSC. The performance evaluation of the different counter electrode materials' effect and utilizing *Strobilanthes cusia* dye extract suggests many more opportunities and pathways to improve the third generation solar cell's performance and cost DSSC belongs.

Table 5 Photovoltaic Performance of chlorophyll based DSSC

Dye	Counter electrodes	Jsc (mA/cm^2)	Voc (V)	ff	η (%)	Ref
Ocimum Gratissimum	Pt	0.044	0.466	0.400	0.021	(Eli et al. 2016)
Green spinach leaves	Pt	0.052	0.590	0.530	0.016	(Hasoon et al. 2015)
Morula leaves	C	0.059	0.472	0.050	0.001	(Maabong et al. 2015)
Lemon leaves	C	1.080	0.592	0.100	0.036	(Maabong et al. 2015)
Black tea leaves	Pt	0.390	0.550	0.400	0.080	(Abdel-Latif et al. 2015)
Green algae (fresh)	Pt	0.134	0.416	0.210	0.010	(Taya et al. 2013)
Green algae (dried)	Pt	0.397	0.559	0.440	0.100	(Taya et al. 2013)
Strobilanthes cusia	FTO glass	0.0003267	0.193	0.203	0.00067	This study
Strobilanthes cusia	Graphite	0.0051833	0.306	0.462	0.0385	This study
Strobilanthes cusia	Pt	0.0031438	0.283394	0.252	0.0118	This study

4.2 Analysis of Malabar Spinach

4.2.1. Anthocyanin Pigment Evaluation

The experiment was conducted in order to determine the Anthocyanin Pigment Content (APC) of the sample. The evaluation of the APC undergoes a series of processes, trial and errors in order to achieve accurate and reliable data. Taken into account that the dyes are sensitive to the light, therefore, it was examined in a little lightroom and kept in a covered bottle to avoid exposure to the light.

For the absorbance, an aliquot of the dye extract was diluted by two different buffers at different dilution factors and was examined by spectrophotometer. Figure 41 shows the color changes that occurred during the process. Thus, it was observed that the color of the extract varies at different pH values. Before the addition of buffers, the initial pH of the sample (for: pure methanol, 50% methanol, 50% methanol & 1% HCl) is: 7.1, 6.82 & 1.45 respectively. When the pH of the dye extract is high, the color is purple, while at low pH its color is red. Furthermore, when acid is added in the extraction process, the color of the resulting dye is darker, as shown in figure 41 (3a) and (3b).

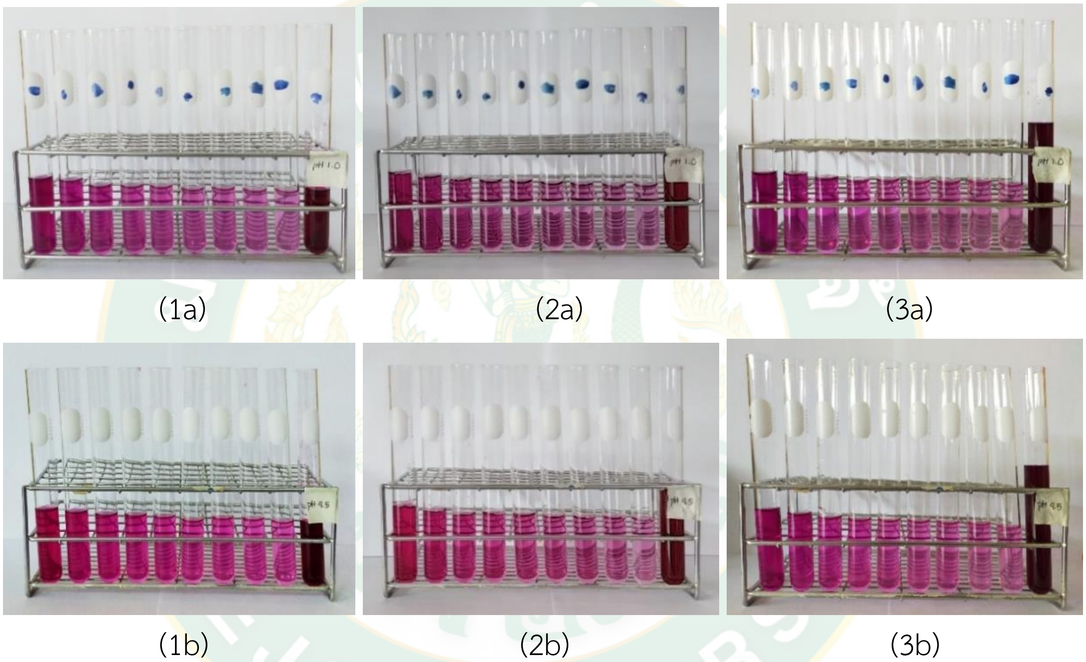

Figure 41 Extracted dye using pure methanol solvent diluted with: (1a) buffer pH 1.0 & (1b) buffer pH 4.5; Extracted dye using 50% methanol solvent diluted with (2a) buffer pH 1.0 & (2b) buffer pH 4.5; Extracted dye using 50% methanol & 1% HCl solvent diluted with (3a) buffer pH 1.0 & (3b) buffer pH 4.5.

The samples were examined at different wavelengths: 510nm, 520nm, 530nm, 540nm, 550nm, & 700nm. Figure 42 (a) & (b) shows that the highest peak of the three processes is at the wavelength of 540 nm. The extraction process using pure methanol solvent gained the highest absorbance for both pH 1 and pH 4.5 buffer having 0.326 & 0.641 respectively.

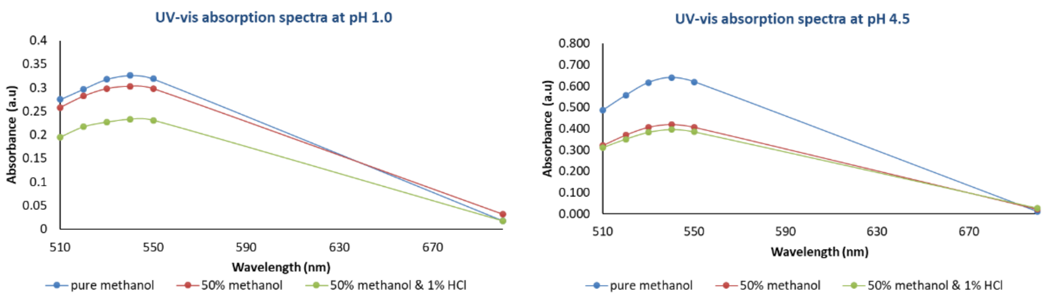

(a) (b)

Figure 42 The absorption spectra at three different solvent: 1.) pure methanol, 2.) 50% methanol, and 3.) 50% methanol & 1% HCl; and diluted at: (a) 0.4M Acetic acid-sodium acetate buffer pH 1.0, (b) 0.1M HCl acid-KCl buffer pH 4.5).

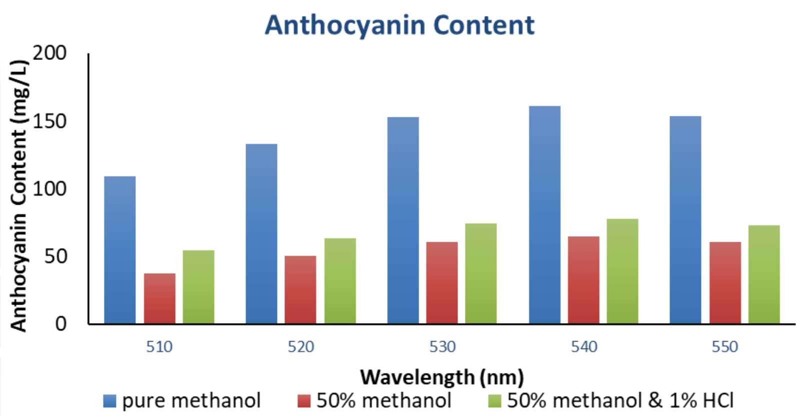

Figure 43 Anthocyanin pigment content of the dye extracted from Malabar spinach fruits.

All three processes gained their highest APC at the wavelength of 540 nm. However, as figure 43 revealed, the highest anthocyanin content extracted was obtained from the extraction process using pure methanol as the solvent having 160.81 mg/L. Hence, followed by 50% methanol & 1% HCl with 64.62 mg/L and lastly, by 50% methanol with 77.65 mg/L. Nevertheless, it can be concluded that using pure methanol to extract APC is more effective and efficient. In comparison, of the result with different plant sources of anthocyanin (table 6); the data gathered from this study is among the highest of APC, which is a good indication that the dye from the fruit of Malabar spinach has a potential to be used as a photosensitizer for dye-sensitized solar cell.

Table 6 Some common fruits and vegetables with their anthocyanin content (Giusti and Wrolstad, 2001; Shamina, 2007).

Plant source		Anthocyanin content	Reference
Prunus avium		150	(Giusti and Wrolstad, 2001)
Aronia melanocarpa		160	(Giusti and Wrolstad, 2001)
Rubus spp.		160	(Giusti and Wrolstad, 2001)
Oryza sativa		200	(Giusti and Wrolstad, 2001)
Red onion		7-21	(Mazza and Miniati, 1993)
Plum		2–25	(Timberlake and Henry, 1988)

Red radishes	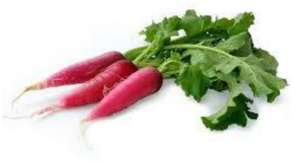	11–60	Giusti et al., 1998
Red Raspberries		20-60	(Mazza and Miniati, 1993)
Strawberries		15–35	(Timberlake and Henry, 1988)
Tradescantia pallida		120	(Shi et al., 1992)
Hibiscus rosa-sinensis		4.63	(Ahmadian, 2011)
Melastomamala bathricum		8.43	(Ahmadian, 2011)
Codiaeumvarieg atum		2.22	(Ahmadian, 2011)
Malabar spinach fruits		160.81	This study

4.2.1.1 Comparison with red cabbage

The color stability of dyes is dependent to the effect of light that passes through it. Characterization of the effect of light is mainly focused by the research regarding the natural dye evaluation. Depending on the state of DSSC, dyes extracted from plants can increase the efficiency in the presence of light.

Figure 44a shows the UV-vis analysis of the three different dye (a. Malabar spinach dye, b. 50% MS + 50% RC, c. Red cabbage), it was found that both red cabbage dye and 50% MS + 50% RC have their highest peak at 520 nm having 0.538 a.u and 0.377 a.u respectively. While the malabar spinach has 0.319 a.u at 540 nm. Figure 44a shows the UV-vis analysis of the three different dye (a. Malabar spinach dye, b. 50% MS + 50% RC, c. Red cabbage), it was found that both red cabbage dye and 50% MS + 50% RC have their highest peak at 520 nm having 0.538 a.u and 0.377 a.u respectively. While the malabar spinach has 0.319 a.u at 540 nm.

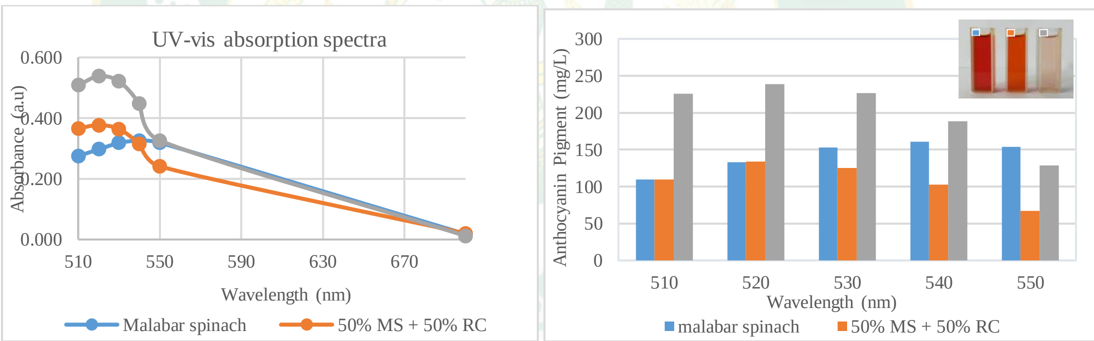

(a) (b)

Figure 44 a.) UV-vis absorption spectra and b.) Anthocyanin content

4.2.1.2 Application of Malabar spinach and red cabbage dye

Anthocyanins are water-soluble pigments. Its appearance is greatly dependent to its pH value. This characteristic of anthocyanin, enables to act as a natural pH indicator. As shown in figure 45b & 45c, there is a significant color change for red cabbage dye and 50% MS + 50% RC sensitized to TiO_2 thin film. The contrast within the appearance of malabar spinach (red to orange), 50% (MS) + 50% (RC) (purple color) , and red cabbage (blue color) is due to the presence of different sort of chemical structure of the pigments and pH. The anthocyanin gathered from red cabbage are delphinidin and cyaniding complexes (Gokilamani et al., 2013). Thus, with this result, it can be concluded that fabrication of multicolored DSSC is feasible.

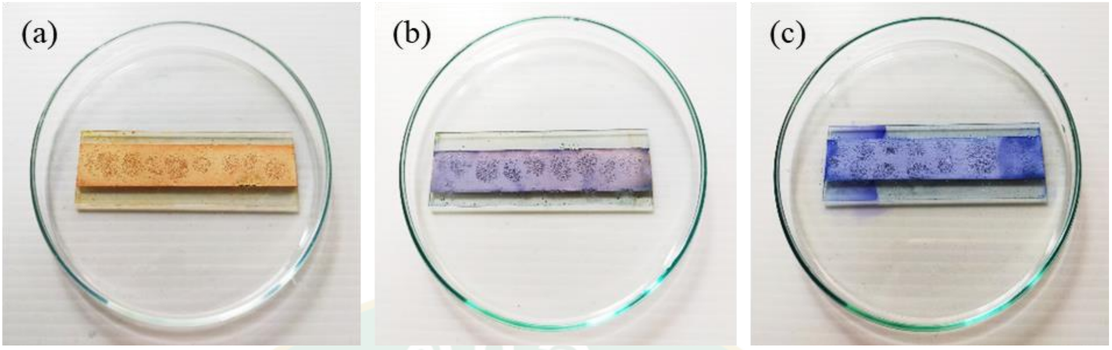

Figure 45 TiO_2 immersed to dye: a.) Malabar spinach, b.) 50% MS with 50% RC and c.) Red cabbage.

Thus, the calculated efficiency showed that dye-sensitized solar cells integrated with red cabbage photosensitizer gained higher efficiency with 0.16654% ± 0.00955, while the malabar based DSSC has an efficiency output of 0.00231% ± 0.00079. A significant difference between the two natural photosensitizers was observed. Hence, red cabbage exhibited higher potential than malabar spinach. Moreover, it can be concluded that the anthocyanin pigment content of the two dye influenced the photons absorbance of the cell, as well as, its energy conversion. Table 7 shows the list of some natural dye-based DSSC. The results of red cabbage show a feasible potential as a photosensitizer. Also, graphite was used as the counter electrode, which is considerably cheaper than platinum; nevertheless, the photoelectric output it exhibited is efficient.

Table 7 Photoelectric performance of DSSC with natural dye from various plants

Natural dye	Jsc (mA/cm^2)	Voc (V)	ff	n (%)	**Ref**
Black rice	-	0.580	0.272	0.0198	(Ahliha, 2017)
Potato	-	0.51	0.53	0.01	(Chandra et al., 2019)
Mulberry		0.55	0.51	0.05	
Turmeric	0.288	0.529	0.48	0.03	
Tomato	0.51	0.14	0.37	0.03	(Supriyanto et al., 2018)
Bloodleaf	-	0.267	0.46	0.04	(Moustafa et al., 2012)
Orange fruit	0.37	0.06	0.58	0.02	
Carrot	0.36	0.04	0.64	0.009	
Bahraini henna	0.368	0.426	24.6	0.128	(Jasim, 2012)
Gree algae	-	0.32	0.37	0.01	(Shalini et al., 2015)
Walnuts	0.73	0.304	0.39	0.0104	(El-Agez et al., 2012)
Malabar spinach	0.001359	0.171426	0.18856	0.00231 ± 0.00079	This study
Red cabbage	0.016349	0.470374	0.41221	0.16654 ± 0.00955	This study

4.2.2. Impacts of pH on anthocyanin pigments for the photovoltaic properties of malabar spinach based dye-sensitized solar cells

Based on table 8, it shows that the higher pH caused efficiency increases, but not in neutral and alkaline conditions. The highest efficiency was obtained when the dye solution of Malabar spinach fruits was adjusted to pH 9, which was equal to 0.1021%. While the lowest efficiency was obtained at pH 1, which is 0.0454%. This is because the dye has deprotonated (loss of H+) from the cation form of flavilium at pH 6. When the pH rises, the flavilium cation gradually changes to the quinonoidal base by losing the proton. At very low pH, electrons are more difficult to deprotonate, so that anthocyanins become very stable and difficult to bind to other molecules. This causes the anthocyanin bond with TiO_2 to become weak. In addition, the charge contained in the flavillium cation can inhibit the movement of electrons on the TiO_2 surface (Chien et al., 2013). The binding of the anthocyanin bonds in an acidic and alkaline state to TiO_2 is shown in figure 46.

Table 8 DSSC parameters with pH variations in dye solutions from Malabar Spinach.

Sample	Isc (mA)	Voc (V)	Jsc (mA/cm^2)	PDm (mW/cm^2)	ff	n (%)
pH = 1	0.0421	0.6936	0.0140	0.0016	0.16346	0.0454
pH = 2	0.0638	0.6121	0.0213	0.0029	0.22523	0.0837
pH = 3	0.0545	0.5245	0.0182	0.0025	0.26089	0.0710
pH = 4	0.0503	0.2356	0.0168	0.0019	0.48121	0.0542
pH = 5	0.0511	0.5580	0.0170	0.0023	0.24548	0.0666
pH = 6	0.0261	0.6123	0.0087	0.0016	0.29960	0.0455
pH = 7	0.0454	0.6185	0.0151	0.0029	0.30702	0.0820
pH = 9	0.0682	0.4877	0.0227	0.0036	0.32252	0.1021
pH = 11	0.0816	0.4316	0.0272	0.0024	0.20174	0.0676

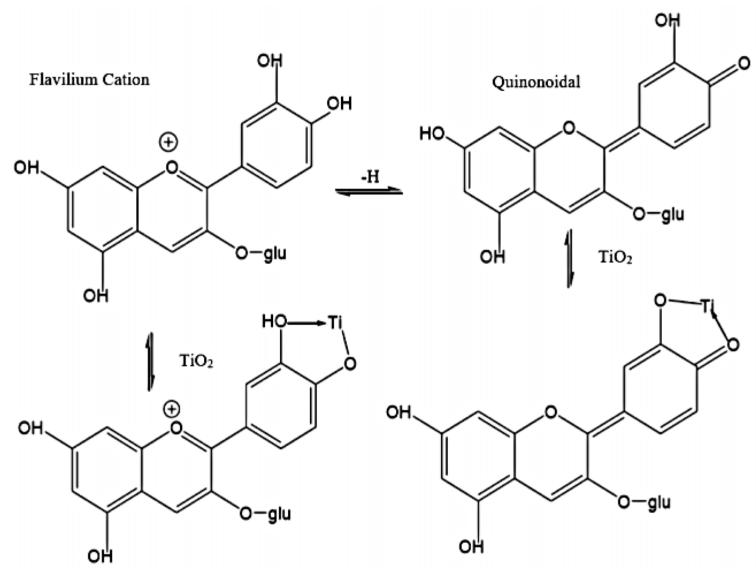

Figure 46 Binding of TiO_2 to anthocyanin in acid (flavilium) and base (quinonoidal) conditions (Cherepy et al., 2013).

In order to assess and distinguish the photovoltaic performance effect of pH variations of the Malabar spinach fruit extract, the unmodified dye, which is pH 6 (original pH of the dye) was set as the standard. As observed in the power density to voltage curve of DSSC in acidic conditions (figure 47-a), the power produced gradually increases as the pH decreases. As shown in the graph, in acidic conditions, Malabar spinach dye produced a higher power of 0.0029 mW/cm^2 at pH 2. However, after it reached its peak pH (pH 2), the power drastically decreased. Whereas, at pH 1, it only produced 0.0016 mW/cm^2. As a result, if the dye is set in an acidic environment, it will damage the TiO_2 particles. According to Faquih et al. (2020), electron diffusion coefficients are often higher in acidic rather than in neutral environments, resulting in a higher electron injection rate. The Fermi level of TiO_2 and the electrolyte redox potential decline when H+ ions interact with LUMO and the TiO_2 conduction band. The electron injection process is accelerated as the amount of H+ ions is increased, resulting in a higher electric current. However, under highly acidic conditions, the dye tends to degrade and denature the TiO_2 particles.Thus, trapping the excited electrons from the dye inhibits them from reaching the TiO_2 conduction band. As a result, electron diffusion rate efficiency is low (Faqih et al., 2020). Furthermore, the Malabar spinach dye performed better in alkaline conditions (figure 47-b), specifically at pH 9. In this condition, the fabricated DSSC was able to produce a power density of 0.0036 mW/cm^2, the highest among the examined DSSCs. The result of this experiment suggests that in alkaline conditions, the Malabar spinach dye was optimized, enhancing its absorbing capacity. Thus, this is due to the different anthocyanin molecules present in the natural dye of the sample. Similarly to acidic conditions, the power produced decreases after the dye reaches its peak alkaline condition (pH 9).Hence, as the pH rises, more protons are taken from the flavylium ion, causing the ring to expand slowly, culminating in the formation of chalcone, a yellow anthocyanin. The yellow color fades as the pH rises, resulting in a lower anthocyanin content evident in the absorption spectra (Prabavathy et al., 2017).

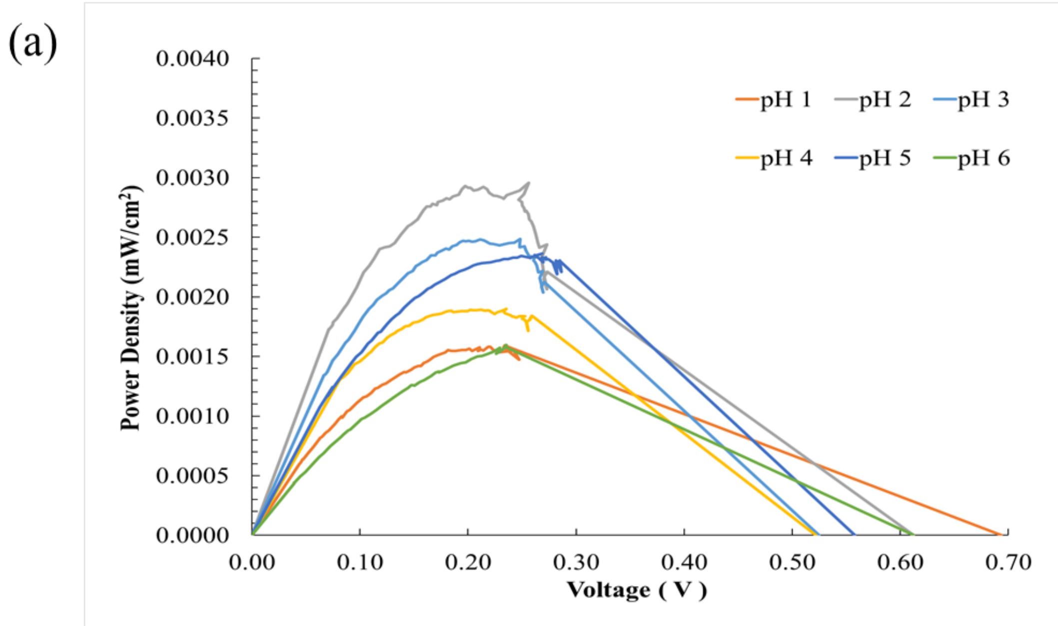

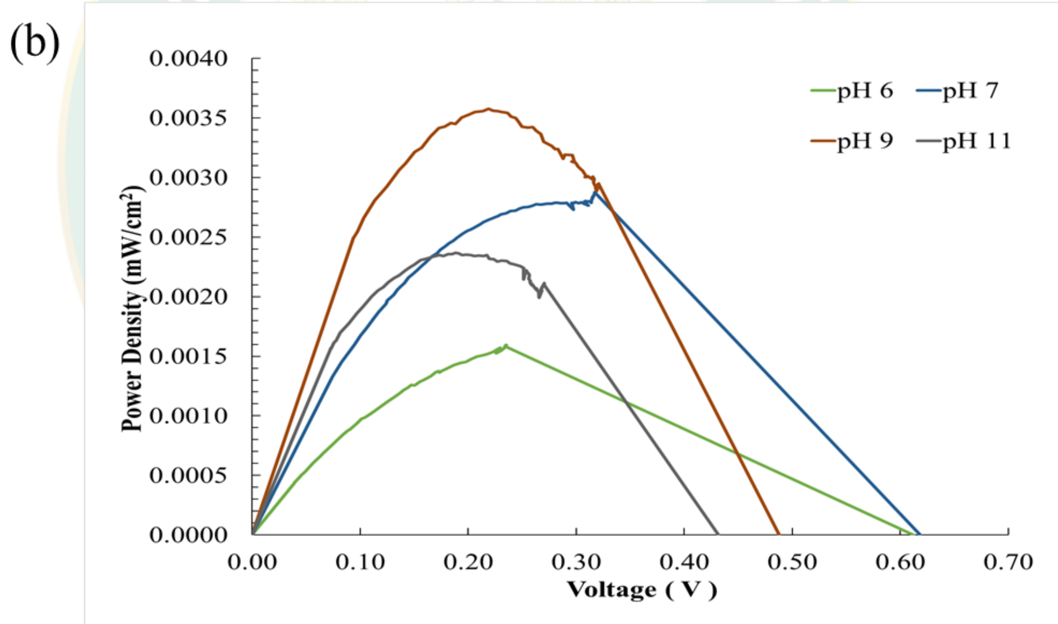

Figure 47 Power density to Voltage curve at (a) acidic conditions, and (b) alkaline conditions.

4.2.2.1 Effect of pH variations to malabar spinach dye extract

The PH value of anthocyanin pigments has the potential to affect their stability and color. The color change caused by changing chemical forms is the most noticeable anthocyanin phenomenon in a pH gradient. Changes in pH cause structural transformations of anthocyanins, which have a significant impact on color.

The pH of anthocyanins is a key component in determining their stability. The color of the malabar spinach anthocyanin is influenced by the pH of the solution. Figure 48 depicts the color scheme of MS extract under various pH conditions (pH 1, pH 2, pH 3, pH 4, pH 5, pH 6, pH 7, pH 9, pH 11, and pH 11.33). The pH of the solution affects the appearance of the anthocyanin in the MS extract, which ranges from magenta to red in acidic to neutral conditions and from purple to yellow in basic conditions. As the pH 1-12 rises, the color of the anthocyanin extract shifts from red to purple to blue to green to yellow. Moreover, for malabar spinach fruit extract at strong acid pH 1, it appears to be magenta then slowly to red as the pH (optimum of pH 7) increases pH turns to purple, and at strong base is yellow. Furthermore, as the pH is raised to 11, more protons are drawn from the flavylium ion, resulting in a delayed opening of the ring, resulting in the production of chalcone, a yellow type of anthocyanin. As the pH rises, the yellow color diminishes, resulting in a reduced anthocyanin concentration, which is visible in the absorption spectra. It may be deduced from the pH research that anthocyanins are particularly persistent in acidic solutions, resulting in maximum anthocyanin content (Prabavathy et al., 2017).

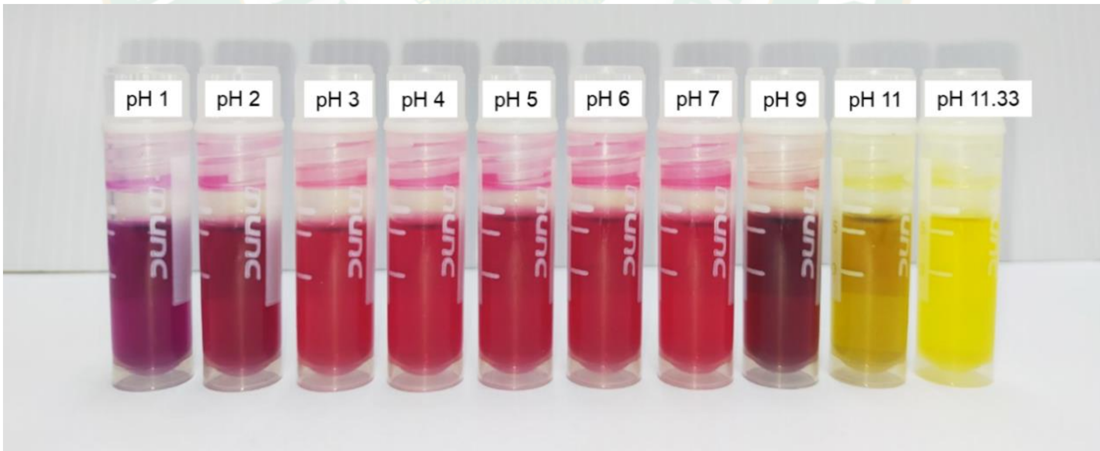

Figure 48 shows the results of dye solution absorbance from malabar spinach fruits with pH variations.

Original malabar spinach dye solution (pH 6) produces the highest absorption peak at 540 nm. The more HCl or NaOH added to the dye solution, the lower the absorption of photons by the dye solution. This is caused by changes in the solvent of the dye solution. The polarity level of pure dye solvents is higher than that of pH-varying dye solvents. This condition causes a decrease in dye absorption intensity as pH changes (hypochromic effect) (Sauer et al., 2011). Besides its effect on concentration, a dye solution with pH variation causes a peak shift in absorption. While the pH increases, the cation flavylium gradually transforms into a quinonoidal base by the loss of protons. The absorption becomes weaker and shifts to 540-550 nm, producing magenta (pH 1.0) or purple (pH 9.0). At neutral pH, blue quinonoidal anions are formed by the loss of other protons, and it's a stronger absorption. The shift within the peak indicates the changes of the anthocyanin pigment present, the molecule structure delocalized due to the effect of the pH variations. Table 9 displays the structural pattern of the common anthocyanidin with its corresponding color appearance.

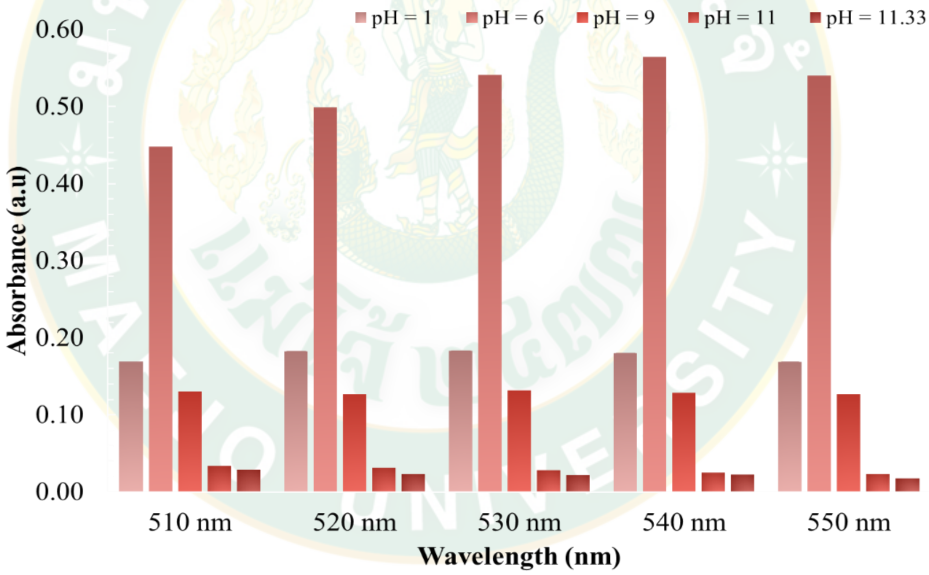

Figure 49 Pigment absorbance of malabar spinach dye.

Table 9 Structural identification of the common anthocyanidins (Giusti et al., 2003).

Classification	Compound pattern		Color	λmax (nm)
	R1	R2		
Cyanidin	OH	H	Orange-red	510
Delphinidin	OH	OH	Blue-red	522
Malvidin	OCH3	OCH3	Blue-red	520
Pelargonidin	H	H	Orange	505
Peonidin	OCH3	H	Orange-red	532
Petunidin	OCH3	OH	Blue-red	546

4.2.2.2 Morphological analysis

SEM characterization is conducted to determine the morphological structure. Figure 50(a1-d1) displays the surface and cross-section figure 50(a2-d2) SEM images of the TiO_2 film and the TiO_2 composite film photoanode under pH variations (pH 1, pH 6 and pH 9). The surface was analyzed with 20000x magnification, in which the samples were observed to have changes in the effect of different pH dye solutions. Figure 50 (a1-a2) displays the TiO_2 film which was assigned as the standard to determine the surface effect of pH variations of the malabar spinach dye. The figure 50-a1 shows that the TiO_2 films were semi-spherical in shape, highly porous morphology and homogenous layer of TiO_2 with large active areas are present, which enables the dye molecules to be easily attached and adsorb, hence improving the short-circuit current density produced. As an outcome, compared to their bulk counterparts, mesoporous electrode materials exhibit improved electrochemical performance (Li et al., 2009). The existence of holes and extensive bonding indicates strongly conducting mesoporous and crystalline TiO_2 layers. The pores in the semiconductor TiO_2 layer can accept the absorbing malabar spinach molecules. Additional dye molecules will be accommodated if more pores are produced in the layer, resulting in a boost in the prototype's solar energy absorption. According to the result of the cross-section shown in figure 50-a2, the approx. thickness of the TiO_2 film is 32.8 μm. In figure 50, degradation of the photosensitizer and TiO_2 was observed. Hence, the acidity of the dye solution causing the anthocyanin pigments to denature. As a result, the active area for redox reaction is inevitably reduced, which affects the current and voltage produced by the DSSC loaded with MS dye at pH 1. In addition, among the examined fabricated DSSCs, pH 1 showed the lowest photovoltaic efficiency of 0.0454%. Moreover, in the cross-section image (figure 50-b2) the average thickness of the TiO_2 composite film under pH 1 was approx. 29.4 µm. Thus, in comparison to the TiO_2 film, the thickness of the film decreases, which suggests that the higher the pH value of the dye, it inhibits the bonding of the molecules and disintegrates the TiO_2 crystalline layer, making it unstable and hollow. Figure 50-c1 displays the TiO_2 composite film loaded with unmodified MS dye (at an original pH of 6). The surface was observed to be homogenous, with spherical nanoparticles of anthocyanin molecules attached to the TiO_2 film. In contrast to the other pH-modified dyes, the molecules of pH 6 are smaller. This is because of the presence of chemical elements such as chlorine (Cl) from HCl in acidic conditions and sodium (Na) from NaOH in alkaline conditions. In the cross-sectional view (figure 50-c2), the thickness was approx. 39.4 µm.

Furthermore, the presence of hollowed points and a thin layer of dye molecules inside the cell results in low electron rate production. Lastly, figure 50-d1 displays the attachment of a thicker clump layer of dye molecules. It was found to be spherical in shape. The cross-section image displayed in figure 50-d2 shows the approximate layer of TiO_2 composite film loaded with pH 9 malabar spinach dye. The thickness was found to be 72.6 µm. Thus, it can be concluded that higher amounts of dye molecules were able to form a bond on the TiO_2 surface. At this condition, the anthocyanin dye molecules were adsorb. As a result, photons from the sun absorb more photons, and the electron injection rate increases. Marcano et al. (2019) reported anthocyanin adsorption on TiO_2, suggesting two possible processes: physisorption (when the pigment's H atoms bond to the oxygen atoms on the TiO_2 surface) or chemisorption (when the anthocyanin's H atoms dissociate, leaving an oxygen atom to bond to Ti atoms on the TiO_2 surface).

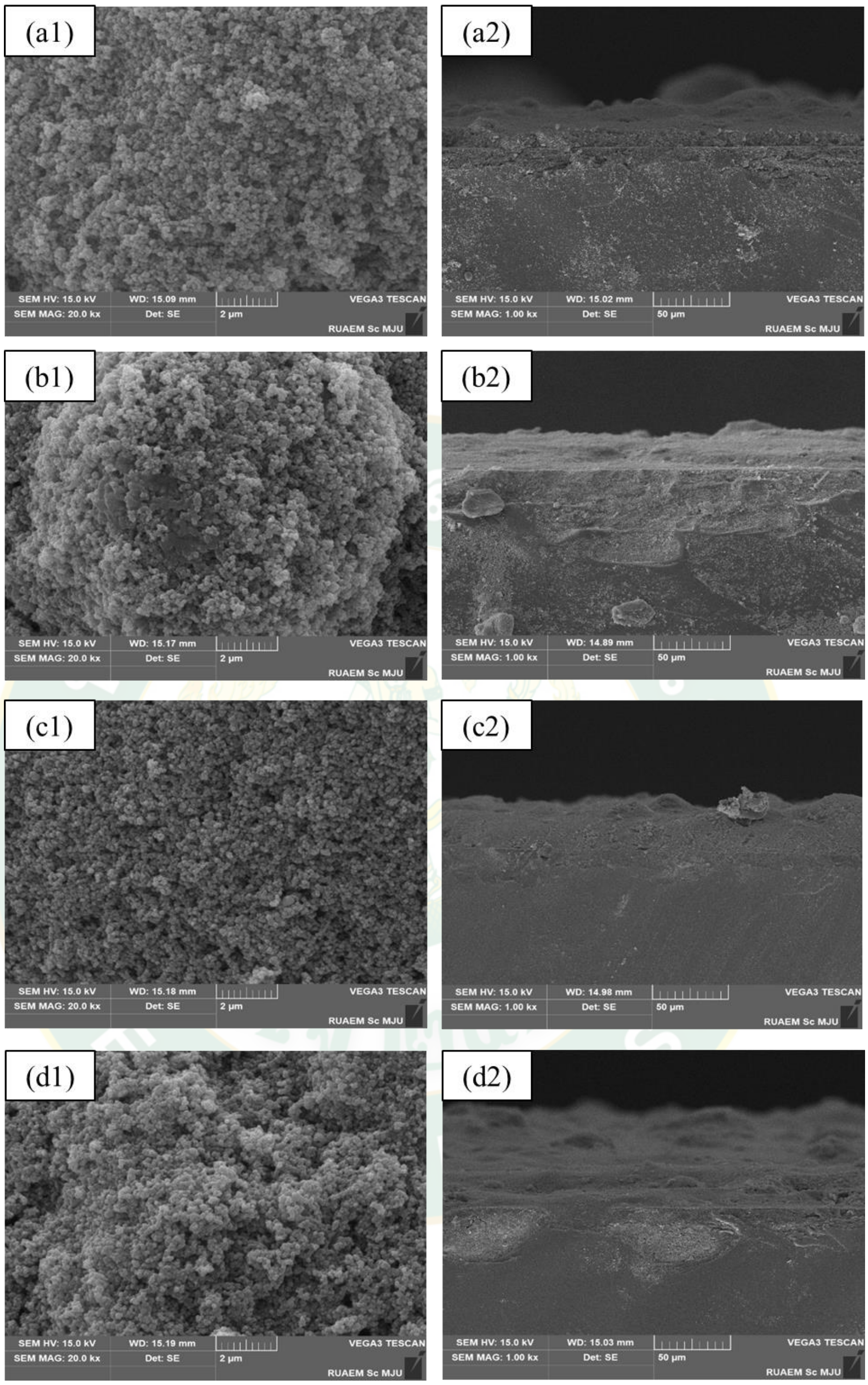

Figure 50 SEM surface and cross-sectional image : TiO_2 film (a1 & a2), TiO_2 composite film with pH 1 dye (b1 & b2), TiO_2 composite film with pH 6 dye, and TiO_2 composite film with pH 9 dye (c1 & c2) (d1 & d2).

The samples were examined using energy dispersive spectroscopy to characterize the chemical elements present. As shown in table 10 and figure 51, the TiO_2 film is mainly composed of 57 (wt%) Ti and 25.5 (wt%) O. The result shows no sign of carbon or any other element. Thus, it is a good indication that the TiO_2 film was not contaminated. For the TiO_2 composite film loaded with dye under pH variations, three conditions were examined : a) pH 1, b) pH 6, and c) pH 9. At pH 1, the elemental weight ratio is composed of 65 (wt%) Ti, 21.3 (wt%) O, 1.65 (wt%) C, and 0.5 (wt%) Cl. Carbon was present due to the presence of the natural dye. The presence of chlorine in pH 1 is because of the HCl used to adjust the acidity of the malabar spinach dye. For pH 6, the elemental weight ratio is composed of 52.2 (wt%) Ti, 26.85 (wt%) O, and 1.75 (wt%) C. As observed, only carbon was added to the elemental composition, because, as previously discussed, the pH of 6 is the original pH of the dye extract. Which means there is no pH adjustment solution added to the dye. Furthermore, for pH 9, it contains 57.6 (wt) Ti, 22.7 (wt O), 2.55 (wt%) C, and 0.5 (wt) Na. The presence of sodium in the pH 9 is from the NaOH used to adjust the solution to alkaline conditions. Among the three conditions, pH 9 has a higher amount of carbon, hence it can be concluded that more dye molecules were adsorbed on the TiO_2 film. The results form EDX, supports the high photovoltaic performance pf the platinum free DSSC. efficiency gained by the DSSC. Since the TiO_2 composite film loaded with pH 9 dye was able to contained more amount of light absorbing anthocyanin molecules, this lead to more capacity of absorbing photons and increasing the electron diffusion of the cell. Hence, resulting to high efficiency of 0.1021%, open circuit voltage of 0.4877 V, short circuit current of 0.0682 mA, and power density of 0.0036 mW/cm^2 .

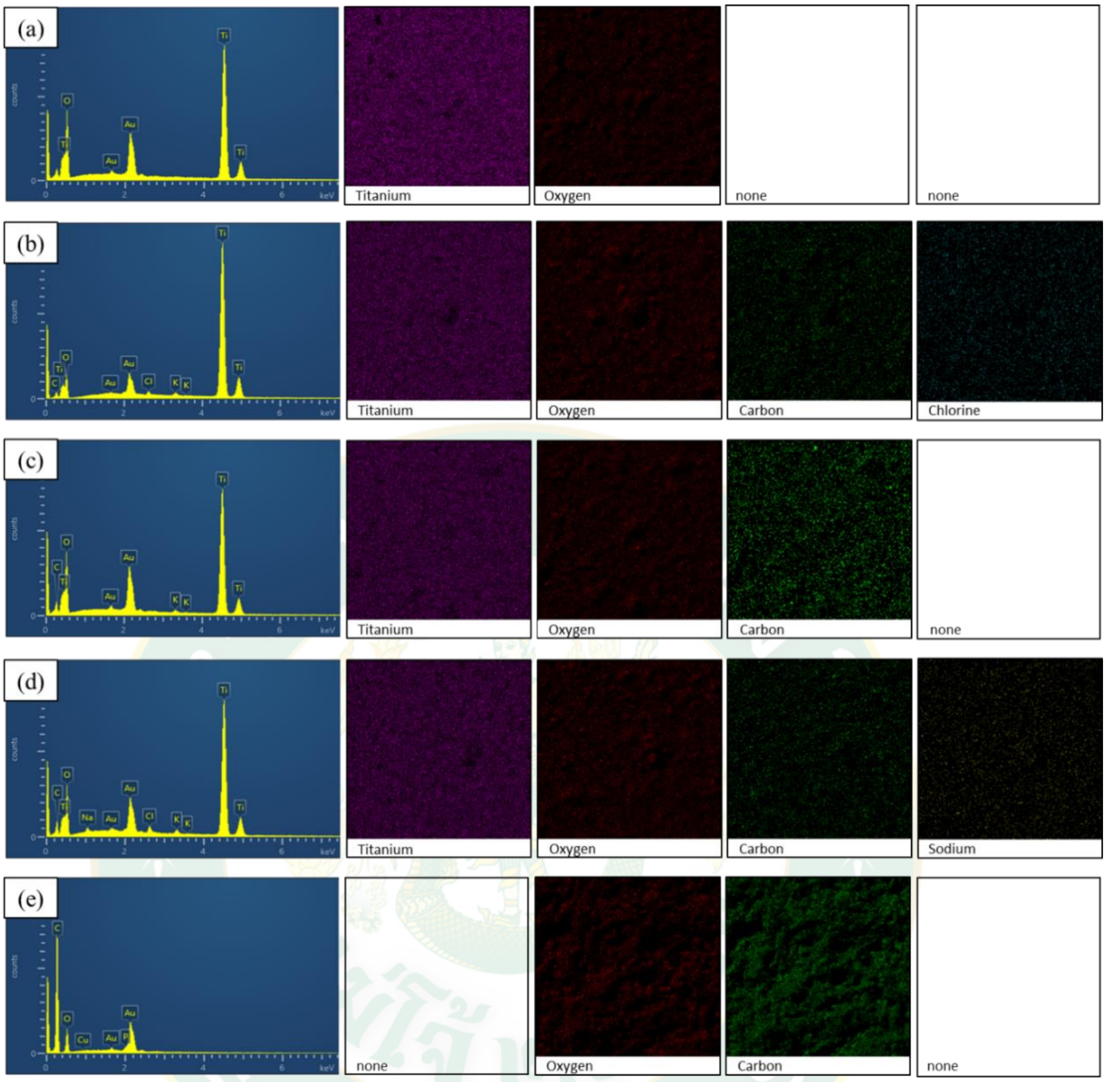

Figure 51 EDX spectrum and mapping of (a) TiO_2 film, (b) TiO_2 film loaded with dye pH 1, (c) TiO_2 film loaded with dye pH 6, (d) TiO_2 film loaded with dye pH 9, and (b) Activated carbon counter-electrode.

Table 10 EDX weight ratio of TiO_2 film, TiO_2 composite film loaded with dye under pH variations (pH 1, pH 6 and pH 9), and counter electrode (activated carbon).

Sample	Titanium (wt%)	Oxygen (wt%)	Carbon (wt%)	Chlorine (wt%)	Sodium (wt%)
TiO_2 film	57.55	25.5	-	-	-
pH 1	65.1	21.3	1.65	0.5	-
pH 6	52.2	26.85	1.75	-	-
pH 9	57.6	22.7	2.55	-	0.5
Activated carbon	-	13.95	60.95	-	-

4.3 Analysis of Longan

The same with *Strobilanthes cusia,* longan is also primarily composed of Chlorophyll pigment. In this study, the absorption qualification of the pigment extraction from longan leaves were examined and an aliquot of the natural dye extract was diluted by methanol and was examined by the UV-Vis spectrophotometer. The absorbance of longan pigment was examined under three wavelength: 470 nm, 645 nm, and 663 nm. The standard absorption wavelength of chlorophyll, the main peak at 662–666 nm and chlorophyll b the shoulder near 650 nm; both were present in the absorption wavelength's red band. In the blue region, the visible absorption wavelength between 430 and 440 nm and 470 and 480 nm is the light absorption by chlorophyll and carotenoids (Lichtenthaler, 1987; Merzlyak et al., 1996; Solovchenko et al., 2001). Moreover, considering the absorption wavelength of carotenoid pigments in the blue region of the spectrum is considerably sophisticated due to an overlapping absorption of chlorophyll appear in most plant tissues (Merzlyak et al., 2003). However, carotenoids' absorption wavelength peak is at 420, 450, and 480 nm (Solovchenko et al., 2001). Consequently, the pigment extraction from longan leaves consist of Chl-a, Chl-b, and carotenoids.

In the evaluation it was found out that longan is consist of 59.35 ± 0.2888 μg/ml chlorophyll a, 14.92 ± 0.2686 μg/ml chlorophyll b, and 10.15 ± 0.3465 μg/ml carotenoids. Furthermore, the results from the photovoltaic evaluation displayed in figure 52, shows that longan based DSSC produced an efficiency of 0.06788%, open circuit voltage of 0.7995 V, short ciruit current of 0.02900 mA. While the calculated maximum current and voltage was found to be 0.0197 mA, and 0.3631 V, respectively. Lastly, the maximum power density is 0.0024 mW/cm^2. In comparison to *Strobilanthes cusia*, longan produced higher photoelectric conversion, due to the presence of carotenoid in the plant. The results suggest that longan pigment has a wider absorbance spectrum which helps in absorbing more light, to be converted into electricity.

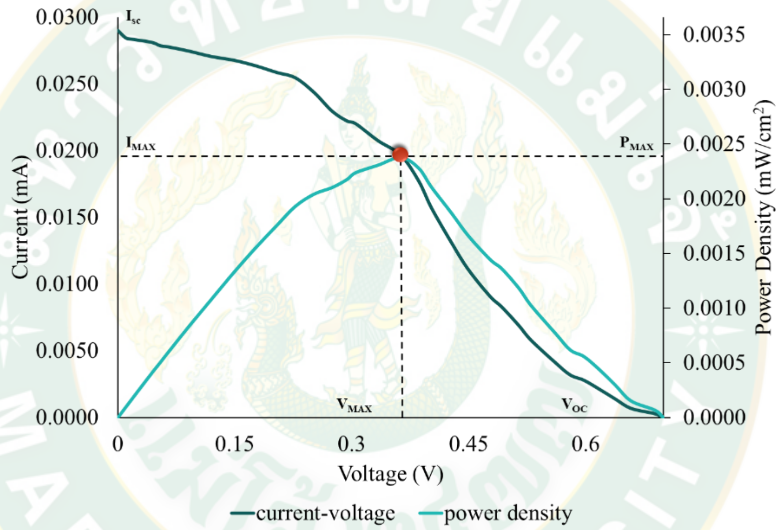

Figure 52 I-V and power density curve of Longan based DSSC.

4.4 Analysis of Inthanin Bok

According to the previous study conducted by Khammee et al., (2020), the absorbance spectra curves from the inthanin bok dyes had three peaks of absorption at the wavelength of 420 nm, 440 nm and 470 nm. The wavelength of 420 nm, 490 nm and 660 nm is the standard maximum absorption wavelength of chlorophylls (Khammee et al., 2020). Thus, the maximum absorption wavelength of inthanin bok dyes feasibility is chlorophylls. On the other hand, the absorption peak of inthanin bok was also matched with the absorption bands of carotenoids, which is 420 nm, 440 nm and 470 nm. In most plant tissues, the considerably sophisticated blue region of the spectrum owing to the absorption wavelength of chlorophylls and carotenoid pigments overlaps absorption wavelength (Khammee et al., 2020). It indicates that the pigments extraction from inthanin bok consists of chlorophylls and carotenoid pigments.

Inthanin contains 3.0996 µg/ml chlorophyll a, 2.8028 µg/ml chlorophyll b, and 15.1431 µg/ml carotenoids, according to the evaluation. In addition, the photovoltaic evaluation findings shown in figure 53 reveal that the Inthanin-based DSSC had an efficiency of 0.953%, an open circuit voltage of 0.7617 V, and a short circuit current of 0.2602 mA. The highest current and voltage estimated were determined to be 0.1847 mA and 0.5426 V, respectively. Finally, 0.0334 mW/cm^2 is the maximum power density.

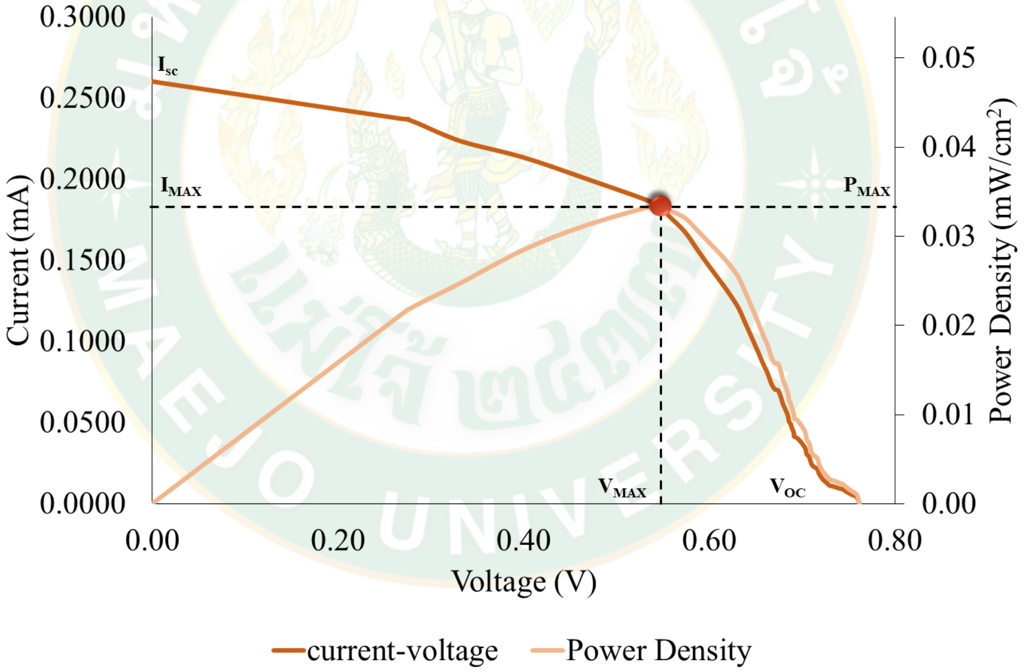

Figure 53 I-V and power density curve of Inthanin based DSSC.

4.5 Surface and Morphology analysis of TiO_2 nanoparticles with Longan and Inthanin dyes

The scanning electron micrographs (SEM) of surface morphology characteristics of TiO_2 nanoparticles pure show in figure 54 and with natural dye extracted from Longan, and Inthanin bok was shown in figure 55. The spherical TiO_2 nanoparticles pure were observed to be homogeneously distributed and porous. No cracks have been identified and stuck on the FTO glass substrate very well, as shown in figure 54 (a) and (b). The agglomeration of small particles brings about to formation of porous structure (Ruhane et al., 2017). The advantages of mesoporous holes of the TiO_2 is to provide the surface of a large hole for higher adsorption of dye molecules and facilitate the penetration of electrolyte within their pores (Jin et al., 2010). Usually, the highest pigment performance consists of the smallest molecule, the highest refractive index, brightness, and scattering coefficient. The chemical adsorption of natural dyes becomes possible because of the condensation of hydroxyl and methoxy protons with the hydroxyl groups on the surface of nanostructured TiO_2 (Kushwaha et al., 2013). Therefore, figure 55. Shows that their pores and surface of the TiO_2 layer were covered with natural dyes extracted from (a) Longan, and (b) Inthanin bok. The spherical, agglomerate grain morphology can predicted; it is the natural pigment. Therefore, the spherical, agglomerate grain morphology and cover on their pores and surface of TiO_2 layer in figure 55. Can forecast; it is a natural pigment extracted from (a) Longan, and (b) Inthanin bok leaves.

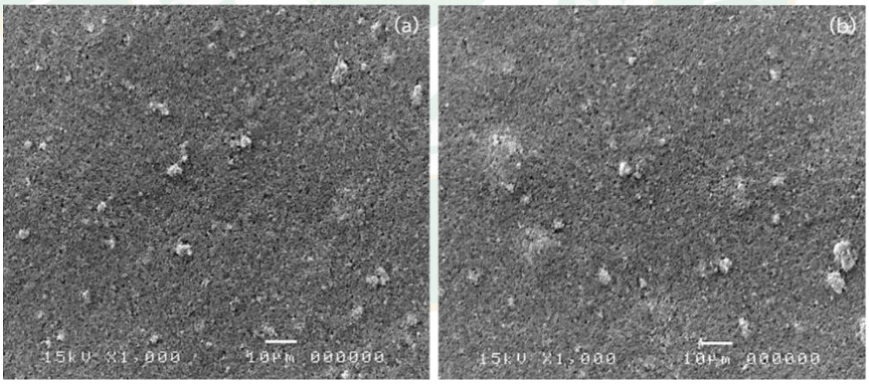

Figure 54 Scanning electron microscope of morphological characteristics of TiO_2 thin.

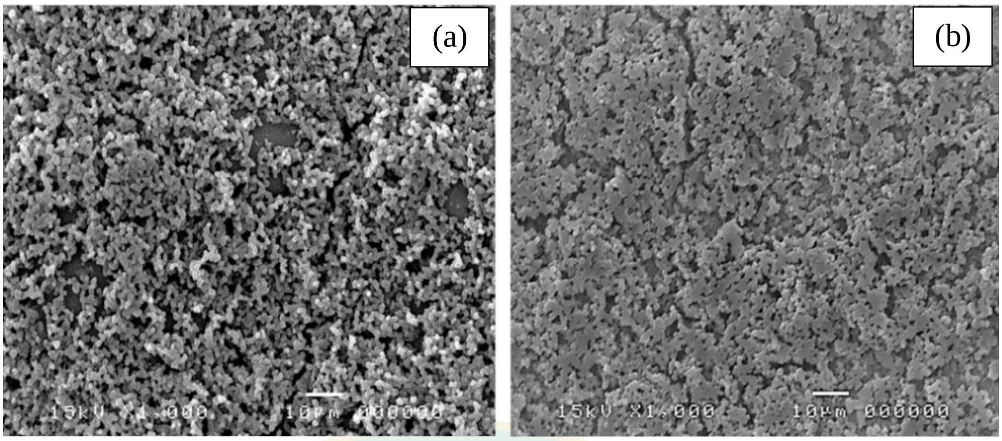

Figure 55 Scanning electron microscope of morphological characteristics of TiO_2 thin films with natural dye extraction from (a) Longan and (b) Inthanin bok leaves dye.

The energy-dispersive X-ray spectroscopy (EDX) was used to analyze the elemental contents of TiO_2 nanoparticles pure as shown in figure 56 and with natural dye extracted as shown in figure 57 a(1&2) Longan, and b(1&2) Inthanin bok leaves. The data of elemental contents were presented in table 5 indicates that the TiO_2 nanoparticles were coated on FTO glass due to elemental contents of oxygen (O), and titanium (Ti). The atomic ratios were 80.33 and 19.67%, respectively. Follow by the natural pigments from Longan and Inthanin bok leaves immersion on TiO_2 nanoparticles. The results show that the highest elemental contents were carbon (C) with 72.28 and 82.29%. This indicated that attendance of natural pigments of functional groups coated on the surfaces of TiO_2 particles. The adsorption of natural dyes on the TiO_2 layer can be enhanced electron transfer rates (Al-Alwani et al., 2018).

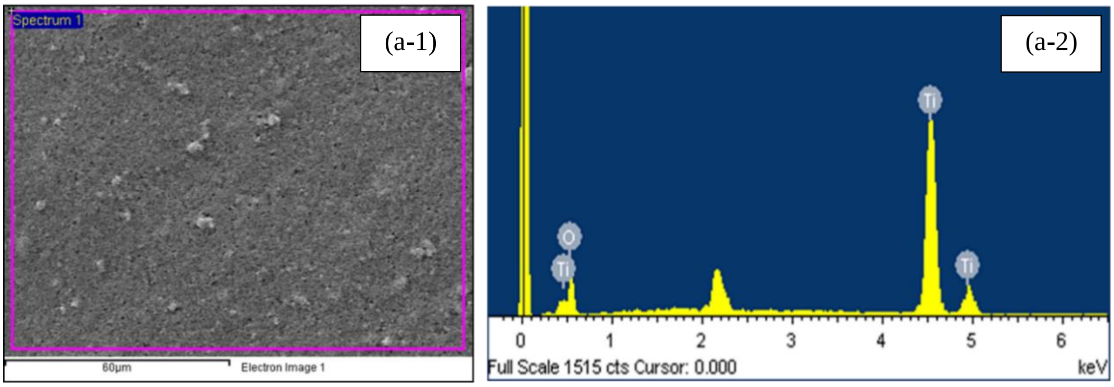

Figure 56 The energy-dispersive X-ray spectroscopy (EDX) analysis of TiO_2 coated on FTO glass substrate (a1,2).

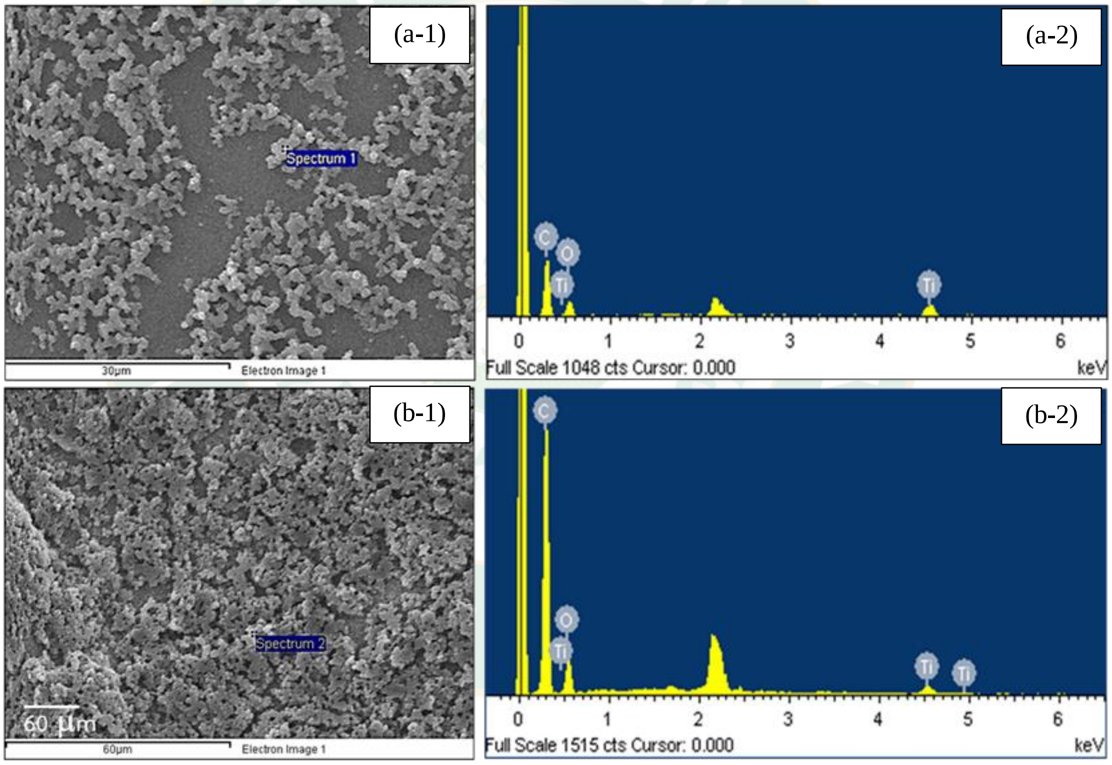

Figure 57 The energy-dispersive X-ray spectroscopy (EDX) analysis of TiO_2 coated on FTO glass substrates with natural dyes immersion a(1&2) Longan, and b(1&2) Inthanin bok leaves.

Table 1 The elemental composition of TiO_2 coated on FTO glass substrate with natural dyes immersion of Indian almond, Yellow cotton, Longan and Inthanin bok leaves.

Methods	Element	Weight %	Atomic %
Blank TiO_2 (spectrum 1) (a-1,2)	O, K	57.70	80.33
	Ti, K	42.30	19.67
Longan	C, K	64.60	72.28
	O, K	31.80	26.71
	Ti, K	3.60	1.01
Inthanin bok	C, K	77.41	82.29
	O, K	21.98	17.54
	Ti, K	0.61	0.16

4.6 DSSC greenhouse and Evaluation of plant growth

For the plant cultivation, *Solanum melongena* was selected to be the experimental plant. The plant *Solanum melongena*, usually known as eggplant or aubergine, is a member of the Solanaceae family, which also includes tomato, potato, and nicotine. Aubergine was first domesticated in India and is now grown all over the world as a favorite ingredient in many traditional dishes. Eggplant is commonly produced for its appealing fruits, which are used as a garnish in a variety of meals all over the world. The fruit is eaten when it is still immature, when it is glossy and vibrant. The flesh gets bitter and stringy as it matures, and the seeds grow hard. Although some species' fruits are eaten raw (as in Southeast Asia), cooking brings out the depth of the flavor, which is comparable to that of mushrooms. Grilled, fried, steamed, roasted, stewed with other vegetables, or served with meat or fish, aubergine flesh has a delicate texture. In addition to its culinary value, eggplant is also used for medical purposes. Diabetes, cholera, bronchitis, dysuria, dysentery, otitis, toothache, skin infections, asthenia, and haemorrhoids are all treated with a decoction of the plant, which also has narcotic, anti-asthmatic, and anti-rheumatic qualities. It is a sign of protection, good health, and female fertility in various countries.

The young eggplant with two to three leaves was purchased from the local market in Sansai, Chiang Mai, Thailand. In this experiment, two conditions was set: a.) Plant growth inside the DSSC roofed greenhouse, and b.) Plant growth outside (natural habitat). Moreover, eight young plants was put in each condition. The first step in the evaluation was to determine the initial height, number of leaves, and identify the first leaf.

Figure 58 Plant preparation (a), and Structure of the DSSC: front view (b), side view, and back view (d).

The circuit of the DSSC roof is composed of 2 series connections, in which each connection is consist of 18 solar cells. Following that, the series connections were then attached to each other in a parallel way. By electrical principle, the series circuit connection catalyze or increased the flow of the voltage inside the system. Moreover, the parallel connection helps to increase the current of the solar cell roof. Through this, the results showed the DSSC greenhouse was able to produce a voltage of 9.0 V and a current of 6 mA.

For the plant growth, the following height data gathered were shown in figure 59 a & b. Inside the DSSC greenhouse, the initial height of plant 1 ($P1_a$) to plant 8 ($P8_a$) were 16.9 cm, 14.62 cm, 13.75 cm, 13.5 cm, 18.7 cm, 15.5 cm, 16 cm, and 13 cm, respectively. With corresponding 2, 3, 3, 3, 4, 3, 2, and 3 number of leaves, respectively. While the plant 1 ($P1_b$) to plant 8 ($P8_b$) outside the greenhouse had an initial height of 12.7 cm, 14 cm, 18.25 cm, 15.15 cm, 15 cm, 16.4 cm, 14 cm, and 12.7 cm, respectively. The number of leaves recorded were 3, 3, 3, 3, 4, 3, 2, and 3, respectively.

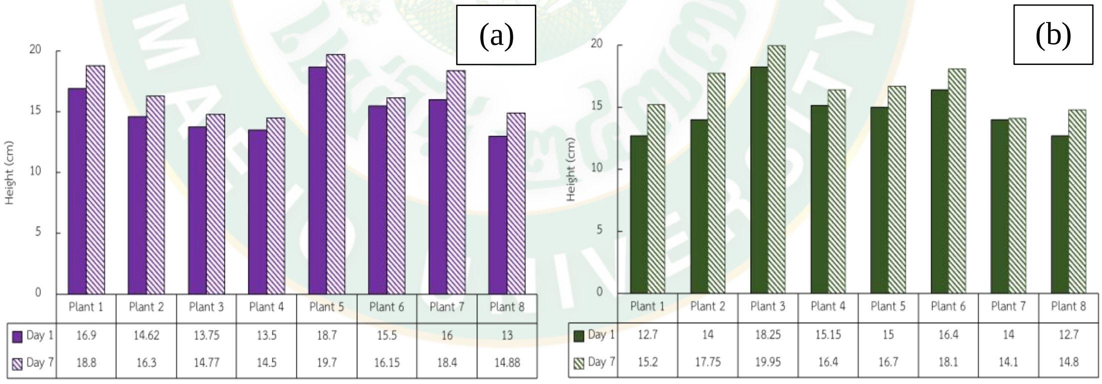

Figure 59 Plant growth: Inside DSSC greenhouse (a), outside (b)

Figures 60 and 61, display the physical changes of the plant in day 1, and day 7. After seven days, the plants were measured again for its height and occurrence of new leaf. Under DSSC greenhouse, the heights of plant 1 to 8 was observed to be 18.8 cm, 16.3 cm, 14.77 cm, 19.7 cm, 16.15 cm, 18.4 cm, and 14.88, respectively. Hence, the height increase from initial data was calculated to be $P1_a$=1.9 cm, $P2_a$=1.68 cm, $P3_a$=1.02 cm, $P4_a$=1.0 cm, $P5_a$=1.6 cm, $P6_a$=0.65 cm, $P7_a$=2.4 cm, and

$P8_a$=1.88 cm. Thus, the height increase is ranging from 0.65 cm to 1.9 cm. Moreover, plant 1, 2, 3, 4, & 8 has a one new leaf each, while plant 7 gained two new leaves.

Figure 60 Plant inside the DSSC greenhouse: day 1(a), and day 7 (b)

Figure 61 Plant outside greenhouse at: Day 1 (a), and Day 7 (b)

On the other hand, the plant outside the greenhouse has also showed physical changes. At the seventh day, the heights of plant 1 to 8 was observed to be 15.2 cm, 17.75 cm, 19.95 cm, 16.4 cm, 16.7 cm, 18.1 cm, 14.1, and 14.8, respectively. Hence, the height increase from initial data was calculated to be $P1_b$=2.5 cm, $P2_b$=3.75 cm, $P3_b$=1.7 cm, $P4_b$=1.25 cm, $P5_b$=1.7 cm, $P6_b$=1.7 cm, $P7_b$=0.1 cm, and

$P8_b$=2.1 cm. Thus, the height increase is ranging from 0.1 cm to 3.75 cm. Moreover, plant 1, 2, 4, 5 & 8 has a one new leaf each, while plant 7 loses two leaves. Thus, from this data, it was observed the higher increase of the plant height. This is because the plants are near with each other and tends to compete with each other to get sufficient sunlight exposure. Outside environment causes different factors that could affect the plant growth. Aside from that, plants are more prone to pests, which is why agricultural sectors resorts to using pesticides. These chemicals are known to be toxic and could affect human health.

The last part of this research study is evaluating the light intensity that passes through the DSSC greenhouse. The temperature and humidity inside and outside are not different from each other since the designed DSSC greenhouse only had an area of $1m^2$. Furthermore, it is well ventilated because it is covered with a screen net, just enough to prevent insects from getting inside. For the light intensity, five locations were checked: Back Left (BL), Back Right (BR), Center (C), Front Left (FL), and Front Right (FR). While for the outside environment, five designated points were also checked. Table 11 and 12, which show the light intensity measured, It was found out that approximately only 50% of light passes through the DSSC greenhouse compared to outside. Moreover, the LED light was connected to the DSSC to increase the light intensity inside the greenhouse. From the results, the light intensity was increased to 55%. Nevertheless, from the physical observations (height and number of new leaves) of the plants, it was found out to be growing successfully. Thus, it concludes that the light passing through the DSSC greenhouse is sufficient for cultivating plants.

Figure 62 LED light powered by DSSC

Table 11 Light intensity at Cloudy weather inside DSSC greenhouse

	Light intensity (LUX)	
Parameter	**Cloudy**	**Mix cloudy & sunny**
Back Left (BL)	4908 ± 33.45	29250 ± 657.65
Back Right (BR)	4689 ± 41.59	18225 ± 521.42
Center (C)	3673 ± 39.61	26325 ± 491.81
Front Left (FL)	4420 ± 39.37	27010 ± 468.29
Front Right (FR)	4130 ± 27.39	26080 ± 536.84

Table 12 Light intensity at Cloudy weather outside

	Light intensity (LUX)	
Parameter	**Cloudy**	**Mix cloudy & sunny**
Point 1	9845 ± 26.22	39335 ± 497.02
Point 2	9015 ± 43.87	36593 ± 589.21
Point 3	7605 ± 36.40	39545 ± 553.92
Point 4	8800 ± 37.42	33230 ± 495.93
Point 5	8345 ± 22.91	35180 ± 501.45

CHAPTER 5
CONCLUSION

Recently, dye-sensitized solar cell has been eyed as alternative energy source. For years, synthetic dye has been a widely used dye sensitizer for the development of dye-sensitized solar cells. However, in producing such dyes, it undergoes complex processes which involve the use of toxic chemicals that pose a health risk and are harmful to the environment. Due to its overall impact on humans and nature, the extraction of natural dyes or pigments from plants such as chlorophyll, anthocyanin, carotenoid, etc., has attracted the interest of research as an alternative dye. Moreover, because of the competition between the use of plants as a food source and as an energy source, PV plays a part in helping the various activities related to food production and subsequent supply chains by providing electricity converted from solar energy. Hence, this study was conducted investigate the potential of natural dye from Malabar spinach (*Basella alba*), Indigo plant (*Strobilanthes cusia Nees*), (*Dimocarpus longan*) and Inthanin bok (*Lagerstroemia macrocarpa*) as photosensitizer.

Based on the results of the evaluation of the natural pigments, Inthanin bok had the highest energy conversion efficiency of 1.134%, V_{oc}= 0.5426 V, I_{sc}= 0.2952 mA. , Isc= 0.2952 mA. Furthermore, the longan leaves had a 0.06788% efficiency with V_{oc}= 0.7 V and I_{sc}=0.02900 mA. The Malabar spinach produced 0.1021% efficiency, V_{oc}= 0.4877 V, and I_{sc}= 0.0682 mA. Lastly, Indigo plant produced the lowest efficiency having 0.0118%, V_{oc}=0.30635 V, and I_{sc}=0.01555 mA.

In addition, Inthanin bok showed the highest potential and was further used in developing the DSSC roofed greenhouse. The voltage and current produced by the DSSC roof were found to be 9 V and 0.5 mA, respectively. *Solanum melongena*, also known as eggplant, was used as an experimental crop to evaluate the effect of DSSC canopy on crops. According to research results, the intensity of light passing through the greenhouse is only about 50% compared to outside. With the addition of the LED by DSSC, the light intensity was increased to 55%. The light intensity inside the greenhouse was measured in five (5) locations: back left (BL), back right (BR), center (C), front left. (FL) and front right (FR) and corresponding measurements are 29,250 ± 657.65 Lux, 18,225 ± 521.42 Lux, 26,325 ± 491.81 Lux, 27,010 ± 468.29 Lux and 26,080 ± 536.84 Lux. Based on the physical observations (height and number of new leaves) of the plants, it was found out to be growing successfully. Therefore, it can be concluded that the light transmitted through the greenhouse from DSSC and connected with LED lamps is sufficient for the cultivation of plants. The resulting data from this research aims to contribute on promoting deeper understanding, knowledge to improve the potential of Dye-sensitized solar cell in converting light to electricity.

For the overall improvement of the DSSC greenhouse, the researchers recommended the following:

1. To further, evaluate the quality and life span of the pigments of the natural dye. And to broaden the wavelength in assessing the pigment's absorbance.
2. To investigate the effect of mixing of different pigments.
3. For the structure of the DSSC roofed, the cover must be open to provide sufficient ventilation for the solar cells. Thus, to prevent the heat to be trapped in solar cells. In addition, to minimize the evaporation of the liquid electrolyte.
4. In addition, measuring the width of the leaves must be included, for better understanding of the effect of light intensity of the plant growth.

APPENDIX A

PROCEEDING PAPER

knowvel
TAKE YOUR RESEARCH TO NEXT LEVEL

GLOBAL JOURNAL OF SCIENCE & ENGINEERING
Vol. 02 (2020) 5-9
www.knowvel.com

Original Research Article

EXTRACTION OF ANTHOCYANIN PIGMENTS FROM MALABAR SPINACH FRUITS AS A POTENTIAL PHOTOSENSITIZER FOR DYE-SENSITIZED SOLAR CELL

GLENNISE FAYE C. MEJICA [1], YUWALEE UNPAPROM [2], PIYAPIT KHONKAEN [3], RAMESHPRABU RAMARAJ [1]

ABSTRACT

The implementation of synthetic dyes gives a better efficiency with higher durability; however, the production process of synthesizing these dyes is more complex, expensive, and involves the use of toxic materials. For these reasons, the production of such dyes can pose harm not only to humans but also to the environment. An alternative for the synthetic dyes is the natural dyes or pigment extracted from plants such as anthocyanin, carotenoid, chlorophyll and many others. These natural dyes are easily extracted from various parts of plants, such as from the fruits, flowers, leaves, and seeds. Regardless of the limited performance of natural dyes, the natural dyes exhibit advantages, including high absorption coefficients, highlight-harvesting efficiency, inexpensive, ecologically friendly, non-toxic, and are easily extractable. Moreover, this research paper is mainly focused on about extraction of anthocyanin dye pigments from Malabar spinach fruits for Dye-sensitized solar cells (DSSC). The experiment was conducted using three different methods; extraction of anthocyanin pigments from Malabar spinach fruits: a.) using pure methanol solvent, b.) using 50% methanol solvent, and c.) using 50% methanol & 1% HCl solvent, and the resulted data were 160.81 mg/L, 64.62 mg/L and 77.65 mg/L respectively. It can be concluded that the extraction of anthocyanin pigments from Malabar spinach fruits using pure methanol solvent has the highest amount of extracted anthocyanin pigment, which is 160.81 mg/L.

Keywords: Dye-sensitized solar cell, anthocyanin, Malabar spinach, photosensitizer, Natural dye

AUTHOR AFFILIATION

[1]School of Renewable Energy, Maejo University, Chiang Mai 50290, Thailand
[2]Program in Biotechnology, Faculty of Science, Maejo University, Chiang Mai 50290, Thailand
[3]Program of Forest Management, Maejo University Phrae Campus, Phrae 54140, Thailand

CORRESPONDENCE

Rameshprabu Ramaraj, School of Renewable Energy, Maejo University, Chiang Mai 50290, Thailand
Email: rrameshprabu@gmail.com

PUBLICATION HISTORY

Received: June 30, 2020
Accepted: July 01, 2020

ARTICLE ID: GJSE-CP-06

1. INTRODUCTION

Based on the prediction conducted by the US Energy Information Administration, by the year 2040, the total world energy consumption will rise to 25 TW. The majority of the world's energy supply is extracted from fossils. The disadvantage of energy derived from fossils is that it is categorized as non-renewable energy resources, which means these energy resources cannot be replenished within a human timescale. Moreover, the resources are depleting at a rapid rate. In addition, within 50-60 years, fossil fuels and natural gas reserves currently available will run out [1, 2].

The consumption of fossil fuels resulted in several environmental issues such as climate change, ozone layer depletion, acid rain, pollution, etc. Furthermore, fossil fuels are the primary contributor to global warming [1]. Greenhouse gas emissions have been increasing rapidly, reaching a rate of 49 gigatons of CO_2-equivalents/year (GT CO_2eq/year) in 2010, with carbon dioxide gas emissions alone from fossil fuels and industrial processes accounting for 78% of total emissions. If present activities continue without any further mitigation efforts, atmospheric greenhouse gas concentrations could potentially increase from 430 ppm CO_2eq in 2011 to 1300 ppm by 2100, which could cause the global mean surface temperature to rise by up to 4.8 °C [2]. To counter the effects of fossil fuels in the environment, this led to an exploration of finding new energy from renewable resources. Among all the sustainable energy, the sun has the most noteworthy potential in providing cleaner, more carbon-neutral energy to fulfill the ever-growing energy demands of the future as its resource base is much larger than all the other renewables combined [2] and are easily extractable by a photovoltaic (PV) system [1].

Over the years, solar PV technologies have been the focus of research studies. These technologies have gone through a lot of innovation, improvement and development. From the birth of the First-generation PV cells, which are the most established type of solar PV cells and dominate the market and commercially available, examples being single-crystalline (scSi) or multi-crystalline (mc-Si) [3]. Then come next is the Second-generation PV systems these are cells that were essentially based upon III-V device structure, GaAs, CdTe, InP, and CIGs solar cells and that were introduced in the field of solar photovoltaics [4]. These P-V systems are still in the premature stage of development; these cells are gradually flourishing and occupying the markets because of its comparatively low manufacturing costs. Lastly, in the early 1990's the third generation of solar cells with Dye-sensitized structure was introduced. These PV cells are still in the experimental and developmental phase or have not yet been widely commercialized [3, 4].

In comparison to a wide variety of solar technologies, the DSSC shows remarkable potential in providing an efficient, low-cost and environmentally friendly solution that could lead us to a society free of fossil fuels. In addition, a study shows that the production of DSSC is inexpensive compared to traditional PV systems and offering a short payback period of less than one year [2]. Since the publication of DSSC in 1990's [5], it has inevitably attracted the interests of researchers because of its feasible characteristics and low process cost. Significantly, the DSSC has the potential to harvest light and convert to electricity, which can be one of the keys to suffice the energy demand of humans. The DSSC is still in the premature stage of research and development.

In comparison to other types of a photovoltaic system, the dye-sensitized solar cell falls behind. Improving the low light to energy conversion efficiency has been the biggest challenge in the fabrication of DSSC. One possible solution to it is by improving the photosensitizers (dye). The photosensitizer plays a vital role in the DSSC; it absorbs the light and supplies electrons to the semiconductor material (such as TiO_2) inside the cell. Hence, the common choices of dyes for DSSC are synthetic dyes [6].

The use of synthetic dyes gives a better efficiency with higher durability; however, the production process of synthesizing these dyes is more complex, expensive, and involves the use of toxic materials. For these reasons, the production of such dyes can pose harm not only to humans but also to the environment. An alternative for the synthetic dyes is the natural dyes or pigment extracted from plants such as anthocyanin, carotenoid, chlorophyll, and many others. These natural dyes are easily extracted from various parts of plants, such as from the fruits, flowers, leaves, and seeds [6]. Regardless of the limited performance of natural dyes, the natural dyes exhibit advantages, including high absorption coefficients, highlight-harvesting efficiency, inexpensive, ecologically friendly, non-toxic, and are easily extractable [1, 7]. Moreover, this research paper is mainly focused on about extraction of anthocyanin dye pigments from Malabar spinach fruits for DSSC. Mostly, these plants are found in tropical countries such as Thailand and are used for various recipes. Unlike its leaves, the ripe fruits (purple to black color) are considered as waste.

2. METHODOLOGY

2.1. Materials

Malabar spinach fruits used in this research were collected from San Kamphaeng District, Chiang Mai, Thailand. HCl and acetic acid were purchased from Union Science. The buffers: (0.4M) Acetic acid-sodium acetate buffer pH 1.0 and (0.1M) HCl acid-KCl buffer pH 4.5, as well as the 50% methanol solvent and 50% methanol & 1% HCl, were prepared in the lab.

2.2. Extraction of the Anthocyanin Pigments

The Malabar spinach fruits were separated from its stalk and then were washed with water and dried at room temperature. The fruit samples were measured by following the ratio of 10 g of sample per 50 mL of solvent. For this study, three different methods were conducted: extraction of anthocyanin pigments from Malabar spinach fruits: a.) using pure methanol solvent, b.) using 50% methanol solvent, and c.) using 50% methanol & 1% HCl solvent. After the Malabar spinach fruits were measured, mortar and pestle were used to pound it and break it down into smaller pieces. The crashed samples were then put into a beaker covered with aluminum foil to avoid light exposure of the sample. Moreover the solvent: a.) using pure methanol solvent, b.) using 50% methanol solvent, and c.) using 50% methanol & 1% HCl solvent is then added and mixed in the beaker and then set aside for 10 mins, to give enough contact time for the solvent to extract the pigments. After 10 mins, the samples were then filtered using a vacuum pump. Lastly the filtrate were then kept in a covered glass bottle to avoid light exposure.

2.3. Determination of Anthocyanin Pigment Content

The filtrate sample of Malabar spinach fruit extract undergoes light absorbance analysis using the spectrophotometer. Its absorbance was checked at different wavelengths (510 nm, 520 nm, 530 nm, 540 nm, & 700 nm). Moreover, the anthocyanin content was calculated using the pH-differential method; in this case, the filtrates were diluted at two different buffers: (0.4M) Acetic acid-sodium acetate buffer pH 1.0 and (0.1M) HCl acid-KCl buffer pH 4.5).

Anthocyanin pigment concentration (APC) was calculated using the following equation (Giusti and Wrolstad, 2001)

$$APC\left(\frac{mg}{L}\right) = \frac{A * MW * Df * 10^3}{\mathcal{E} * L} \quad (1)$$

Where,

$A = (A_\omega - A_{700nm})_{pH\ 1.0} - (A_\omega - A_{700nm})_{pH\ 4.5}$, MW (molecular weight) = 449.2 g/mol, Df is dilution factor, $\mathcal{E}$= 26,900 L/cm mol, 10^3 is the converting factor for g to mg, and L is the path length in cm.

3. RESULTS AND DISCUSSION

Figure 1 (a) & (b) shows the image of the fruits of Malabar spinach and the dye extracted after the extraction process. The experiment was conducted in order to determine the Anthocyanin Pigment Content (APC) of the sample. The evaluation of the APC undergoes a series of processes, trial and errors in order to achieve accurate and reliable data. Taken into account that the dyes are sensitive to the light, therefore, it was examined in a little lightroom and kept in a covered bottle to avoid exposure to the light.

For the absorbance, an aliquot of the dye extract was diluted by two different buffers at different dilution factors and was examined by spectrophotometer. Figure 3 shows the color changes that occurred during the process. Thus, it was observed that the color of the extract varies at different pH values. Before the addition of buffers, the initial pH of the sample (for: pure methanol, 50% methanol, 50% methanol & 1% HCl) is: 7.1, 6.82 & 1.45 respectively. When the pH of the dye extract is high, the color is purple, while at low pH its color is red. Furthermore, when acid is added in the extraction process, the color of the resulting dye is darker, as shown in Figure 2 (3a) and (3b).

(a) (b)

Figure 1. (a) Malabar spinach fruit (purple to black color; (b) Extracted dye from Malabar spinach fruits

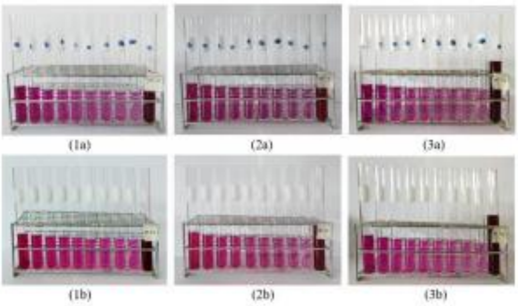

(1a) (2a) (3a) (1b) (2b) (3b)

Figure 2. Extracted dye using pure methanol solvent diluted with: (1a) buffer pH 1.0 & (1b) buffer pH 4.5; Extracted dye using 50% methanol solvent diluted with (2a) buffer pH 1.0 & (2b) buffer pH 4.5; Extracted dye using 50% methanol & 1% HCl solvent diluted with (3a) buffer pH 1.0 & (3b) buffer pH 4.5

The samples were examined at different wavelengths: 510nm, 520nm, 530nm, 540nm, 550nm, & 700nm. Figure 3 (a) & (b) shows that the highest peak of the three processes is at the wavelength of 540 nm. The extraction process using pure methanol solvent gained the highest absorbance for both pH 1 and pH 4.5 buffer having 0.326 & 0.641 respectively.

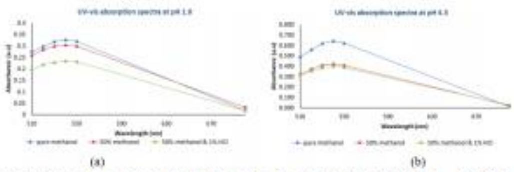

(a) (b)

Figure 3. The absorption spectra (wavelengths: 510nm, 520nm, 530nm, 540nm, 550nm, & 700nm) of the extracts of Malabar spinach fruit extracted by three different solvent: 1.) pure methanol, 2.) 50% methanol, and 3.) 50% methanol & 1% HCl; and diluted at: (a) 0.4M Acetic acid-sodium acetate buffer pH 1.0, (b) 0.1M HCl acid-KCl buffer pH 4.5).

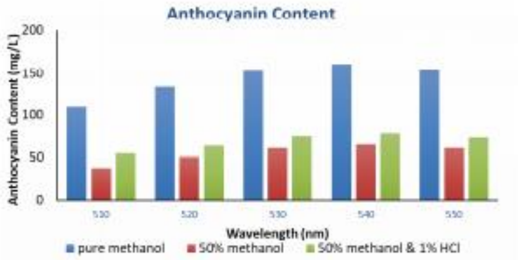

Figure 4. Anthocyanin pigment content of the dye extracted from Malabar spinach fruits

All three processes gained their highest APC at the wavelength of 540 nm. However, as Figure 4 revealed, the highest anthocyanin content extracted was obtained from the extraction process using pure methanol as the solvent having 160.81 mg/L. Hence, followed by 50% methanol & 1% HCl with 77.65 mg/L and lastly, by 50% methanol with 64.62 mg/L. Nevertheless, it can be concluded that using pure methanol to extract APC is more effective and efficient. In comparison, of the result with different plant sources of anthocyanin (Table 1), the data gathered from this study is among the highest of APC, which is a good indication that the dye from the fruit of Malabar spinach has a potential to be used as a photosensitizer for dye-sensitized solar cell.

4. Conclusions

The present study explored the potential of the natural dye from the fruit of Malabar spinach. Also, it examined the effect of using three different methods; extraction of anthocyanin pigments from Malabar spinach fruits: a.) using pure methanol solvent, b.) using 50% methanol solvent, and c.) using 50% methanol & 1% HCl solvent. Based on the outcomes of the study, extraction using pure methanol showed higher and more effective in extracting dye from Malabar spinach. Having the highest amount of anthocyanin with 160.81 mg/L. This finding can help to convert the agricultural waste into a potential material that can absorb light and convert it to electricity. Furthermore, the methods used in this study can contribute to the development of low-cost and effective natural dye as photosensitizers for the dye-sensitized solar cell.

Table 1. Some common fruits and vegetables with their anthocyanin content [9, 10]

Plant source		Anthocyanin content	Ref.
Prunus avium		150	[10]
Aronia melanocarpa		160	[10]

Rubus spp.		160	[10]
Oryza sativa		200	[10]
Red onion		7-21	[11]
Plum		2-25	[12]
Red radishes		11-60	[10]
Red Raspberries		20-60	[11]
Strawberries		15-35	[12]
Tradescantia pallida		120	[13]
Hibiscus rosa-sinensis		4.63	[14]
Melastoma malabathricum		8.43	[14]
Codiaeum variegatum		2.22	[14]
Malabar spinach fruits		160.81	This study

CONFLICT OF INTERESTS

The authors declare that there is no conflict of interest related to the publication of this article.

REFERENCES

[1] F. Kabir, M. M. H. Bhuiyan, M. S. Manir, M. S. Rahaman, M. A. Khan, and T. Ikegami, "Development of dye-sensitized solar cell based on combination of natural dyes extracted from Malabar spinach and red spinach," Results Phys., vol. 14, 2019.

[2] K. K. S. Lau and M. Soroush, "Chapter 1 - Overview of Dye-Sensitized Solar Cells," M. Soroush and K. K. S. B. T.-D.-S. S. C. Lau, Eds. Academic Press, 2019, pp. 1–49.

[3] V. Sugathan, E. John, and K. Sudhakar, "Recent improvements in dye sensitized solar cells: A review," Renewable and Sustainable Energy Reviews, vol. 52. pp. 54–64, 2015.

[4] P. Roy, N. Kumar Sinha, S. Tiwari, and A. Khare, "A review on perovskite solar cells: Evolution of architecture, fabrication techniques, commercialization issues and status," Solar Energy, vol. 198. pp. 665–688, 2020.

[5] B. O'Regan and M. Grätzel, "A low-cost, high-efficiency solar cell based on dye-sensitized colloidal TiO2 films," Nature, vol. 353, no. 6346, pp. 737–740, 1991.

[6] N. T. R. N. Kumara, A. Lim, C. M. Lim, M. I. Petra, and P. Ekanayake, "Recent progress and utilization of natural pigments in dye sensitized solar cells: A review," Renewable and Sustainable Energy Reviews, vol. 78. pp. 301–317, 2017.

[7] S. Shalini, R. Balasundara Prabhu, S. Prasanna, T. K. Mallick, and S. Senthilarasu, "Review on natural dye sensitized solar cells: Operation, materials and methods," Renewable and Sustainable Energy Reviews, vol. 51. pp. 1306–1325, 2015.

[8] M. M. Giusti and R. E. Wrolstad, "Characterization and Measurement of Anthocyanins by UV-Visible Spectroscopy," Curr. Protoc. Food Anal. Chem., vol. 00, no. 1, pp. F1.2.1–F1.2.13, 2001.

[9] A. Shamina, K. N. Shiva, and V. A. Parthasarathy, "Food colours of plant origin," CAB Reviews: Perspectives in Agriculture, Veterinary Science, Nutrition and Natural Resources, vol. 2. 2007..

[1] M. M. Giusti, L. E. Rodriguez-Saona, J. R. Baggett, G. L. Reed, R. W. Durst, and R. E. Wrolstad, "Anthocyanin Pigment Composition of Red Radish Cultivars as Potential Food Colorants," J. Food Sci., vol. 63, no. 2, pp. 219–224, 2008..

[11] G. Mazza, "Anthocyanins in fruits, vegetables, and grains," CRC press, 2018.

[12] C. F. Timberlake, and B. S. Henry, "Anthocyanins as natural food colorants," Progress in clinical and biological research, vol. 280, pp. 107-121, 1988.

[13] Z. U. Shi, M. I. Lin, and F. J. Francis, "Stability of anthocyanins from Tradescania pallida," Journal of Food Science, vol. 57(3), pp.758-770, 1992.

[14] R. Ahmadian, "Estimating the impact of dye concentration on the photoelectrochemical performance of anthocyanin-sensitized solar cells: a power law model," J. Photonics Energy, vol. 1, no. 1, p. 011123, 2011.

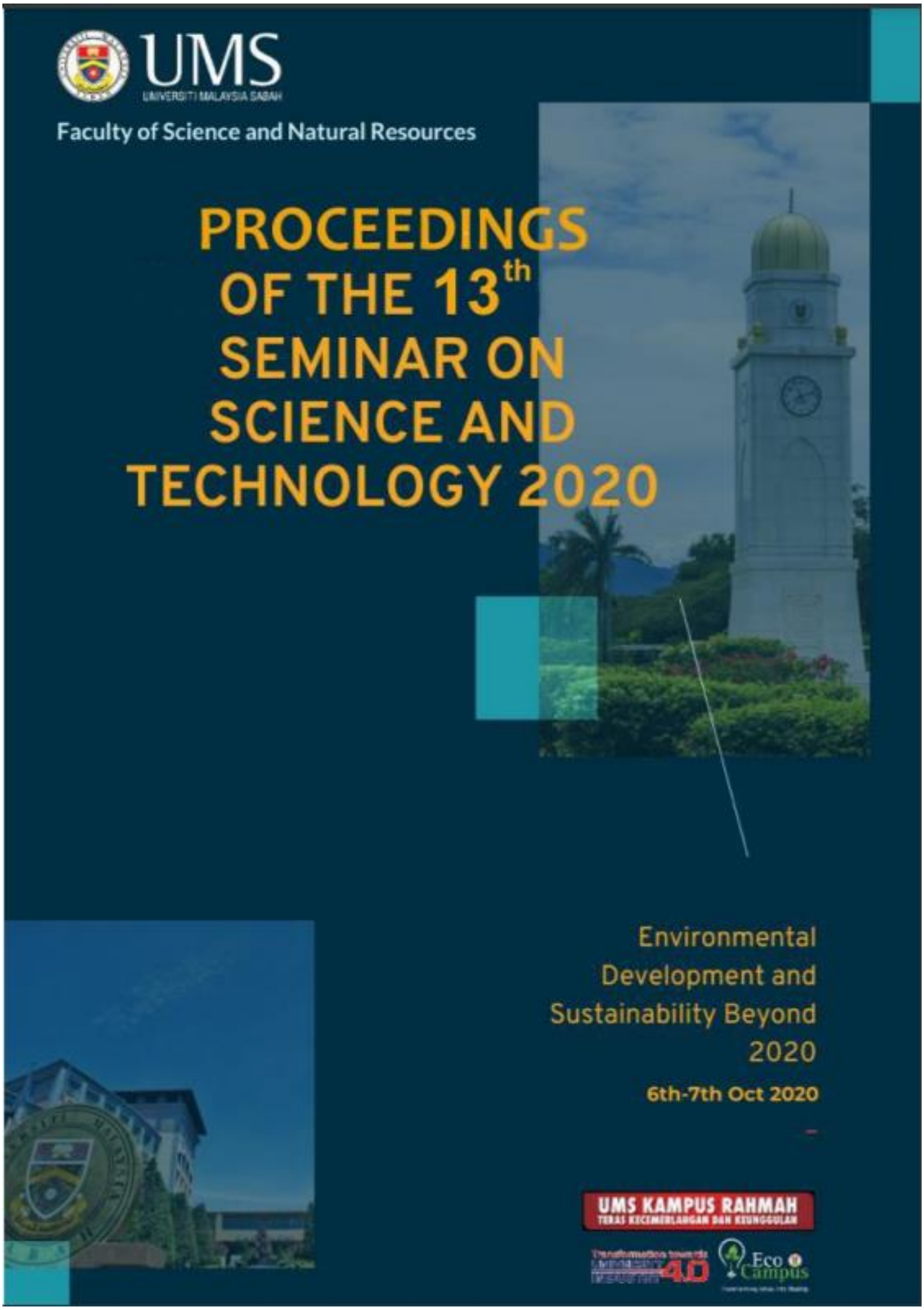
UMS
UNIVERSITI MALAYSIA SABAH
Faculty of Science and Natural Resources
PROCEEDINGS OF THE 13th SEMINAR ON SCIENCE AND TECHNOLOGY 2020
Environmental Development and Sustainability Beyond 2020
6th-7th Oct 2020
UMS KAMPUS RAHMAH
TERAS KECEMERLANGAN DAN KEUNGGULAN
Eco Campus

ANTHOCYANIN PIGMENT EVALUATION AND DEVELOPMENT OF MULTICOLORED NATURAL DYE FROM MALABAR SPINACH AND RED CABBAGE AS A POTENTIAL DYE SENSITIZER FOR DYE-SENSITIZE SOLAR CELL

G.F.C. Mejica*[1], Y. Unpaprom[2] and R. Ramaraj[1]

[1]School of Renewable Energy, Maejo University, Chiang Mai 50290, Thailand
[2]Program in Biotechnology, Faculty of Science, Maejo University, Chiang Mai 50290, Thailand

mejicag@yahoo.com, rrameshprabu@gmail.com

Abstract: For years, synthetic dye has been widely used dye sensitizer for the development of dye-sensitized solar cell (DSSC) because of its efficiency and durability. However, in producing such dyes, it undergoes complex processes which involve the use of toxic chemicals that poses a health risk and harmful to the environment. Due to its overall impact to human and nature, extraction of natural dyes or pigments from plants such as chlorophyll, anthocyanin, carotenoid and etc. has attracted the interest of researches as an alternative dye. Hence, the objective of this research study centers on the evaluation of anthocyanin pigments and development of multicolored dye from malabar spinach, red cabbage and combination of malabar spinach and red cabbage dyes. In this experiment, solvent extraction method was used for the extraction of the dye from malabar spinach and red cabbage. Overall, the dyes evaluated were the following: malabar spinach (MS), 50% malabar spinach (MS) + 50% red cabbage (RC) and red cabbage (RC).

Keywords: Anthocyanin pigment, Malabar spinach, Red cabbage, Titanium dioxide, Dye-sensitized solar cell

1. INTRODUCTION

To mitigate the use of fossil fuels, researchers are focusing to the development of renewable energy. Such energy is from the photovoltaic (PV) technology, it converts solar energy to electricity. However, in order to meet the energy demand, production of energy from the sun requires a larger plot area. Hence, it will catalyze the increase of competition of land resources for food cultivation and for energy production [3]. This land competition led to the development of agrivoltaic system. This system is based on the principle of combining crop cultivation and electricity production within the same unit area [4].

Currently, the main challenge manifested by agrivoltaic, is the rivalry between PV roof and plants to get incident solar radiation. Thus, Dye-sensitized solar cell or also known as DSSC is seen as a potential alternative to the conventional solar cell due to its low light level sensitivity and inexpensive fabrication cost.

The DSSC was first reported by Gratzel and O'Regan in the 90's [5] have attracted the interest of researchers due to its inexpensive process cost, potential to absorb light and convert it to electricity and environmentally safe [6]. Furthermore, the color of the dye-sensitized solar cell can be determined and modify by the dye, in which it can propagate the plant growth or can modify the solar light spectrum that passes through it [4]. In addition, chlorophyll, which gives the green pigment or the abundant color found in plants, has the ability to absorb blue and red lights. Hence, this research is mainly focused in the anthocyanin pigment evaluation and development of multicolored natural dye from malabar spinach and red cabbage.

2. METHODOLOGY

The Malabar spinach (MS) and red cabbage (RC) used for this research were collected from Chiang Mai, Thailand. The MS fruits were crushed using mortar and pestle and mix with solvent for 10 mins. Then the RC was chopped into smaller pieces and put in the blender together with the solvent. After it was blended, the solution was kept in a beaker.

Both the MS and RC were kept in dark storage to avoid light exposure. In addition, the combination of 50% MS with 50% RC was prepared by mixing 50 mL of dye from both extracts.

Three grams of TiO2 paste was prepared and thoroughly mixed using a magnetic stirrer for 2hrs. Lastly, the natural dye was added to the surface of TiO2. For the anthocyanin pigment concentration, the procedure was adopted from Mejica et al. [6].

2 RESULTS & DISCUSSION

3.1 ABSORPTION SPECTRA OF NATURAL DYE & ANTHOCYANIN PIGMENT The color stability of dyes is dependent to the effect of light that passes through it. Characterization of the effect of light is mainly focused by the research regarding the natural dye evaluation. Depending on the state of DSSC, dyes extracted from plants can increase the efficiency in the presence of light.

This study result, the UV-vis analysis of the three different dye, it was found that both red cabbage dye and 50% MS + 50% RC have their highest peak at 520 nm having the absorbance of 0.538 a.u and 0.377 a.u respectively. While the malabar spinach has 0.319 a.u at 540 nm.

3.2 APPLICATION OF NATURAL DYE

Anthocyanins are water-soluble pigments. Its appearance is greatly dependent to its pH value. This characteristic of anthocyanin enables to act as a natural pH indicator. There was a significant color change for red cabbage dye and 50% MS + 50% RC sensitized to TiO2 thin film. The contrast within the appearance of malabar spinach (red to orange), 50% (MS) + 50% (RC) (purple color), and red cabbage (blue color) is due to the presence of different sort of chemical structure of the pigments and pH. The anthocyanin gathered from red cabbage are delphinidin and cyaniding complexes [8]. Thus, with this result, it can be concluded that fabrication of multicolored DSSC is feasible.

3 CONCLUSION

The resulted data from this study shows the capability of the natural dye extracted from Malabar spinach and red cabbage to absorb green light and release blue to red light. With the modification of dye composition, changes in color was vividly seen. In relation to this, the results can help in the development of multicolored dye-sensitized solar cell, which can be useful in agrivoltaic system. The next step for this project is to fabricate multicolored dye-sensitized solar cell based on malabar spinach, 50% MS + 50% RC, and red cabbage.

ACKNOWLEDGEMENT

Authors would like to thank School of Renewable Energy, Maejo University for funding this research and Program in Biotechnology, Faculty of Science, Maejo University, Chiang Mai, Thailand for providing the research facilities during the conduct of the study

REFERENCES

[1] Lau, K. K. S. & Soroush, M. (). 'Overview of Dye-Sensitized Solar Cells. In Dye-Sensitized Solar Cells. 2019, pp. 1-49.

[2] Kabir, F., Bhuiyan, M. M. H., Manir, M. S., Rahaman, M. S., Khan, M. A. & Ikegami, T. (2019). 'Development of dye-sensitized solar cell based on combination of natural dyes extracted from Malabar spinach and red spinach'. Results in Physics.

[3] Dinesh, H. & Pearce, J. M. . The potential of agrivoltaic systems. Renewable and Sustainable Energy Reviews, 2016, 54, pp 299-308.

[4] Roslan, N., Ya'acob, M. E., Radzi, M. A. M., Hashimoto, Y., Jamaludin, D. & Chen, G. . Dye Sensitized Solar Cell (DSSC) greenhouse shading: New insights for solar radiation manipulation. Renewable and Sustainable Energy Reviews, 2018, 92, pp 171-186.

[5]O'Regan, B. & Grätzel, M. 1991. 'A low cost, high-efficiency solar cell based on dye-sensitized colloidal TiO2 films'. NATURE.

[6] Mejica, G., Unpaprom, Y., Khonkaen, P. & Ramaraj, R. 'Extraction of anthocyanin pigments from malabar spinach fruits as a potential photosensitizer for dye-sensitized solar cell', Global Journal of Science & Engineering, 2020, pp 5-9.

[7] Giusti, M. & Wrolstad, R. E. (2001). Characterization and Measurement of Anthocyanins by UV-Visible Spectroscopy. Current Protocols in Food Analytical Chemistry.

[8] Gokilamani, N., Muthukumarasamy, N., Thambidurai, M., Ranjitha, A. & Velauthapillai, D. . 'Utilization of natural anthocyanin pigments as photosensitizers for dye-sensitized solar cells', Journal of Sol-Gel Science and Technology, 2013, 66, (2), pp 212-219.


PROCEEDING E-BOOK
ICSTI-MJU 2021
Science Technology & Innovation-Maejo University
THE 1ST INTERNATIONAL CONFERENCE ON
SCIENCE TECHNOLOGY & INNOVATION-MAEJO UNIVERSITY
MARCH 19, 2021, CHIANG MAI, THAILAND

Development of natural dye based Dye-sensitized solar cell utilizing natural pigment from malabar spinach and red cabbage

Glennise Faye C. Mejica [1,2], Yuwalee Unpaprom [2,3], Ubonwan Subhasaen[4], Thidarat Siriboon[5] and, Rameshprabu Ramaraj[2,3,*]

[1] School of Renewable energy, Maejo University, Chiang Mai 50290, Thailand
[2] Sustainable Resources and Sustainable Engineering research laboratory, Maejo University, Chiang Mai 50290, Thailand
[3] Program in Biotechnology, Faculty of Science, Maejo University, Chiang Mai 50290, Thailand
[4] Program of Political Science, Maejo University Phrae campus, Phrae 54140, Thailand
[5] Program in Agronomy, Faculty of Agricultural Production, Maejo University, Chiang Mai 50290, Thailand

*Corresponding author email: rameshprabu@mju.ac.th ; rrameshprabu@gmail.com

Abstract. Dye-sensitized solar cell (DSSC) a new innovation of photovoltaic cell has gained popularity due to its inexpensive fabrication cost and promising potential to absorb light and convert it to electricity. For decades, the artificial dye has been employed as a photosensitizer for dye-sensitized solar cells due to its performance output. In contrast, manufacturing such dyes undergoes complicated processes that involve the utilization of costly and harmful chemicals that poses a health risk and harmful to human and environment. Hence, the extraction of dyes or pigments from nature has been eyed for various researches that can be an alternative to artificial dyes as a photosensitizer for DSSC. Hence, this research investigates and evaluates natural dye utilization from the malabar spinach (MS) and red cabbage (RC) as a photosensitizer for DSSC. The experiment was conducted by using the solvent extraction method for the natural dye extraction; the doctor blade technique was adapted for the coating of TiO_2 paste, while graphite was employed for the counter electrode material. The experimental results concluded the potential of natural dye from MS and RC to absorb light and produce electricity. The energy conversion efficiency of red cabbage and Malabar spinach-based DSSC was 0.16654% ± 0.00955 and 0.00231% ± 0.00079.

Keywords: dye-sensitized solar cell; natural dye; photosensitizer; graphite; malabar spinach; red cabbage.

1. Introduction

Energy is one of the necessities of humans for everyday needs, from food, water and transportation [1]. Population growth and modernization has contributed to the high increase of energy usage. For generations, people have depended upon non-renewable energy to

supply the everyday energy needs [2,3]. Such energy is extracted from fossils and natural gas, which are classified as nonsustainable energy sources. Due to its limited amount left and inavailability to replenish within human timescale [4]. Moreover, both the extraction process and utilization of non-renewable energy have resulted in various environmental problems that threaten human health and the environment [5,6]. Hence, this crisis has paved the way for sustainable, renewable, and environmentally friendly energy [7].
Renewable energy plays a vital role in mitigating the global energy demand while protecting and preserving the safety of nature and people [8]. Nowadays, energy from the sun is eyed as potential alternative energy due to its wide range of source availability. Solar energy is harvested using photovoltaic (PV) technology [9]. For years, PV technology has been improving since the development of its first generation of solar cells. In the 1990's, the dye-sensitized solar cell was published by Gratzel and O'Regan [10].

Dye-sensitized solar cell is categorized as a third generation of the solar cell. This concept PV cell is to harvest the solar light energy, also known as photons and convert it into electricity. Moreover, it has gained popularity due to its low cost and easy fabrication process. This photoelectrochemical cell utilizes dye molecules or photosensitizers to absorb photons from a light source, injecting the electrons into the electron capture material such as TiO_2 [11]. Currently, the DSSC is still at the early stage of development compared to the conventional solar cell panels that are commercially available. Thus, improving its low light to energy conversion is necessary to increase its performance output.

Over the years, artificial dyes are utilized as photosensitizers due to some advantages [6]. However, making such dyes are complicated, and it uses toxic chemicals that are dangerous to the environment and people. For this reason, researchers are now exploring the use of natural dyes. These dyes are pigments (chlorophyll, anthocyanin, carotenoid and etc.) extracted from different plants found in nature. Notably, natural dyes are easier to produce and cheaper [12]. Furthermore, this study focuses on developing natural dye-based dye-sensitized solar cells utilizing photosensitizer extracted from Malabar spinach fruits and red cabbage.

2. Methodology

2.1. Materials

Natural dye was extracted from Malabar spinach fruits and red cabbage. The Malabar spinach and red cabbage used for this research were collected from Chiang Mai, Thailand and the chemicals such as acetonitrile, methanol, surfactant (Tween 20), acetic acid, iodine were used. Potassium Iodide, Ethylene glycol, HCl, and TiO_2 powder were purchased from Union Science. While the (0.4M) Acetic acid-sodium acetate buffer pH 1.0 and (0.1M) HCl acid-KCl buffer pH 4.5 were prepared in the laboratory. The (FTO) glass was purchased from Hangzhou, Zhejiang, China.

2.2. Extraction of natural dyes

To prepare the malabar spinach dye (MS), the fruits were removed from the stalk and were washed with distilled water and dried at room temperature. Then the fruits were crushed using mortar and pestle and mix with solvent for 10 mins., then filtered using a vacuum pump; the filtrate was stored in a covered container.

For the red cabbage (RC) dye, the vegetable was chopped into smaller pieces and then put in the blender together with the solvent. After it was blended, the solution was kept in a beaker and set aside for 10 mins at room temperature. Lastly, the solid residues were filtered out while the dye extract was stored in a container covered with aluminum foil. Both the Malabar spinach dye and red cabbage dye were kept in the dark storage to avoid light exposure. The combination of 50% malabar spinach (MS) with 50% red cabbage (RC) was prepared by mixing 50 mL of dye from malabar spinach and 50 mL of red cabbage dye. Figure 1c shows the extracted dye from the experiment.

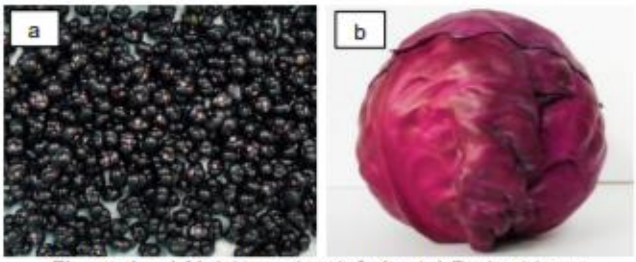

Figure 1. a.) Malabar spinach fruits, b.) Red cabbage

2.3. Anthocyanin pigment content determination

For determining the anthocyanin pigment content of the malabar spinach dye, 50% MS with 50% RC dye and red cabbage dye, light absorbance analysis through spectrophotometer was utilized. The extracted dyes were diluted using two different buffers: (0.4M) Acetic acid-sodium acetate buffer pH 1.0 and (0.1M) HCl acid-KCl buffer pH 4.5. Then, each dye's absorbance at a different wavelength (510 nm, 520 nm, 530 nm, 540 nm, & 700 nm) was checked and examined. In addition, the anthocyanin pigment was calculated using the following equation:

$$APC\left(\frac{mg}{L}\right) = \frac{A * MW * Df * 10^3}{\varepsilon * L} \quad (1)$$

where $A = (A_{\omega} - A_{700nm})_{pH\ 1.0} - (A_{\omega} - A_{700nm})_{pH\ 4.5}$, MW (molecular weight)= 449.2 g/mol, Df is dilution factor, ε= 26,900 L/cm mol, 10^3 is the converting factor for g to mg, and L is the path length in cm.

2.4. Photo-electrode and Counter-electrode preparation

TiO_2 paste was prepared by slowly adding 5% acetic acid to 3g of TiO_2 powder & 0.5 mL surfactants until the paste's desired consistency is achieved. For the homogeneity of the paste, it was thoroughly mixed using a magnetic stirrer for 1hr. Furthermore, after the TiO2 paste preparation, it was coated on the glass, Subsequently, annealed at 240°C for 30 min, then let it cool down. Lastly, the natural dye is added to the surface of TiO_2. The counter electrode was also prepared by adding graphite to the FTO glass and was sintered at 240 ºC for 20 min.

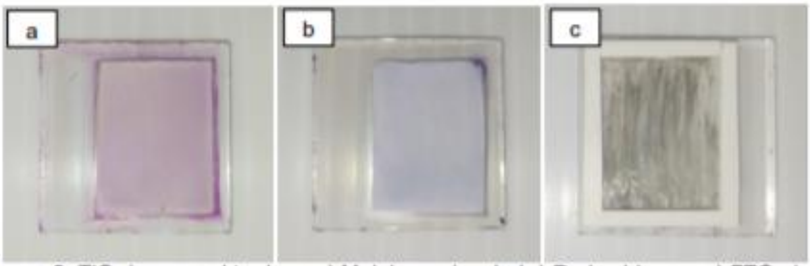

Figure 2. TiO_2 immersed to dye: a.) Malabar spinach, b.) Red cabbage; c.) FTO glass with graphite

2.5 Fabrication of dye-sensitized solar cell

The prepared photo-electrode and counter-electrode film were then assembled and the three sides were sealed with hot-melt glue. Then the electrolyte was injected inside the cell, and the remaining unsealed side was closed. Subsequently, the solar cells' photovoltaic parameters were measured instantly to ensure accurate determination and prevent degradation of photoelectric values caused by aging.

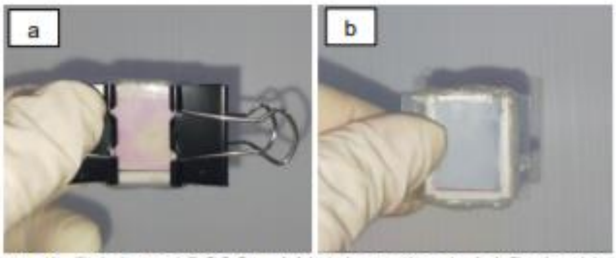

Figure 3. Fabricated DSSC: a.) Malabar spinach, b.) Red cabbage

3. Results & Discussion

3.1. Absorption spectra and Anthocyanin pigment

The color stability of dyes is dependent on the effect of light that passes through them. Characterization of light's effect is mainly focused on by the research regarding the natural dye evaluation [11]. Depending on the state of DSSC, dyes extracted from plants can increase the efficiency in the presence of light. Figure 4a shows the UV-vis analysis of the two different dyes (Malabar spinach dye and Red cabbage); it was found that red cabbage dye had its highest peak at 520 nm, having 0.538 a.u. At the same time, the malabar spinach had 0.319 a.u at 540 nm.

Figure 4b, shows the anthocyanin content recorded at a different wavelength (510 nm, 520 nm, 530 nm,540 nm, & 550) of the natural dye. Moreover, the total anthocyanin pigment of Malabar spinach was 709.87 mg/L and 1007.44 mg/L for Red cabbage. It was observed that red cabbage contains a higher amount of anthocyanin.

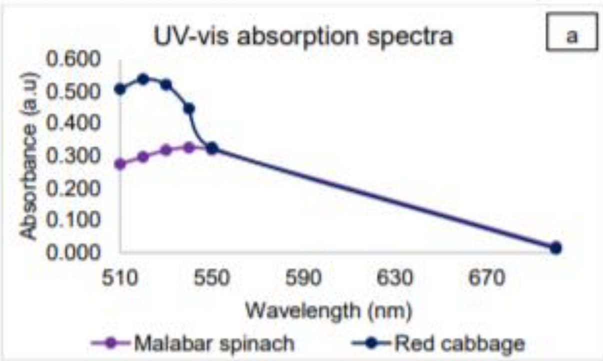

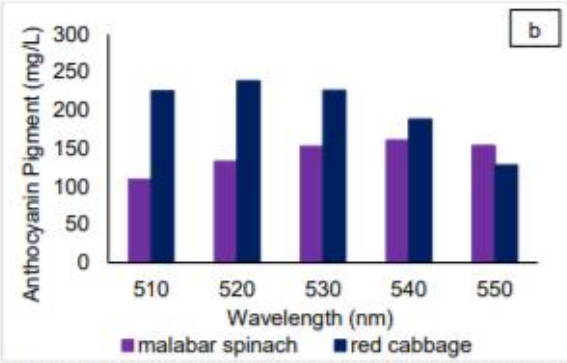

Figure 4. a.) UV-vis absorption spectra and b.) Anthocyanin content.

3.2. Application of natural dye

Anthocyanins are pigments that are soluble in water. Its pH value influences its appearance. Thus, these characteristics pg the pigments enable to act as a natural pH indicator. The contrast in the color appearance of malabar and red cabbage (blue color) is due to the different sort of chemical structure of the pigments and pH. The anthocyanin presents in the red cabbage are delphinidin and cyaniding complexes [13]. Thus, with this result, it can be concluded that the fabrication of multicolored DSSC is feasible

3.3. Photovoltaic performance evaluation

In characterizing the performance output of the fabricated dye-sensitized solar cell, photovoltaic parameters are evaluated: short circuit current density (J_{sc}), open-circuit voltage (V_{oc}), fill factor (ff), and efficiency (η). Moreover, these parameters are determined using the current density-voltage or I-V curve [14].

The photovoltaic performance evaluation of the MS and RC-based solar cell was conducted under the solar irradiation of LED light (white) of 13000 LUX at room temperature. The recorded values of open-circuit voltage (V_{OC}) and short-circuit current density (J_{SC}) of Malabar spinach were 0.171426 V and 0.001359 mA/cm^2, respectively. While the Red cabbage produced V_{OC} = 0.470374 V and J_{SC}= 0.016349 mA/cm^2. Furthermore, the gathered data were then used to calculate the energy conversion efficiency of the DSSC. The efficiency was calculated by using the following equation:

$$n = \frac{P_{max}}{P_{in}} = \frac{(J_{sc} \times V_{oc} \times FF)}{P_{in}} \tag{2}$$

Thus, the calculated efficiency showed that dye-sensitized solar cells integrated with red cabbage photosensitizer gained higher efficiency with 0.16654% ± 0.00955, while the malabar based DSSC has an efficiency output of 0.00231% ± 0.00079. A significant difference between the two natural photosensitizers was observed. Hence, red cabbage exhibited higher potential than malabar spinach. Moreover, it can be concluded that the anthocyanin pigment content of the two dye influenced the photons absorbance of the cell, as well as, its energy conversion. Table 1 shows the list of some natural dye-based DSSC [15-21]. The results of red cabbage show a feasible potential as a photosensitizer. Also, graphite was used as the counter electrode, which is considerably cheaper than platinum; nevertheless, the photoelectric output it exhibited is efficient.

Table 1 Photoelectric performance of DSSC with natural dye from various plants

Natural dye	Jsc (mA/cm²)	Voc (V)	ff	n (%)	Ref
Black rice	-	0.580	0.272	0.0198	[15]
Potato	-	0.51	0.53	0.01	[16]
Mulberry		0.55	0.51	0.05	
Turmeric	0.288	0.529	0.48	0.03	
Tomato	0.51	0.14	0.37	0.03	[17]
Bloodleaf	-	0.267	0.46	0.04	[18]
Orange fruit	0.37	0.06	0.58	0.02	
Carrot	0.36	0.04	0.64	0.009	
Bahraini henna	0.368	0.426	24.6	0.128	[19]
Gree algae	-	0.32	0.37	0.01	[20]
Walnuts	0.73	0.304	0.39	0.0104	[21]
Malabar spinach	0.001359	0.171426	0.18856	0.00231 ± 0.00079	This study
Red cabbage	0.016349	0.470374	0.41221	0.16654 ± 0.00955	This study

4. Conclusion

This study's resulting data shows the natural dye's potential extracted from Malabar spinach and red cabbage as a photosensitizer. With the fabrication of dye-sensitized solar cells, it was found out that red cabbage has an efficiency of 0.16654% ± 0.00955 while Malabar spinach has an efficiency of 0.00231% ± 0.00079. Concerning this, the higher total amount of anthocyanin was evaluated from red cabbage dye having 1007.44 mg/L. In comparison, the Malabar spinach dye has 709.87 mg/L. Thus, it can be concluded that the higher pigment content in red cabbage dye made it possible for the DSSC to absorb more light and converted it into electricity. In conclusion, the methods used in this experimental study can contribute to the development and improvement of inexpensive and effective natural dye as photosensitizers for the dye-sensitized solar cell.

5. Acknowledgement

The authors would like to thank the School of Renewable Energy, Energy Research Center, and Program in Biotechnology, Maejo University, Chiang Mai, Thailand, for the research facilities to accomplish this research.

References

[1] Mejica GFC, Unpaprom Y, Ramaraj R (2020). Anthocyanin pigment evaluation and development of multicolored natural dye from malabar spinach and red cabbage as a potential dye sensitizer doe dye-sensitized solar cell. Proceedings of the 13th Seminar on Science & Technology, 6 – 7

[2] Mejica GFC, Unpaprom Y, Whangchai K and Ramaraj R 2021 Cellulosic-derived bioethanol from *Limnocharis flava* utilizing alkaline pretreatment. Biomass Conversion and Biorefinery. https://doi.org/10.1007/s13399-020-01218-7

[3] Kabir F, Bhuiyan MMH, Manir MS, Rahaman MS, Khan MA and Ikegami T, Development of dye-sensitized solar cell based on combination of natural dyes extracted from Malabar spinach and red spinach. Results Phys., vol. 14, 2019

[4] Tu N, Unpaprom Y, Tandee K, Whangchai K and Ramaraj R 2020 Physical pretreatment and algal enzyme hydrolysis of dried low-grade and waste longan fruits to enhance its fermentable sugar production. Biomass Conversion and Biorefinery. 1-9. 10.1007/s13399-020-01176-0.

[5] Nong H, Unpaprom Y, Whangchai K, Buochareon S and Ramaraj R 2020 Assessment of the effects of anaerobic co-digestion of water primrose and cow dung with swine manure on biogas yield and biodegradability. Biomass Conversion and Biorefinery. 1-11. 10.1007/s13399-020-01115-z.

[6] Sophanodorn K, Unpaprom Y, Whangchai K, Duangsuphasin A, Manmai, N and Ramaraj R 2020 A biorefinery approach for the production of bioethanol from alkaline-pretreated, enzymatically hydrolyzed Nicotiana tabacum stalks as feedstock for the bio-based industry. Biomass Conversion and Biorefinery. 1-9. 10.1007/s13399-020-01177-z.

[7] Manmai N, Unpaprom Y, Ponnusamy VK and Ramaraj R 2020 Bioethanol production from the comparison between optimization of sorghum stalk and sugarcane leaf for sugar production by chemical pretreatment and enzymatic degradation. Fuel. 278. 118262. 10.1016/j.fuel.2020.118262.

[8] Unpaprom Y, Pimpimol T, Whangchai K and Ramaraj R 2020 Sustainability assessment of water hyacinth with swine dung for biogas production, methane enhancement, and biofertilizer. Waste and Biomass Valorization. 1-12. 10.1007/s13399-020-00850-7.

[9] Lau KKS and Soroush M 2019 Chapter 1 - Overview of Dye-Sensitized Solar Cells," M. Soroush and K. K. S. B. T.-D.-S. S. C. Lau, Eds. Academic Press, pp. 1–49.

[10] O'Regan B and Grätzel M 1991 'A low cost, high-efficiency solar cell based on dyesensitized colloidal TiO2 films'. NATURE

[11] Mejica GFC, Unpaprom Y, Ramaraj R (2020). Extraction of anthocyanin pigments from malabar spinach fruits as a potential photosensitizer for dye-sensitized solar cell. Global Journal of Science & Engineering 02:5–9

[12] Khammee P, Unpaprom Y, Whangchai K andRamaraj, R 2020 Comparative studies of the longan leaf pigment extraction as a photosensitizer for dye-sensitized solar cells' purpose. Biomass Conversion and Biorefinery. 1-8. 10.1007/s13399-020-01060-x.

[13] Gokilamani N, Muthukumarasamy N, Thambidurai M, Ranjitha A and Velauthapillai D 2013 Utilization of natural anthocyanin pigments as photosensitizers for dye-sensitized solar cells, Journal of Sol-Gel Science and Technology, 66, (2), pp 212-219

[14] Kumara NTRN, Lim A, Lim CM, Petra MI and Ekanayake P 2017 "Recent progress and utilization of natural pigments in dye sensitized solar cells: A review," Renewable and Sustainable Energy Reviews 78:301–317

[15] Ahliha AH, Nurosyid F, Supriyanto A and Kusumaningsih T 2017 The chemical bonds effect of anthocyanin and chlorophyll dyes on TiO2 for dye-sensitized solar cell (DSSC). InJournal of Physics: Conference Series 909(1): 012013, IOP Publishing.

[16] Chandra Maurya I, Singh S, Srivastava P, Maiti B and Bahadur L 2019 Natural dye extract from Cassia fistula and its application in dye-sensitized solar cell: Experimental and density functional theory studies. Optical Materials, 90(273-280)

[17] Supriyanto A, Nurosyid F and Ahliha AH 2018 Carotenoid pigment as sensitizers for applications of dyesensitized solar cell (DSSC). IOP Conf. Series: Materials Science and Engineering.

[18] Moustafa KF, Rekaby M, El Shenawy ET, Khattab NM 2012 Green dyes as photosensitizers for dye-sensitized solar cells. J Appl Sci Res;8 4393-04

[19] Jasim KE 2012.Natural dye-sensitized solar cell based on nanocrystalline TiO2. Sains Malaysiana; 41:1011–6.

[20] Shalini S, Prabhu R, Mallick, Tapas & Sundaram, Senthilarasu. (2015). Review on natural dye sensitized solar cells: Operation, materials and methods. Renewable and Sustainable Energy Reviews.

[21] El-Agez TM, El Tayyan AA, Al-Kahlout A, Taya SA, Abdel-Latif MS, 2012 DyeSensitized solar cells based on ZnO films and natural dyes. International Journal of Materials and Chemistry 2:105–110

Poster Presentation at International Conference on Challenges and Progress in Biosciences and Engineering – (ICCPBE 2021)

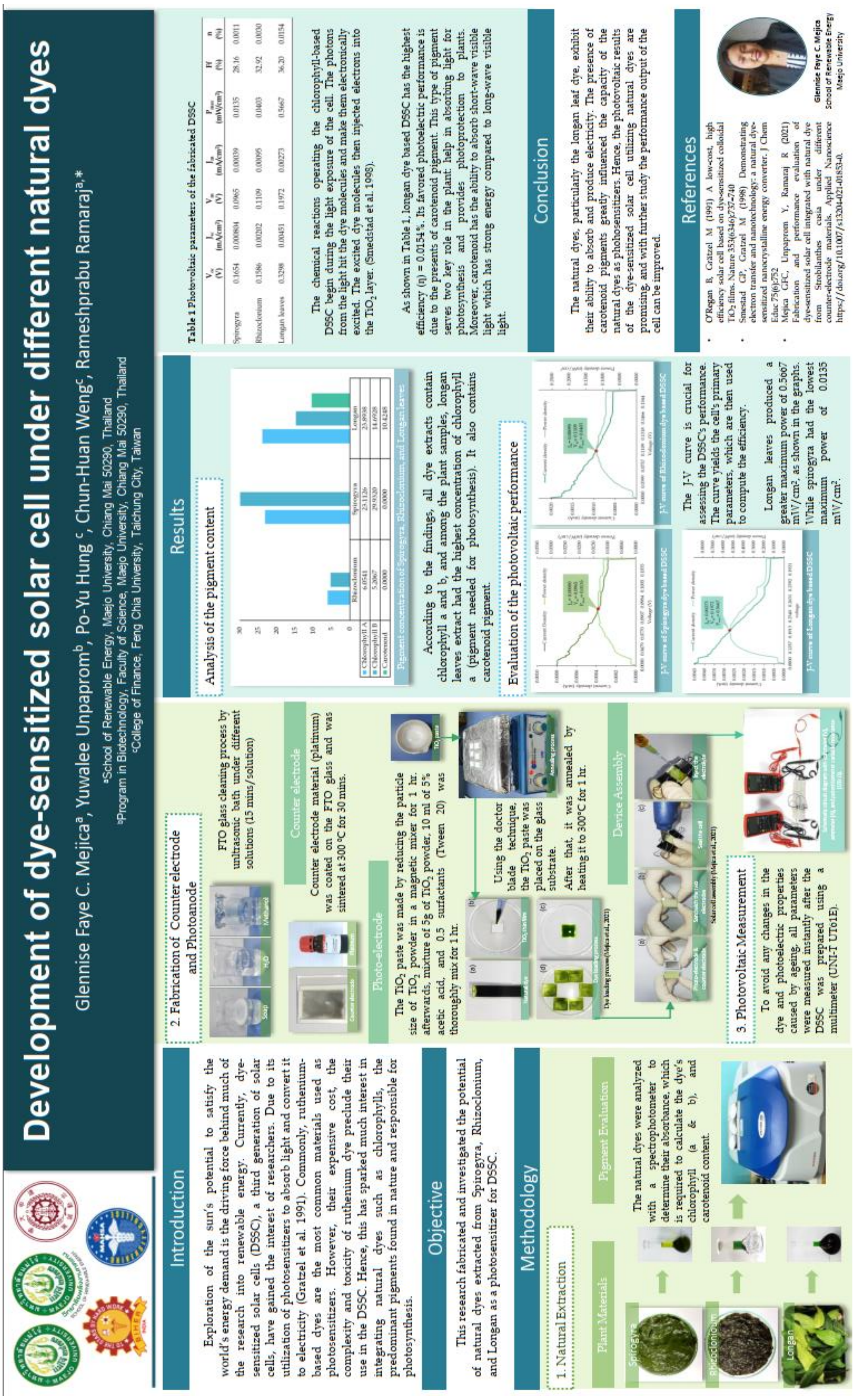

APPENDIX B

PUBLICATION

Biomass Conversion and Biorefinery
https://doi.org/10.1007/s13399-020-01218-7

ORIGINAL ARTICLE

Cellulosic-derived bioethanol from *Limnocharis flava* utilizing alkaline pretreatment

Glennise Faye C. Mejica [1,2] · Yuwalee Unpaprom [2,3] · Kanda Whangchai [4] · Rameshprabu Ramaraj [1,2]

Received: 21 October 2020 / Revised: 7 December 2020 / Accepted: 14 December 2020

Abstract
Increasing demand for energy and environmental issues has laid various opportunities for research and development of sustainable, renewable, and environmentally friendly energy. Production of ethanol from biomass has been the focus of researchers due to its feasible characteristics in meeting global energy demands. Moreover, the second-generation ethanol or the ethanol derived from lignocellulosic biomass has been favored due to its diverse biomass resources such as wood, grass, agricultural residue, and municipal waste (newspaper). Hence, *Limnocharis flava*, an aquatic plant and considered a weed, was investigated and converted into bioethanol. For optimization, the lignocellulosic biomass was examined by various alkaline treatments (0% alkaline, 1% CaO, 2% CaO, and 2% NaOH) to distinguish the suitable pretreatment that can break down lignin, cellulose, and hemicellulose to form sugars that can be fermented to produce bioethanol. Significantly, 1% CaO showed favorable results of ethanol yield of 6.31 ± 0.72 g/L with a total and reducing sugars of 50.81 g/L and 28.88 g/L, respectively. Thus, it can be concluded that bioethanol can be derived from *L. flava*.

Keywords Lignocellulosic biomass · Bioethanol · *Limnocharis flava* · Alkaline pretreatment · Cellulosic-derived ethanol

1 Introduction

Population explosion and industrialization escalated global energy demand. Throughout history, human has relied upon fossils as the primary source of energy [1–3]. However, fuels derived from such sources have brought huge drawbacks that resulted in serious environmental issues and posed a risk to human health [4, 5]. The researchers are finding ways to lessen people's reliance on energy derived from non-renewable sources to mitigate the problem. The main goal is to search and develop sustainable, renewable, also environmentally friendly energy [6, 7]. Hence, bioethanol production from biomass has captured different institutions' interests due to its feasible characteristics and potential to suffice the global energy demand.

Derivation of bioethanol from renewable organic material, or also known as biomass, exhibits promising potential to replace fossil fuels [8]. It is a type of renewable fuel produced by fermenting the sugar and starch content of the biomass. The well-established source of bioethanol is from sugarcane and corn. Hence, such sources are categorized as the first generation of bioethanol production. Moreover, the utilization of this sort of biomass has been debated considering its effect on food supply [9, 10]. Another type of bioethanol production is the second generation, known as bioethanol's derivation from lignocellulosic biomass. In this generation, the feedstock used is from the lignocellulosic plant, such as wood, grasses, weeds, and agricultural waste [11]. Lignocellulosic-based bioethanol has gained researchers' interest due to the wide availability of lignocellulosic biomass. Consequently, it can reduce agricultural crops' consumption as feedstock for producing ethanol [12]. In addition, lignocellulosic material is inexpensive; as raw material cost contributes more than 50% to the production cost, it is economically competitive [13].

Lignocellulosic biomass is generally composed of three structural polymers: cellulose, hemicellulose, and lignin.

✉ Rameshprabu Ramaraj
rameshprabu@mju.ac.th; rrameshprabu@gmail.com

1 School of Renewable Energy, Maejo University, Chiang Mai 50290, Thailand

2 Sustainable Resources & Sustainable Engineering Research Lab, Maejo University, Chiang Mai 50290, Thailand

3 Program in Biotechnology, Faculty of Science, Maejo University, Chiang Mai 50290, Thailand

4 Center of Excellence in Bioresources for Agriculture, Industry and Medicine, Chiang Mai University, Chiang Mai 50200, Thailand

Published online: 06 January 2021

Among these polymers, only cellulose and hemicellulose are convertible to fermentable sugar. One of the simplest ways to convert such biomass into sugars is through enzymatic hydrolysis or saccharification. However, the main problem is the low accessibility of cellulose and hemicellulose due to cellulose's strong chemical bond with lignin. Therefore, pretreatment is necessary to break down the lignin, which hinders the saccharification process [14, 15].

Nevertheless, the trend for bioethanol production is mainly focused on utilizing invasive plant species or inedible crops as feedstock and enhancing its bioethanol conversion efficiency [16]. This concept is beneficial in mitigating the competition between first-generation ethanol and food supply for humans. This will valorize the purpose of unwanted plant species, especially the aquatic weeds, which often obstruct the irrigation system's water flow and occupy vast areas. The utilization of aquatic weed is advantageous due to being inedible, widely available, and faster without human labor [11, 12, 15]. This will help solve the problem due to the rampant growth of invasive aquatic weed in the waterways channel.

One kind of invasive aquatic plant is the *L. flava* also known as yellow velvet. This plant is commonly found in canals, rice fields, and rivers. Due to its proliferation in the waterways, it causes floods and hinders the flow of water. The yellow velvetleaf is also widely available inside the Maejo University Campus; unfortunately, it causes a lot of labor and cost for the temporary solution of controlling the plant's fast growth in the waterways channel. Moreover, finding ways to convert this undesired weed into renewable energy can valorize its presence. Also, there is no data about lignocellulosic-based bioethanol from *Limnocharis flava*. Hence, it would be an opportunity to investigate the plant's potential as a raw material for bioethanol. This study investigated bioethanol's derivation from lignocellulosic biomass: *Limnocharis flava*, an aquatic weed, and employment of different alkaline pretreatments (1% CaO, 2% CaO, and 2% NaOH) to distinguish the optimal pretreatment that can disintegrate lignin.

2 Materials and methods

2.1 Substrate preparation

The aquatic weed *Limnocharis flava*, also known as yellow velvetleaf, was collected from the waterways channel inside Maejo University, Chiang Mai, Thailand. The roots were removed, subsequently thoroughly rinsed with tap water to remove dirt, chopped to smaller size, dried in the oven at 60 °C for 3 days, and blended to pulverize the dried sample (Fig. 1).

2.2 Alkaline pretreatment

The pulverized lignocellulosic *L. flava* was treated with 300 mL of varying concentrations of CaO (1% and 2%) and 2% NaOH at a 5% proportion biomass loading, and the mixture was kept in a 1000-mL Duran glass bottle at room temperature and settled for 3 days. Following that, total sugar (TS) and reducing sugar (RS) were assessed by preparing an aliquot of the pretreated mixture, centrifuged at 700 rpm for 15 min. Sulfuric acid and 5% phenol were used to estimate the reducing sugar and the DNS method was utilized for total sugar. Total sugar and reducing sugar concentration estimation procedures were adopted from Dubois et al. [16] and Miller [17].

2.3 Enzymatic hydrolysis

The process was conducted by adjusting the pH of each pretreated solution to pH 5 using 5 N HCl. Afterward, 2% (v/v) of commercial cellulase (2398 units/g, 577 units/g β-glucosidase, and pH 4) purchased from Union Science Company, Chiang Mai, Thailand and 0.125% (v/v) surfactant (Tween 20) were added to each solution. Subsequently, the enzymatic solution was incubated at 30 °C for 2 days (Fig. 2). Three replicates were prepared in all the experiments, and non-chemicalized (0% chemical) substrate was set as control.

2.4 Fermentation of *Limnocharis flava*

Liquid hydrolysates obtained after saccharification were examined for TS and RS content. The hydrolysate that showed the favorable amount of TS and RS, which is then hydrolyzed as substrate pretreated with 1% CaO, was chosen and proceeded to the fermentation process. The hydrolyzed substrate's pH was adjusted to pH 5.6 using 5 N HCl, succeeded by the addition of 2% (w/v) dry yeast (*Saccharomyces cerevisiae*). The resulting concoction was then incubated at 30 °C for 5 days.

2.5 Ethanol estimation

The ethanol estimation and TS and RS calculation were done every 24 h of fermentation for 5 days. The evaluation was prepared by getting 60 mL (including for TS and RS analysis) of the solution, centrifuged at 1000 rpm for 15 min. Ebulliometer (Dujardin-Salleron, Alcohol Burner, France) was then used to check the fermented concoction's alcohol percentage [11].

2.6 Statistical analysis

The experiment was conducted with three replicates. Hence, the data were presented as mean ± standard deviation (SD).

Fig. 1 Sample collection and preparation of *Limnocharis flava* (**a**–**d**)

Statistical analyses were performed using computer-based software SPSS. The difference in values is indicated in the form of probability ($p < 0.05$) values.

3 Results and discussion

3.1 Characteristics of *Limnocharis flava*

The proliferation of various aquatic weeds such as *L. flava* in waterways obstructs the water flow for irrigation and can flood. *Limnocharis flava*, also known as yellow velvetleaf, is an aquatic plant commonly found in waterways channel and rice fields. Moreover, this plant is considered an aquatic weed due to its undesirability in the waterways system. In some regions, the flowers and leaves are utilized as an ingredient for various dishes. According to Saupi et al. [18], *L. flava* leaves contain 79.34% moisture content, 0.79% ash, 0.28% crude protein, 1.22% crude protein of 3.81% crude fiber, and 14.56% total carbohydrate. Ooh et al. [19] reported, in comparison to other plants, yellow velvetleaf consists of a larger amount of phenolic such as p-HBA (hydroxybenzoic acids), CFA. In addition, the plant was also detected with rutin.

3.2 Effect of alkaline pretreatment on *Limnocharis flava*

The complex chemical structure of lignin to cellulose has difficulty accessing the carbohydrate polymers (cellulose and hemicellulose), making it complicated to disintegrate and convert cellulose hemicellulose into fermentable sugar [19, 20]. Therefore, pretreatment is necessary to break down lignin barriers and make the cellulosic fraction responsive to enzymatic hydrolysis or saccharification. Pretreatment is a major factor in overall bioconversion efficiency [7, 8]. Delignifying lignocellulosic biomass with alkaline pretreatment has been one of the pioneer pretreatment processes used due to its number of desirable characteristics.

Delignification of *L. flava* was conducted by employing different alkaline pretreatments (1% CaO, 2% CaO, and 2% NaOH) and substrate treated with H_2O was set as control. Among the above pretreatment solutions, 1% CaO produced higher reducing sugar (38.125 g/L) followed by 2% NaOH (21.125 g/L), as shown in Fig. 3.

Fig. 2 Hydrolysis of pretreated substrate and incubation for 2 days (a and b), laboratory scale of fermentation process of substrate pretreated with 1% CaO

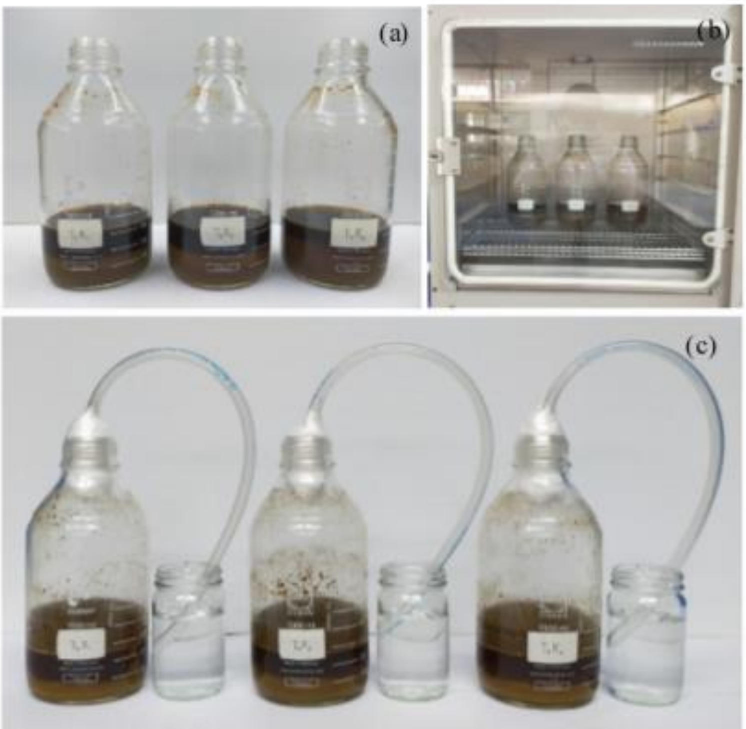

Mood et al. [22] and Kim et al. [23] mentioned that during the alkaline pretreatment process, the substrate mainly undergoes disintegration of lignin, dissolution of cellulose, and hemicellulose as well as saponification of intermolecular bonds of ester, destroying the chemical bond of hemicellulose and other chemical compounds resulting to delignification of lignocellulosic substrate. In addition, this also alters the intensity of cross-linking polymers, hence, resulting to changes in the porosity, surface range, and crystallinity of the treated substrates.

In evaluating the pretreatment's reducing sugar, results suggested that 1% CaO is more effective for delignifying *L. flava*. The utilization of CaO for pretreatment is also advantageous due to its cheaper cost, availability,

Fig. 3 Total and reducing sugar accumulated after pretreatment

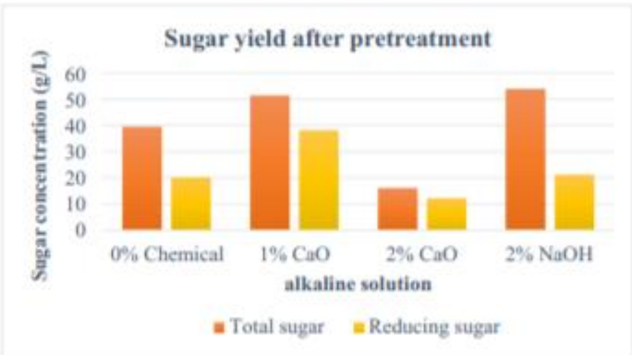

Table 1 Enzymatic hydrolysis yields of *Limnocharis flava* after alkaline pretreatment

Sugar	Alkaline concentration (% w/v)			
	0%	1% CaO	2% CaO	2% NaOH
Reducing sugar (g/L)	49.52 ± 0.18	57.73 ± 0.46	30.92 ± 0.69	52.75 ± 0.47
Total sugar (g/L)	68.65 ± 0.14	78.65 ± 0.29	62.71 ± 0.13	77.01 ± 0.13

innocuous feature, and easy usage [7, 8]. According to Hammel et al. [24], the hydrocarbon chains (ether and ester) in the lignocellulosic substrate are severed by the alkaline treatments making the cellulose and hemicellulose more accessible for enzymatic hydrolysis. Considering the characteristics of *L. flava*, ester bonds are mainly found to this biomass; hence, the application of CaO pretreatment is more suitable and effective for grass pretreatment [7, 8]. The crucial role of lime in pretreatment is that it detaches acetyl groups and disintegrates 30% of the lignin in the substrate. Moreover, lower lignin concentration promulgates better enzymatic hydrolysis or saccharification.

3.3 Enzymatic hydrolysis

Enzymatic hydrolysis of the pretreated substrate is a crucial step in bioethanol derivation. It is the key component that converts the accessible polysaccharide (cellulose and hemicellulose) after breaking down the lignin barriers during pretreatment into fermentable sugar (glucose and fructose) [21]. The process is aided by the use of microbial enzymes, known as cellulase. The cellulase speeds up the hydrolysis and breaks down cellulose into simple sugar (monosaccharides). The saccharification process determines the effective pretreatment in destroying the cross-linkage bond of lignin barriers, releasing the polysaccharides. Cellulase is more responsive in breaking down cellulose into glucose [10, 11, 21].

The results in Table 1 showed the sugar yield after hydrolyzing the substrate pretreated with a different alkaline solution (0% chemical, 1% CaO, 2% CaO, and 2% NaOH). Among the treatment above, 1% CaO exhibited higher TS and RS, having 78.27 ± 3.09 g/L and 59.60 ± 2.66 g/L, respectively, while 2% NaOH produced 77.01 ± 0.13 g/L TS and 52.75 ± 0.47 g/L RS, followed by 0% (control) having 68.65 ± 0.14 g/L TS and 49.52 ± 0.18 g/L RS. Moreover, 2% CaO gained the lowest amount of sugar concentration; it can be concluded that increasing the amount of CaO was not effective in breaking down the lignocellulosic biomass: *Limnocharis flava*. Considering the cost, safe characteristics, and effectiveness of 1% CaO, the solution was determined as the suitable treatment and further used for the fermentation process.

During hydrolysis, various sugars are generated, such as hexose ($C_6H_{12}O_6$) and pentose ($C_5H_{10}O_5$), mainly comprised of the carbohydrates found in lignocellulosic biomass through enzymes using monosaccharides and resulting in the conversion of bioethanol. Furthermore, the hydrolyzed substrate contains a higher amount of sugar [25]. Nevertheless, the cost of producing ethanol must be considered throughout the process. It is essential in order to achieve economically friendly bioethanol production [26]. Hence, the implementation of 1% CaO can suffice the standard with relatively good effectivity.

3.4 Ethanol fermentation

Conversion of fermentable sugar into ethanol is the principal key to the production of bioethanol. Fermentation is a biological process of converting fermentable sugar using a microorganism isolated in an anaerobic condition. The utilization of dry yeast, *S. cerevisiae*, is one of the pioneer microorganisms in the bioethanol industry. It is known to convert fermentable sugar into ethanol [26, 27] efficiently.

In this study, the 1% CaO liquid hydrolysate was selected to undergo fermentation. The fermentation process was conducted for 5 days (120 h) to investigate the highest ethanol yield of *L. flava*. Every 24 h for 5 days, the ethanol content and the sugar concentration (TS and RS) of the concoction were checked. As shown in Table 2, the highest ethanol yield of 6.31 ± 0.72 g/L was achieved at 24 h of fermentation with a

Table 2 Sugar and bioethanol concentration yield within 120 h of fermentation

Sugar	Fermentation time				
	24 h	48 h	72 h	96 h	120 h
Reducing sugar (g/L)	28.88	16.54	16.83	15.31	12.30
Total sugar (g/L)	50.81	39.79	34.74	30.44	25.22
Bioethanol content (g/L)	6.31 ± 0.72	5.79 ± 1.18	5.02 ± 1.13	4.76 ± 0.84	4.31 ± 1.11

Table 3 Ethanol production from lignocellulosic biomass

Lignocellulosic biomass	Pretreatment	Enzyme	EtOH production	Reference
Limnocharis flava	1% CaO	*S. cerevisiae*	6.31 g/L	This study
Vetiveria zizanioides	Alkaline peroxide	*S. cerevisiae* TISTR 5339 + *P. stipitis* CBS 5773	0.14 g/L	[28]
Panicum maximum cv. TD 53	Calcium hydroxide	*S. cerevisiae*	5.9 g/L	[29]
Laminaria japonica	Thermal	*Pichia stipites* KCTC 7228	2.9 g/L	[30]
Sago pith flour	Sulfuric acid	*Issatchenkia orientalis*	2.8 g/L	[31]
Bagasse	Ionic liquid	*S. cerevisiae* MT8-1	0.69 g/L	[32]

total and reducing sugars of 50.81 g/L and 28.88 g/L, respectively. It was observed that after 24 h of fermentation, the ethanol production was constantly decreasing until the 5th day of the experiment. On the other hand, the results gained from this study prove the potential of *L. flava* as a feedstock for the derivation of lignocellulosic-based ethanol. In addition, Table 3 presents the ethanol production from various lignocellulosic biomass, such as weeds and agricultural waste. For comparison, *L. flava* produced a significant amount of 6.31 g/L ethanol. Therefore, it can be concluded that bioethanol can be derived from *L. flava*.

4 Conclusion

This present study investigated the potential of *L. flava* as an alternative and inexpensive feedstock for the derivation of bioethanol. Thus, it examined various alkaline treatments (0%, 1% CaO, 2% CaO, and 2% NaOH) in delignifying the lignocellulosic biomass. Based on the research results, 1% CaO showed a significant amount of total sugar and reducing sugar with 50.81 g/L and 28.88 g/L, respectively, and an ethanol yield of 6.31 ± 0.72 g/L. The highest ethanol production was observed after 24 h of the fermentation, subsequently decreasing for the next 24 h until the last day of fermentation. Aside from the sugar produced, the cost and harmless characteristic of CaO made it an ideal pretreatment due to its low environmental impact and safer usage. This experiment showed the capability of *L. flava* to produce ethanol compared to other invasive plants. Hence, this study can valorize the yellow velvetleaf plant to provide an alternative and more sustainable feedstock for bioethanol.

Acknowledgments The authors gratefully acknowledged the School of Renewable Energy, Program in Biotechnology, and Energy Research Center, Maejo University, Chiang Mai, Thailand for the research facilities to accomplish this experimental study.

Compliance with ethical standards

Conflict of interest The authors declare that they have no conflict of interest.

References

1. Nguyen TVT, Unpaprom Y, Tandee K, Whangchai K, Ramaraj R (2020) Physical pretreatment and algal enzyme hydrolysis of dried low-grade and waste longan fruits to enhance its fermentable sugar production. Biomass Conv Bioref. https://doi.org/10.1007/s13399-020-01176-0
2. Saengsawang B, Bhuyar P, Manmai N, Ponnusamy VK, Ramaraj R, Unpaprom Y (2020) The optimization of oil extraction from macroalgae, *Rhizoclonium* sp. by chemical methods for efficient conversion into biodiesel. Fuel 274:117841
3. Mejica GFC, Unpaprom Y, Ramaraj R (2020) Extraction of anthocyanin pigments from malabar spinach fruits as a potential photosensitizer for dye-sensitized solar cell. Global Journal of Science & Engineering 02:5–9
4. Nguyen TV, Unpaprom Y, Manmai N, Whangchai K, Ramaraj R (2020) Impact and significance of pretreatment on the fermentable sugar production from low-grade longan fruit wastes for bioethanol production. Biomass Convers Biorefin. https://doi.org/10.1007/s13399-020-00977-7
5. Bhuyar P, Sundararaju S, Rahim MH, Ramaraj R, Maniam GP, Govindan N (2019) Microalgae cultivation using palm oil mill effluent as growth medium for lipid production with the effect of CO_2 supply and light intensity. Biomass Convers Biorefin 26:1–9
6. Ramaraj R, Kawaree R, Unpaprom Y (2016) A newly isolated green alga, *Pediastrum duplex* Meyen, from Thailand with efficient hydrogen production. IJSGE 4:7–12
7. Sophanodorn K, Unpaprom Y, Whangchai K, Duangsuphasin A, Manmai N, Ramaraj R (2020, 2020) A biorefinery approach for the production of bioethanol from alkaline-pretreated, enzymatically hydrolyzed *Nicotiana tabacum* stalks as feedstock for the bio-based industry. Biomass Conv Bioref. https://doi.org/10.1007/s13399-020-01177-z
8. Sophanodorn K, Unpaprom Y, Whangchai K, Homdoung N, Dussadee N, Ramaraj R (2020) Environmental management and valorization of cultivated tobacco stalks by combined pretreatment for potential bioethanol production. Biomass Conv Bioref. https://doi.org/10.1007/s13399-020-00992-8
9. Khammee P, Ramaraj R, Whangcha NBP, Unpaprom Y (2020) The immobilization of yeast for fermentation of macroalgae *Rhizoclonium* sp. for efficient conversion into bioethanol. Biomass Conv Bioref. https://doi.org/10.1007/s13399-020-00786-y
10. Ramaraj R, Unpaprom Y (2019) Optimization of pretreatment condition for ethanol production from *Cyperus difformis* by response surface methodology. 3. Biotech 9(6):218
11. Vu PT, Unpaprom Y, Ramaraj R (2018) Impact and significance of alkaline-oxidant pretreatment on the enzymatic digestibility of *Sphenoclea zeylanica* for bioethanol production. Bioresour Technol 247:125–130

12. Manmai N, Siriboon T, Tipnee S, Unpaprom Y, Ramaraj R (2017) Bioconversion of lignocellulosic biomass, *Sorghum bicolor* L. into bioethanol. Proceedings of Academics World 73rd International Conference, Taipei, Taiwan, 41–45
13. Chuanchai A, Ramaraj R (2018) Sustainability assessment of biogas production from buffalo grass and dung: biogas purification and bio-fertilizer. 3. Biotech 8(3):151
14. Tu V, Yuwalee U, Piyapat C, Rameshprabu R (2020) Improvement of bioethanol production from low grade and damaged longan fruits with thermal pretreatment and different types of the enzymatic hydrolysis. Int J Eng Sci 3:10–15
15. Vu P, Unpaprom Y, Ramaraj R (2017) Evaluation of bioethanol production from rice field weed biomass. Emerg Life Sci Res 3: 42–49
16. Dubois M, Gilles K, Hamilton J, Rebers P, Smith F (1956) Colorimetric method for determination of sugars and related substances. Anal Chem 28(3):350–356
17. Miller G (1959) Use of dinitrosalicylic acid reagent for determination of reducing sugar. Anal Chem 31(3):426–428
18. Saupi N, Zakaira MH, Bujang JS (2009) Analytic chemical composition and mineral content of yellow velvetleaf (*Limnocharis flava* L. Buchenau)'s edible parts. J Appl Sci 9(16):2969–2974
19. Ooh KF, Ong HC, WONG F, Chai TT (2015) HPLC profiling of phenolic acids and flavonoids and evaluation of anti-lipoxygenase and antioxidant activities of aquatic vegetable *Limnocharis flava*. Acta Pol Pharm 72(5):973–979
20. Nong HT, Whangchai K, Unpaprom Y, Thararux C, Ramaraj R Development of sustainable approaches for converting the agro-weeds *Ludwigia hyssopifolia* to biogas production. Biomass Conv Bioref. https://doi.org/10.1007/s13399-020-01083-47
21. Ramaraj R, Unpaprom Y (2019) Enzymatic hydrolysis of small-flowered nutsedge (*Cyperus difformis*) with alkaline pretreatment for bioethanol production. Maejo Int J Sci Technol 13(2):110–120
22. Mood SH, Golfeshan AH, Tabatabaei M, Jouzani GS, Najafi GH, Gholami M, Ardjmand M (2013) Lignocellulosic biomass to bioethanol, a comprehensive review with a focus on pretreatment. Renew Sust Energ Rev 27:77–93
23. Kim JS, Lee YY, Kim TH (2016) A review on alkaline pretreatment technology for bioconversion of lignocellulosic biomass. Bioresour Technol 199:42–48
24. Hammel KE, Cullen D (2008) Role of fungal peroxidases in biological ligninolysis. Curr Opin Plant Biol 11(3):349–355
25. Manmai M, Bautista K, Unpaprom Y, Ramaraj R (2019) Optimization of combined pretreatments on sugarcane leaves for bioethanol production. Maejo Int J Energ Environ Comm 1(1):30–39
26. Manmai N, Siriboon T, Unpaprom Y, Ramaraj R (2017) Bioethanol from lignocellulosic biomass: a comparison between sunflower stalk and sorghum stalk. Proceedings of the 24th Tri-University International Joint Seminar and Symposium, Mie University, Japan, 1–4
27. Manmai N, Unpaprom Y, Ramaraj R (2018) Effect of chemical pretreatment on enzymatic hydrolysis and fermentation of corn stalks for ethanol production. Proceedings of the 6th ASCON-IEEChE 2018, Sun Moon Lake, Taiwan, 375–382
28. Ullah K, Kumar Sharma V, Dhingra S, Braccio G, Ahmad M, Sofia S (2015) Assessing the lignocellulosic biomass resources potential in developing countries: a critical review. Renew Sust Energ Rev 51(Supplement C):682–698
29. Prasertwasu S, Khumsupan D, Komolwanich T, Chaisuwan T, Luengnaruemitchai A, Wongkasemjit S (2014) Efficient process for ethanol production from Thai Mission grass (*Pennisetum polystachion*). Bioresour Technol 163:152–159
30. Lee SM, Lee JH (2012) Ethanol fermentation for main sugar components of brown-algae using various yeasts. J Ind Eng Chem 18: 16–18
31. Sunarti TC, Yanti SD, Ruriani E (2017) Twosteps microwave-assisted treatment on acid hydrolysis of sago pith for bioethanol production. InIOP Conf. Series: Earth Environ Sci 65:1755–1315
32. Yamada R, Nakashima K, Asai-Nakashima N, Tokuhara W, Ishida N, Katahira S, Kamiya N, Ogino C, Kondo A (2017) Direct ethanol production from ionic liquid-pretreated lignocellulosic biomass by cellulase-displaying yeasts. Appl Biochem Biotechnol Appl Biochem Biotechnol 182(1):229–237

Applied Nanoscience
https://doi.org/10.1007/s13204-021-01853-0

ORIGINAL ARTICLE

Fabrication and performance evaluation of dye-sensitized solar cell integrated with natural dye from *Strobilanthes cusia* under different counter-electrode materials

Glennise Faye C. Mejica[1,2] · Yuwalee Unpaprom[2,3] · Rameshprabu Ramaraj[1,2]

Received: 6 March 2021 / Accepted: 15 April 2021

Abstract
The ruthenium-based dye and platinum (pt) are the most common materials used as photosensitizer and counter electrode (CE), respectively, in the production of the dye-sensitized solar cell (DSSC), the third generation of photovoltaic technologies. However, their expensive cost, the complexity and toxicity of ruthenium dye, and the scarcity of pt's sources preclude their use in the DSSC. Thus, this has sparked much interest in integrating natural dyes such as chlorophylls, the predominant pigments found in nature and responsible for photosynthesis, and exploring platinum-free CE in developing DSSC. This research investigated the natural dye from *Strobilanthes cusia* (SC) and evaluated the performance output under the three various counter electrode materials: a. fluorine-doped tin oxide (FTO) CE; b. graphite/FTO CE; and c. pt/FTO CE. Hence, from this study's results, it was found that the SC dye is primarily composed of Chl-a with 64.5345 ± 0.4226 μg/ml followed by Chl-b with 41.4341 ± 0.2636 μg/ml. While in the photovoltaic performance of the SC dye-based DSSC the graphite/FTO CE showed higher photoelectric output having an open-circuit voltage (V_{oc}) of 306.35 mV, short circuit current (I_{sc}) of 15.55 μA, ff = 0.462, maximum power (P_{MAX}) of 0.734 μW/cm^2 and an efficiency (η) of 0.0385%. For the pt/FTO CE, the values obtained were V_{oc} = 283.39 mV, I_{sc} = 9.43 μA, ff = 0.252, P_{MAX} = 0.225 μW/cm^2 and η = 0.0118%, and last, for FTO CE, V_{oc} = 192.62 mV, I_{sc} = 2.94 μA, ff = 0.203, P_{MAX} = 0.0128 μW/cm^2, and η = 0.00067%. It can be concluded that graphite presents feasible potential as an alternative to platinum due to its affordable cost and performance output.

Keywords Dye-sensitized solar cell · Natural dye · Nano TiO_2 · Natural dye · Fabrication · Performance

Introduction

Throughout the century, humans have relied upon non-renewable energy for everyday activities. As the population rapidly increases, the demand for such energy has also escalated. Moreover, synthesizing such energy from fossils has contributed to worldwide environmental issues and endangered people's health (Mejica et al. 2020; Nong et al. 2020). In addition, it has been predicted that for the next few decades, the non-renewable energy sources will not be enough to suffice the future generation's energy needs (Sophanodorn et al. 2020; Van Tran et al. 2020). Hence, one of the main topics of scientific studies is to develop an alternative which is safe, sustainable, environmentally friendly, and renewable energy (Mejica et al. 2021). Presently, the sun's energy has gained research interest due to its widely available sources and feasible characteristics that can meet the energy demand (Lau and Soroush 2019). The sun's energy is extracted using photovoltaic technologies (Kabir et al. 2019).

The photovoltaic technologies have been evolving from the establishment of the first generation or the conventional solar cell examples being single-crystalline (scSi) or multi-crystalline (mc-Si) (Sugathan et al. 2015). Among the advantages of the commercial solar cell is the high light to electricity conversion. In contrast, this solar cell becomes an issue after a certain period of time due to the materials' degradation; the unavailability of recycling adds

✉ Rameshprabu Ramaraj
rrameshprabu@gmail.com; rameshprabu@mju.ac.th

1 School of Renewable Energy, Maejo University, Chiang Mai 50290, Thailand

2 Sustainable Resources and Sustainable Engineering Research Lab, Maejo University, Chiang Mai 50290, Thailand

3 Program in Biotechnology, Faculty of Science, Maejo University, Chiang Mai 50290, Thailand

Published online: 27 April 2021

to toxic non-biodegradable waste. The second-generation PV systems introduced in solar photovoltaics are based on III–V device structure, GaAs, CdTe, InP, and CIGs solar cells (Roy et al. 2020). Last, the third generation, which composes dye-sensitized solar cells, has gained scientists' attention due to its ability to harvest light and transform it into electrical energy (O'Regan and Grätzel 1991). Furthermore, the process of fabricating such solar cells is inexpensive.

Roslan et al. (2018) stated that dye-sensitized solar cells are electrochemical devices that utilize photosensitizer to collect light energy, called photons, and convert it into electricity. The process is as shown in Fig. 1: (1) light penetrates into the photoanode by which a dye molecule absorbs sufficient energy of photons, causing electron excitation from the highest occupied molecular orbital (HOMO) level to the lowest unoccupied molecular orbital (LUMO) level as a result of the absorbed light energy (Supriyanto et al. 2021), (2) the excited electron is then injected into the conduction band of a semiconductor material such as TiO_2, then (3) flows out through the external circuit to the counter electrode, then (4) to the charge mediator/electrolyte (I^-/I_3^-). Lastly, (5) to regenerate the missing electrons in the dye, the iodine/triiodide electrolyte generates a redox chemical reaction (Lau and Soroush 2019). This cycle repeats itself under a light source of sufficient intensity to generate electricity. The DSSC is still in the early stage of development to be commercially available (Roy et al. 2020; Sugathan et al. 2015). Thus, extensive studies are done in order to improve its performance output and durability. The photosensitizer played a key role in the DSSC, and it is the one that absorbs photons or energy from the sunlight, which paves the way for the conversion into electricity.

For years, synthetic dye such as ruthenium-based dye with a light absorption range of 300–800 nm has been used for photosensitizer (Kumara et al. 2017; Li and Chen 2019). However, producing such dye is expensive, complex, and toxic to humans and the environment. Due to this, natural dyes or pigments (chlorophyll, anthocyanin, carotenoid, etc.) extracted from plants have been subjected as an alternative to synthetic dye (Khammee et al. 2020a, b). Chlorophyll is known to be the green pigment naturally found in plants (Ramaraj et al. 2013). Moreover, it absorbs photons from the sun, necessary for the photosynthesis process (Ardo and Meyer 2009). Through this, the photons absorbed by chlorophyll together with carbon dioxide (CO_2) and water (H_2O) produce the much-needed oxygen (O_2) and sugars (Scheer 2006).

Aside from photosensitizer, counter electrodes are crucial in improving the output of the solar cell. Their purpose is to continue the electron cycle within the cell. The counter electrodes (CE) made it possible for the electron to transfer from the external circuit to the mediator (I^-/I_3^-). The CEs are typically made of a few nanometre-thick platinum (pt) layer acting as a catalyst (O'Regan and Grätzel 1991). pt is expensive due to its small global reserves. The creation of alternative electrode materials was necessitated by the Pt electrode's current cost, commonly used as a counter electrode in DSSCs. The research goal on alternative counter electrode development is to establish a low-cost material that can replace the traditional counter electrode (Bayram et al. 2020). Furthermore, when in contact with the I^-/I_3^- liquid electrolyte, Pt continues to degrade over time, decreasing the efficiency of DSSC (Koo et al. 2006).

Hence, this study is focused on evaluating the application of chlorophyll pigment from *Strobilanthes cusia* (SC),

Fig. 1 Schematic diagram of the DSSC mechanism

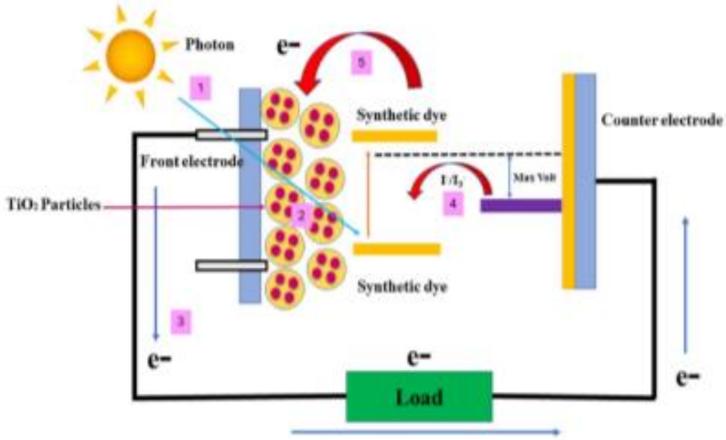

also known as indigo plant, as a photosensitizer for dye-sensitized solar cells. This plant is noted for its properties for producing the indigo dye, which is famously used for textile dyeing. This study evaluated the performance output of the fabricated natural dye-based DSSC under three different counter electrode materials: a. fluorine-doped tin oxide (FTO) CE, b. graphite/FTO CE, and c. pt/FTO CE.

Materials and methods

Chemicals such as acetonitrile, methanol, surfactant (Tween 20), acetic acid, and iodine were used. Potassium Iodide, Ethylene glycol, TiO_2 powder HCl, acetic acid, and nano TiO_2 powder were purchased from Union Science, while the (0.4 M) acetic acid-sodium acetate buffer pH 1.0 and (0.1 M) HCl acid-KCl buffer pH 4.5 were prepared in the laboratory. The fluorine-doped tin oxide (FTO) glass was purchased from Hangzhou, Zhejiang, China.

Extraction of photosensitizer

The extraction process used was adopted and modified from Sumanta et al. (2014). The *Strobilanthes cusia* (SC), commonly known as the Indigo plant, was collected from Chiang Mai Province, Thailand. The plant sample was thoroughly rinsed with water, subsequently air-dried at room temperature until free from moisture, then cut into smaller size using a blender together with the organic solvent. After it was blended, the solution was kept in a beaker and set aside for 10 min at room temperature. Last, the solid residues were filtered out using Whatman filter paper, while the dye extract was stored in a container (Fig. 2).

Chlorophyll determination

The experiment was conducted in order to determine the chlorophyll pigment content (CPC) of the sample. The CPC evaluation undergoes a series of processes trial and errors to achieve accurate and reliable data. Taking into account that the dye is sensitive to light, therefore, it was examined in a little lightroom and kept in a covered bottle to avoid exposure to the light. Khammee et al. (2020a,b) study was used to calculate the chlorophyll a (Chl-a) and chlorophyll b (Chl-b) of the natural dye. The absorbance of the *Strobilanthes cusia* dye was examined using a UV–Vis spectrophotometer (Drawell Artist of Science, China) at 663 nm, 645 nm, and 470 nm.

For the determination of chlorophyll a (Chl-a) and chlorophyll b (Chl-b), the following equations were used (Khammee et al. 2020a, b):

$$\text{Chlorophyll a} = \left(12.25 \times A_{663} - 2.79 \times A_{645}\right) \times \text{DF}, \quad (1)$$

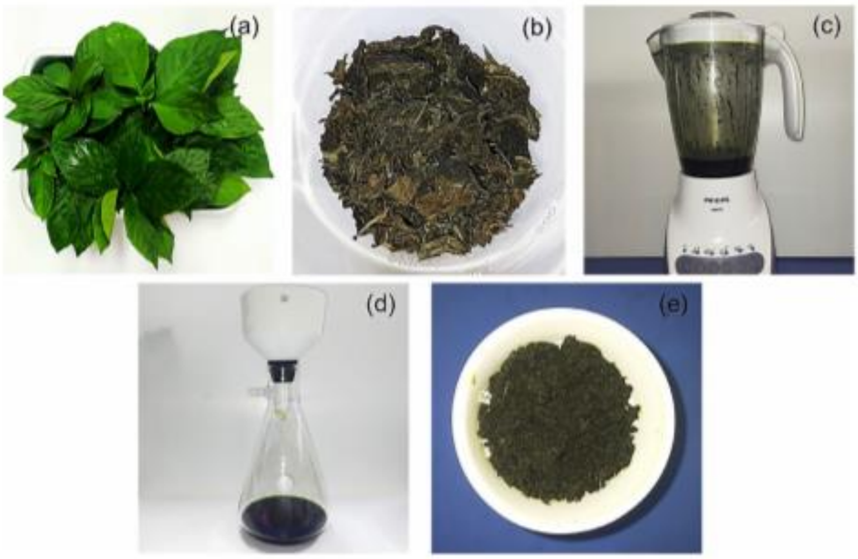

Fig. 2 *Strobilanthes cusia* sample preparation and dye extraction process (**a**–**d**), residue (**e**)

$$\text{Chlorophyll b} = (21.50 \times A_{645} - 5.10 \times A_{663}) \times \text{DF}, \quad (2)$$

$$\text{Carotenoid} = \frac{(1000 \times A_{470} - 1.43 \times C_a - 35.87 \times C_b) \times \text{DF}}{205},$$

where DF = dilution factor, A_{663}, A_{645}, and A_{470} are the absorbance at 663 nm, 645 nm, and 470 nm, respectively.

Photo-electrode preparation

Different processes were used to prepare the photoanode, also known as the working electrode. First, the FTO glass was cleaned by ultrasonic under three different solutions (soap, distilled H_2O, and methanol) for 10 min each, consecutively. Afterward, the FTO glass was air-dried, then was checked for the conductive side by measuring its resistance, and then the four corner sides were taped to get the desired surface area of 3 cm^2 (Fig. 3). Simultaneously, the TiO_2 paste was prepared by reducing the particle size of the TiO_2 powder by setting it to a magnetic mixer for 1 h. Hence, 5 g of TiO_2 powder, 10 ml of 5% acetic acid, and 0.5 surfactants (Tween 20) were thoroughly mixed using a magnetic stirrer for 1 h, then kept in a sealed container to avoid evaporation of the paste. Last, the TiO_2 paste was deposited on the glass substrate using the doctor blade technique. Subsequently, the annealing process was done by heating it at a constant temperature of 240 °C for 30 min and then letting it cool down.

Dye loading to TiO_2

As shown in Fig. 4, SC photosensitizer was loaded into the TiO_2 by slowly putting ten drops of the dye and then letting it dry for 5 min. Subsequently, the process was repeated two more times. After the dye loading, the excess dye from the FTO glass was removed.

Counter-electrode preparation

An adhesive tape was put on the four corners of the FTO glass's conductive surface to get the desired surface area of 3 cm^2. For the counter electrode material (Fig. 5), three materials were prepared: 1. FTO glass for FTO CE, 2. FTO glass coated with graphite for graphite/FTO CE, and 3. FTO glass coated with platinum for pt/FTO CE. The counter electrode material platinum was coated on the FTO glass and dried at room temperature for 5 min. Afterward, the film was gradually sintered at 240 °C for 20 min. Subsequently, for graphite-based counter electrode, the method used was adopted and modified from Setyawati et al. (2017); graphite

Fig. 3 Ultrasonic cleaner (**a**), putting tape for area boundary (**b**)

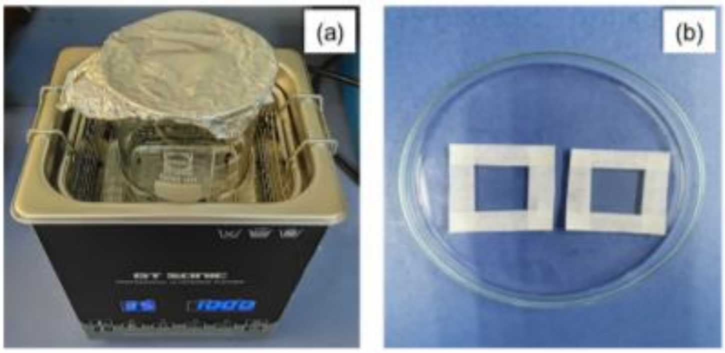

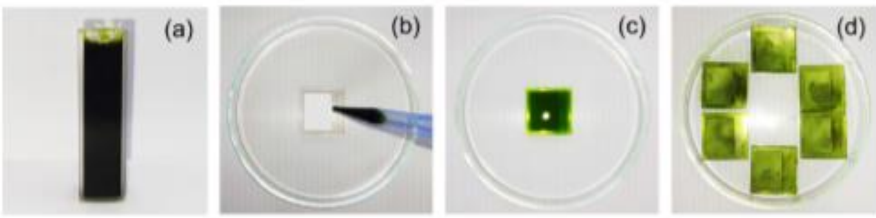

Fig. 4 *Strobilanthes cusia* photosensitizer (**a**), dye loading to TiO_2 (**b–d**)

from graphite pencil was added to the FTO glass and was sintered at 240 °C for 20 min. Last, the counter electrode film was cooled at room temperature.

Electrolyte

In the liquid electrolyte, preparation process was adopted and modified from Gu et al. (2017): 20 ml of ethylene glycol mixed with 80 ml acetonitrile was taken in a beaker. Then, 0.21 g of iodine (I) was added to the liquid solution. After that, 1.08 g of potassium iodide was added. The mixture was mixed using the glass rod until no grains of iodine and potassium iodide were visible.

Fabrication of DSSC

Dye-sensitized solar cells were assembled by sandwiching the prepared photo-anode with a counter electrode and sealed with hot-melt glue. Figure 6 shows the assembly and overall view of the fabricated DSSC. Then the electrolyte was injected inside the cell (Fig. 7). Furthermore, after the preparation of the DSSC, all the parameters were measured instantly to avoid any changes in the dye and photoelectric properties caused by aging.

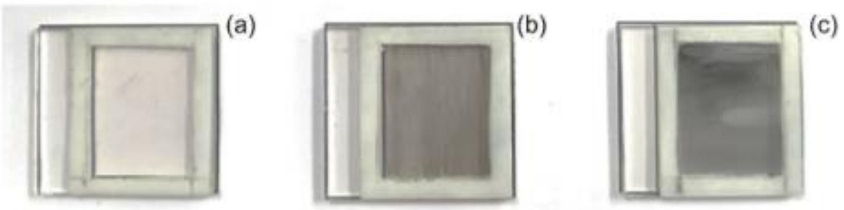

Fig. 5 Counter electrodes: FTO glass (**a**), FTO glass with graphite (**b**), FTO glass coated with platinum (**c**)

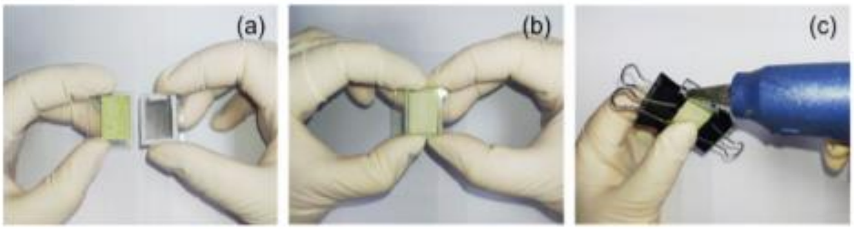

Fig. 6 Photoanode and counter electrode (**a**) cell assembly (**b**), sealing (**c**)

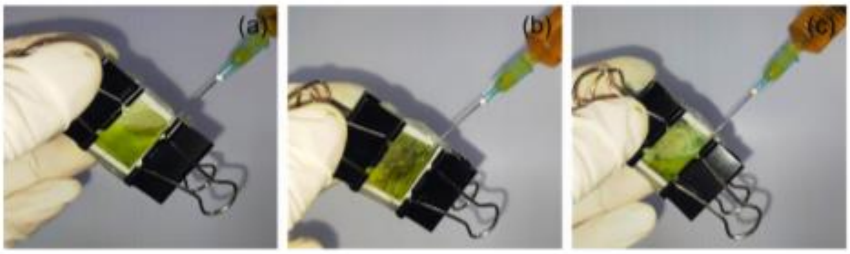

Fig. 7 Injection of electrolyte to different counter electrodes: FTO glass (**a**), FTO glass with graphite (**b**), FTO glass coated with platinum (**c**)

Statistical analysis

The experiment was conducted with three replicates. Hence, the data were presented as mean ± standard deviation (SD).

Results and discussion

Evaluation of chlorophyll pigment content of *Strobilanthes cusia*

In this research, methanol was used to extract the chlorophyll pigment from *Strobilanthes cusia*. Methanol is an excellent chlorophyll extractant, particularly for algae and recalcitrant vascular plants (Ritchie 2006). During the experiment, three replicates of the SC dye were prepared to ensure reliable data. Chlorophyll is a type of cyclic tetrapyrrole, similar to porphyrin and phthalocyanines. Calogero et al. (2014) mentioned that Caventou and Pelletier discovered chlorophyll as a chlorin ring with a magnesium ion at its center. These green pigments contain reduced pyrrole rings and a phytol group. Among the chlorophyll chemical structures, chlorophyll a ($C_{55}H_{72}O_5N_4Mg$, blue-green) and chlorophyll b ($C_{55}H_{70}O_6N_4Mg$, yellow-green) are distinguished as common chlorophyll pigments (Calogero et al. 2014).

The result of the chlorophyll estimation of the natural dye showed that the amount of CPC from SC was primarily composed of Chl-a with 64.5345 ± 0.4226 (µg/ml) followed by Chl-b with 41.4341 ± 0.2636. According to Zielewicz et al. (2020), the typical ratio of Chl-a:Chl-b is 3:1 since Chl-a is the primary pigment of photosynthesis that absorbs light from the sun. At the same time, Chl-b is considered an accessory pigment because it is not needed during photosynthesis. Furthermore, the key structural distinction between chlorophyll a and chlorophyll b is the composition of a single side chain of the cyclic tetrapyrrole, which in Chl-a is a $-CH_3$ and in Chl-b is a –CHO. Chlorophylls have a highly stable polycyclic network of alternating single- and double-bond- (polyenes) conjugated structure that allows the orbitals to delocalize, making them suitable for photosensitizers (Kay et al. 1994; Calogero et al. 2014).

Surface morphologic analysis of TiO_2 film and SC dye/TiO_2 composite film

The assessment of the surface morphology of a dye-sensitized solar cell is part of the study of its properties. According to Khammee et al. (2020a, b, 2021), the hydroxyl groups on nanostructured TiO_2 allow for natural dyes' chemical adsorption. For establishing the chemical bonding of the carbonyl and hydroxyl groups, it is essential to analyze the morphological surface of TiO_2/FTO film TiO_2/FTO film's morphological surface after dye loading of *Strobilanthes cusia* extract (SC dye/TiO_2/FTO composite film). The morphology of the TiO_2/FTO film and SC dye/TiO_2/FTO composite film was evaluated using a scanning electron microscope (SEM). Moreover, Fig. 8a1 displays the assessment of the morphology of a TiO_2 film. Herewith, the substrate was assayed at a total magnification of 1000×. A heterogeneous nanoparticle made of mesoporous TiO_2 and a porous surface was shown. The highlighted factor of TiO_2 film is its porous configuration, which secures the adsorbing dye molecules and the diffusion path of electrolyte in the DSSCs (Wei et al. 2011).

Moreover, the pores could increase the contact area between dye molecules and the electrolyte contributing to the oxidized dye reduced immediately by I_3^- in the electrolyte. The DSSC is a rather complicated system that includes light absorption, charge injection, charge collection, and electrolyte diffusion (Ni et al. 2008). In addition, Fig. 8b1 shows the SEM picture of SC dye/TiO_2/FTO composite film at a magnification of 1000×. The composite film's surface was observed to be less porous, indicating dye molecules penetrating between the gap/pores in the TiO_2 substrate.

For further assessment, the SEM samples (TiO_2/FTO film and SC dye/TiO_2/FTO composite film) were examined for energy-dispersive X-ray spectroscopy (EDX), an elemental technique to distinguish the chemical elements present in the composite. Figure 8a2 displays that the elemental composition of TiO_2 film consists solely of titanium and oxygen, supported by the results shown in Table 1, where the film consists of 20.99 atomic% titanium (Ti) and 79.01 atomic% oxygen (O). TiO_2 usually exhibits a characteristic spectrum of fundamental Ti–O bond absorption in the UV region between 320 and 400 nm, with a characteristic peak of about 350 nm (band edge) for TiO_2. These rely on the production of highly reactive free radicals like the hydroxyl radical, which aid in the degradation of organic pollutants. These hydroxyl radicals can be made using several methods, including photocatalysis with semiconductors and light (Pawar et al. 2019; Khammee et al. 2020a, b, 2021). In comparison, Fig. 8b2 and Table 1 display the presence of carbon in SC dye/TiO_2/FTO composite film. Thus, this shows the sensitization of the dye molecules on the TiO_2 film. It is known that generally, plant composition consists of 45% C and 45% O; as mentioned by Calogero et al. (2014), chlorophyll chemical structures contain chlorophyll a (*Chl-a*) ($C_{55}H_{72}O_5N_4Mg$) and chlorophyll b (*Chl-b*) ($C_{55}H_{70}O_6N_4Mg$.), alternating conjugated structures of the C=O (carbonyl) and C–O. Chlorophylls have strong absorption bands in the blue and red regions of the visible spectrum (λmax, ≈ 430 and 665 nm in Chl-a, and 425 and 655 nm in Chl-b). Hence, it is a feasible compound for photosensitizer application in the dye-sensitized solar cell.

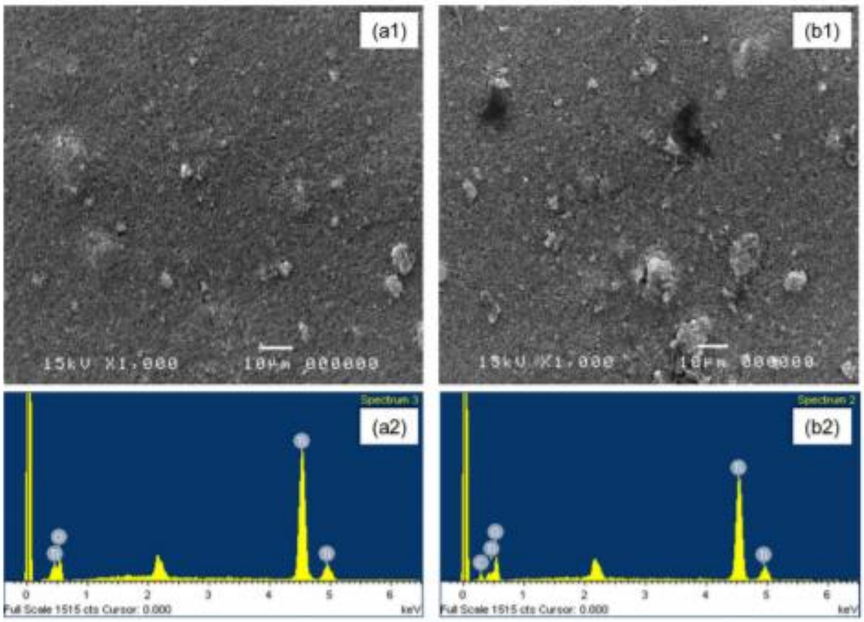

Fig. 8 SEM and EDX image of TiO_2 film (**a1** and **a2**), and TiO_2 film loaded with *Strobilanthes cusia* dye (**b1** and **b2**)

Table 1 EDX weight ratio of TiO_2 film and TiO_2 photoanode loaded with *Strobilanthes cusia* dye

Photoanode	Titanium (Ti)		Oxygen (O)		Carbon (C)	
	Weight (%)	Atomic (%)	Weight (%)	Atomic (%)	Weight (%)	Atomic (%)
TiO_2 film	44.30	20.99	55.70	79.01	–	–
TiO_2 loaded with SC dye	33.25	13.50	53.49	65.03	13.26	21.47

Fig. 9 Schematic circuit diagram of the experimental setup used for measuring the current–voltage characteristics of DSSC with voltmeter (*V*), ammeter (*A*), and potentiometer variable resistance (10 k Ω)

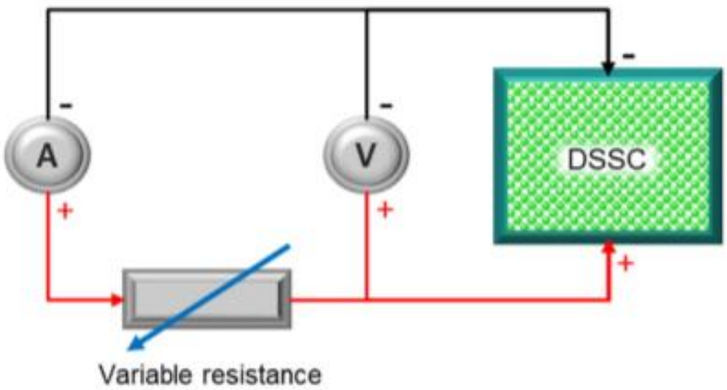

Characterization and performance analysis of fabricated DSSC

The chemical reactions operating the chlorophyll-based DSSC begin during the light exposure of the cell. The photons from the light hit the dye molecules and make them electronically excited. The excited dye molecules then injected electrons into the TiO_2 layer. Moreover, within the electrolyte, the mediator (I^-/I_3^-) undergoes oxidation at the dye and regeneration at the catalyst-coated counter electrode as current flows through the electrical load (Smestad et al. 1998).

Kumara et al. (2017) reported that the performances of DSSC are evaluated using the current–voltage (I–V) characteristic curve and the power density–voltage curve (P_ρ–V). In this study, the photovoltaic performance of the fabricated DSSCs was carried out under irradiation of white LED light at 13,000 lx (0.001903367 W/cm^2) in the ambient atmosphere using an experimental setup. Moreover, the schematic circuit diagram for measuring the photovoltaic parameters is shown in Fig. 9, and the circuit is composed of a voltmeter (V) for measuring the voltage, ammeter (A) for current, and potentiometer variable resistance (10 k Ω). According to Dinesh et al. (2019), an important factor on the I–V curve is the point at which maximum power (P_{MAX}) is supplied (also referred to as the 'knee of the curve'), the short circuit current (I_{sc}) when $V = 0$; the knee point is $\{I_{MAX}, V_{MAX}\}$ which is the point of maximum power, and V_{OC} the open-circuit voltage, when $I = 0$. Figure 10 displays the I–V and power density–voltage curve recorded from this experiment wherein SC dye-based DSSCs were examined under three different counter electrodes: FTO CE, graphite/FTO CE, and pt/FTO CE, respectively. Figure 10a shows the point at which the FTO CE obtained its maximum power of 0.0128 μW/cm^2, $V_{oc} = 192.62$ mV, $I_{sc} = 2.94$ μA, and ff = 0.203. Moreover, Fig. 10b displays the higher photoelectric output of graphite/FTO CE having $V_{oc} = 306.35$ mV, $I_{sc} = 15.55$ μA, ff = 0.462, and $P_{MAX} = 0.734$ μW/cm^2. And the pt/FTO CE (Fig. 10c) obtained $V_{oc} = 283.39$ mV, $I_{sc} = 9.43$ μA, ff = 0.252, and $P_{MAX} = 0.225$ μW/cm^2.

The data parameters from the I–V and power density–voltage were then used to quantify the performance of the assembled DSSC. The efficiency was calculated by using the following equation (Dawoud 2016):

$$n = \frac{P_{max}}{P_{in}} = \frac{J_{sc} \times V_{oc} \times FF}{P_{in}}, \tag{3}$$

where P_{max} is the maximum power output of the solar cell, P_{in} is the solar irradiation of the light source, J_{sc} = short circuit density, and FF = fill factor.

One of the most critical components in DSSCs is the counter electrode (CE). The CE's primary function is to either (a) catalyze by reducing redox species, which are charge mediators for regenerating the sensitizer (dye) after electron insertion into TiO_2 semiconductor film (Thomas et al. 2014). Thus, the DSSC without counter electrode

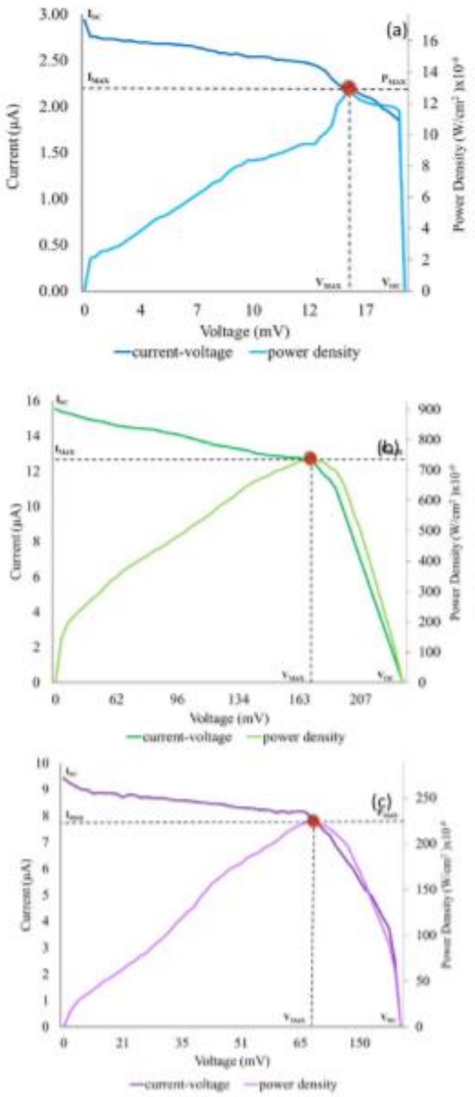

Fig. 10 I–V and power–density curve of DSSC using different counter electrode: FTO glass (a) graphite/FTO glass (b), and pt/FTO glass (c)

Table 2 Photovoltaic performance of chlorophyll-based DSSC

Dye	Counter electrodes	J_{sc} (mA/cm^2)	Voc (V)	ff	η (%)	Reference
Ocimum Gratissimum	Pt	0.044	0.466	0.400	0.021	Eli et al. (2016)
Green spinach leaves	Pt	0.052	0.590	0.530	0.016	Hasoon et al. (2015)
Morula leaves	C	0.059	0.472	0.050	0.001	Maabong et al. (2015)
Lemon leaves	C	1.080	0.592	0.100	0.036	Maabong et al. (2015)
Black tea leaves	Pt	0.390	0.550	0.400	0.080	Abdel-Latif et al. (2015)
Green algae (fresh)	Pt	0.134	0.416	0.210	0.010	Taya et al. (2013)
Green algae (dried)	Pt	0.397	0.559	0.440	0.100	Taya et al. (2013)
Strobilanthes cusia	FTO glass	0.0003267	0.193	0.203	0.00067	This study
Strobilanthes cusia	Graphite	0.0051833	0.306	0.462	0.0385	This study
Strobilanthes cusia	Pt	0.0031438	0.283394	0.252	0.0118	This study

material limits the cycle of the electron flow within the device. This corresponds to the efficiency output of 0.00067% of not employing counter electrode material (FTO glass only) to the DSSC. The absence of counter electrode material restricts the movement of the electron, which slows down the recharge of electrolyte mediator (I^-/I_3^-), hence, resulting in low values of short-circuit current (I_{sc}) = 2.94 µA and open-circuit voltage (V_{oc}) = 192.62 mV.

The majority of DSSC research focuses on improving performance by increasing the short-circuit current (I_{sc}), and open-circuit voltage (V_{oc}). As a CE, a Pt-coated FTO is usually used. The experiment results show the improvement of the cell's photovoltaic output integrating pt/FTO CE compared to FTO CE, having an efficiency of 0.0118%. The fill-factor (FF) of the cell increases as the CE material improves, which is primarily influenced by the cell's series resistance (Rs) related to the tangent line's slope to the *I–V* curve at V_{oc}. The Warburg impedance concerning the Nernst diffusion of the I_3^- species in the electrolyte is used to calculate the series resistance (Zn), which is the electrical hindrance of charge-transfer at the CE and the regeneration of dye and electrolyte, resistance at the fluorine-doped tin oxide glass, and charge-transfer resistance at the CE, and the electrolyte interface (Thomas et al. 2014). Platinum deposited on transparent conducting oxide, with a thickness of 0.2–2 micron, acts as a catalyst (O'Regan and Grätzel 1991) to improve the flow of electrons from dye molecules to the electrolyte (regeneration of dye molecules and electrolyte). These CE films have excellent electrical conductivity, catalytic behavior against I_3^-, and reflectivity. However, pt is expensive due to its small global reserves. Additionally, according to (Koo et al. 2006), when in contact with the I_3^-/I^- liquid electrolyte, pt continues to degrade over time, decreasing the efficiency of DSSC.

Considering the cost of platinum, a low-cost dye-sensitized solar cell, the use of an alternative, a cheap and plentiful material found in the Earth's crust as the counter electrode, which can replace Pt in DSSC, is being investigated. The graphite counter electrode is a cheaper alternative to platinum, which is commonly used in these cells. The use of a graphite pencil as a source of graphite for graphite/FTO CE was tested. Among the three conditions evaluated (FTO CE, graphite/FTO CE, and pt/FTO CE), graphite exemplifies significant DSSC performance, in which the efficiency obtained was 0.0385%. The difference in graphite counter electrodes' performance is primarily due to the high degree of mechanical stability (Wang and Hu 2012) and wide surface area (Marques et al. 2020; Smestad and Gratzel 1998).

Table 2 shows some of the available photovoltaic performances of chlorophyll dye-based dye-sensitized solar cells. It can be concluded that the results from this scientific research are within the range of the developed DSSC. The performance evaluation of the different counter electrode materials' effect and utilizing *Strobilanthes cusia* dye extract suggests many more opportunities and pathways to improve the third-generation solar cell's performance and cost DSSC belongs.

Conclusion

This present study investigated the development and performance evaluation of dye-sensitized solar cells integrated with natural dye from *Strobilanthes cusia* under different counter electrode materials. The results showed the potential of the natural dye from *Strobilanthes cusia* as a photosensitizer. Significantly, counter electrode utilizing graphite (graphite/FTO CE) exhibited higher photoelectric having an open-circuit voltage (V_{oc}) of 306.35 mV, short circuit current (I_{sc}) of 15.55 µA, ff = 0.462, maximum power (P_{MAX}) of 0.734 µW/cm^2, and an efficiency (η) of 0.0385%. For the pt/FTO CE, the values obtained were V_{oc} = 283.39 mV, I_{sc} = 9.43 µA, ff = 0.252, P_{MAX} = 0.225 µW/cm^2 and η = 0.0118%, and last, for FTO CE, V_{oc} = 192.62 mV, I_{sc} = 2.94 µA, ff = 0.203, P_{MAX} = 0.0128 µW/cm^2, and

$\eta = 0.00067\%$. Hence, it can be concluded that graphite presents feasible potential as an alternative to platinum due to its affordable cost and performance output. The performance evaluation of the effect of the different counter electrode materials and utilizing *Strobilanthes cusia* dye extract suggests many opportunities and pathways to improve the third-generation solar cell performance dye-sensitized solar cell.

Acknowledgements The authors kindly acknowledged the School of Renewable Energy, Energy Research Center, Maejo University, Chiang Mai, Thailand and Program in Biotechnology for the research fund and facilities to accomplish this experimental study.

Compliance with ethical standards

Conflict of interest The authors declare that they have no conflict of interest.

References

Abdel-Latif MS, Abuiriban MB, Dahoudi NA, Al-Kahlout AM, Taya SA, El-Agez TM, El-Ghamri HS (2015) Dye-sensitized solar cells using fifteen natural dyes as sensitizers of nanocrystalline TiO_2. Sci Technol Dev 34:135–139

Ardo S, Meyer GJ (2009) Photodriven heterogeneous charge transfer with transition-metal compounds anchored to TiO_2 semiconductor surfaces. Chem Soc Rev 38(1):115–164

Bayram O, Igman E, Guney H, Demir Z, Yurtcan MT, Cirak C, Hasar UU, Simsek O (2020) Graphene/polyaniline nanocomposite as platinum-free counter electrode material for dye-sensitized solar cell: its fabrication and photovoltaic performance. J Mater Sci Mater Electron 31(13):10288–10297

Calogero G, Bartolotta A, Marco GD, Carlo AD, Bonaccorso F (2014) Vegetable-based dye-sensitized solar cells. Chem Soc Rev 44(10):3244–3294

Dawoud AM (2016) Natural pigments extracted from plant leaves as photosensitizers for dye-sensitized solar cells. Master Degree of Science (M.Sc.) in Physics. Islamic University of Gaza

Dinesh VP, Sriram R, Sukhananazerin A, Mary Sneha J, Manoj Kumar P, Biji P (2019) Novel stainless steel based, eco-friendly dye-sensitized solar cells using electrospun porous ZnO nanofibers. Nanostructure Nanoobjects 19:100311

Eli D, Musa GP, Ezra D (2016) Chlorophyll and betalain as light-harvesting pigments for nanostructured TiO_2 based dye-sensitized solar cells. J Energy Nat Resour Law 5:53–58

Gu P, Yang D, Zhu X, Sun H, Wangyang P, Li J, Tian H (2017) Influence of electrolyte proportion on the performance of dye-sensitized solar cells. AIP Adv 7(10):105219

Hasoon SA, Al-Haddad RMS, Shakir OT, Ibrahim IM (2015) Natural dye-sensitized solar cell based on zinc oxide. Int J Eng Res 6:137–142

Kabir F, Bhuiyan MMH, Manir MS, Rahaman MS, Khan MA, Ikegami T (2019) Development of dye-sensitized solar cell based on combination of natural dyes extracted from *Malabar spinach* and red spinach. Results Phys 14:102474

Kay A, Humphry-Baker R, Graetzel M (1994) Artificial photosynthesis. 2. Investigations on the mechanism of photosensitization of nanocrystalline TiO2 solar cells by chlorophyll derivatives. J Phys Chem 98:952–959

Khammee P, Unpaprom Y, Whangchai K, Ramaraj R (2020a) Comparative studies of the longan leaf pigment extraction as a photosensitizer for dye-sensitized solar cells' purpose. Biomass Convers Biorefinery. https://doi.org/10.1007/s13399-020-01060-x

Khammee P, Unpaprom Y, Subhasaen U, Ramaraj R (2020b) Potential evaluation of yellow cotton (*Cochlospermum regium*) pigments for dye sensitized solar cells application. Glob J Sci Eng 2:16–21. https://doi.org/10.37516/global.j.sci.eng.2020.008

Khammee P, Unpaprom Y, Thurakitseree T, Dussadee N, Kojinok S, Ramaraj R (2021) Natural dyes extracted from Inthanin bok leaves as light-harvesting units for dye-sensitized solar cells. Appl Nanosci. https://doi.org/10.1007/s13204-021-01769-9

Koo BK, Lee DY, Kim HJ, Lee WJ, Song JS, Kim HJ (2006) Seasoning effect of dye-sensitized solar cells with different counter electrodes. J Electroceramics 17(1):79–82

Kumara NTRN, Lim A, Lim CM, Petra MI, Ekanayake P (2017) Recent progress and utilization of natural pigments in dye sensitized solar cells: a review. Renew Sustain Energy Rev 78:301–317

Lau KKS, Soroush M (2019) Chapter 1 - overview of dye-sensitized solar cells. Academic Press, pp 1–49

Li D, Chen G (2019) Chapter 9 - upconversion-enhanced dye-sensitized solar cells. Dye Sensitized Solar Cells. https://doi.org/10.1016/B978-0-12-814541-8.00009-4

Maabong K, Muiva CM, Monowe P, Sathiaraj TS, Hopkins M, Nguyen L, Malungwa K, Thobega M (2015) Natural pigments as photosensitizers for dye-sensitized solar cells with TiO_2 thin films. Int J Eng Res 5:54–60

Marques ADS, Da Silva VAS, Ribeiro ES (2020) Dye-sensitized solar cells: components screening for glass substrate, counter-electrode, photoanode and electrolyte. Mater Res 23(5):e20200168. https://doi.org/10.1590/1980-5373-mr-2020-0168

Mejica GFC, Unpaprom Y, Ramaraj R (2020) Extraction of anthocyanin pigments from malabar spinach fruits as a potential photosensitizer for dye-sensitized solar cell. Glob J Sci Eng 2:5–9

Mejica GFC, Unpaprom Y, Whangchai K, Ramaraj R (2021) Cellulosic-derived bioethanol from *Limnocharis flava* utilizing alkaline pretreatment. Biomass Convers Biorefin.. https://doi.org/10.1007/s13399-020-01218-7

Ni M, Leung MKH, Leung DYC (2008) Theoretical modelling of the electrode thickness effect on maximum power point of dye-sensitized solar cell. Can J Chem Eng 86(1):35–42

Nong HTT, Unpaprom Y, Whangchai K, Buochareon S, Ramaraj R (2020) Assessment of the effects of anaerobic co-digestion of water primrose and cow dung with swine manure on biogas yield and biodegradability. Biomass Convers Biorefinery. https://doi.org/10.1007/s13399-020-01115-z

O'Regan B, Grätzel M (1991) A low-cost, high-efficiency solar cell based on dye-sensitized colloidal TiO_2 films. Nature 353(6346):737–740

Pawar KS, Baviskar PK, Nadaf AB, Salunke-Gawali S, Pathan HM (2019) Layer-by-layer deposition of TiO_2–ZrO_2 electrode sensitized with pandan leaves: natural dye-sensitized solar cell. Mater Renew Sustain Energy 8:12

Ramaraj R, Tsai DD, Chen PH (2013) Chlorophyll is not accurate measurement for algal biomass. Chiang Mai J Sci 40(4):547–555

Ritchie RJ (2006) Consistent sets of spectrophotometric chlorophyll equations for acetone, methanol and ethanol solvents. Photosynth Res 89:27–41

Roslan N, Ya'acob ME, Radzi MAM, Hashimoto Y, Jamaludin D, Chen G (2018) Dye sensitized solar cell (DSSC) greenhouse shading: new insights for solar radiation manipulation. Renew Sustain Energy Rev 92:171–186

Roy P, Kumar Sinha N, Tiwari S, Khare A (2020) A review on perovskite solar cells: evolution of architecture, fabrication techniques, commercialization issues and status. Sol Energy 198:665–688

Scheer H (2006) Chlorophylls and bacteriochlorophylls: biochemistry, biophysics, functions and applications, vol 25, Chp 1. In: Grimm B, Porra RJ, Rüdiger W, Scheer H (eds) Springer

Setyawati H, Darmokoesoemo H, Rochman F, Permana AJ (2017) Affordable dye sensitizer by waste. Mater Renew Sustain Energy 6(4):1–6

Smestad GP, Gratzel M (1998) Demonstrating electron transfer and nanotechnology: a natural dye-sensitized nanocrystalline energy converter. J Chem Educ 75(6):752

Sophanodorn K, Unpaprom Y, Whangchai K, Homdoung N, Dussadee N, Ramaraj R (2020) Environmental management and valorization of cultivated tobacco stalks by combined pretreatment for potential bioethanol production. Biomass Convers Biorefinery. https://doi.org/10.1007/s13399-020-00992-8

Sugathan V, John E, Sudhakar K (2015) Recent improvements in dye sensitized solar cells: a review. Renew Sustain Energy Rev 52:54–64

Sumanta N, Haque CI, Nishika J, Suprakash R (2014) Spectrophotometric analysis of chlorophylls and carotenoids from commonly grown fern species by using various extracting solvents. Res J Chem Sci 2231:606X

Supriyanto A, Saputri DG, Ahmad MKB, Ramelan AH, Ramadhani F (2021) Significant efficiency improvement of TiO_2:LEG4-Ag layer dye sensitized solar cells by incorporating small concentration of Ag. Optik 231:166429

Taya SA, El-Agez TM, El-Ghamri HS, Abdel-Latif MS (2013) Dye-sensitized solar cells using fresh and dried natural dyes. Int J Mater Sci Eng 2:37–42

Thomas S, Deepak TG, Anjusree GS, Arun TA, Nair SV, Nair AS (2014) A review on counter electrode materials in dye-sensitized solar cells. J Mater Chem A 2(13):4474–4490

Van Tran G, Unpaprom Y, Ramaraj R (2020) Methane productivity evaluation of an invasive wetland plant, common reed. Biomass Convers Biorefinery 10:689–695

Wang H, Hu YH (2012) Graphene as a counter electrode material for dye-sensitized solar cells. Energy Environ Sci 5(8):8182–8188

Wei YS, Jin QQ, Ren TZ (2011) Expanded graphite/pencil-lead as counter electrode for dye-sensitized solar cells. Solid State Electron 63(1):76–82

Zielewicz W, Wróbel B, Niedbała G (2020) Quantification of chlorophyll and carotene pigments content in mountain melick (*Melica nutans* L.) in relation to edaphic variables. Forests 11(11):1197

APPENDIX C

CERTIFICATE OF PRESENTATION

CERTIFICATE OF ATTENDANCE, PARTICIPATION, & PRESENTATION

THIS IS PROUDLY GIVEN TO

GLENNISE FAYE C. MEJICA

for attending, participating and conducting an oral presentation at

THE INTERNATIONAL ONLINE CONFERENCE ON INNOVATIVE SCIENCE, ENGINEERING, AND TECHNOLOGY (IOCISET-2020) (JULY 03, 2020 - JULY 05, 2020)

as per the details below:

Submission Type: Full Paper
Title: Extraction of Anthocyanin Pigments from Malabar Spinach Fruits as a Potential Photosensitizer for Dye-Sensitized Solar Cell

KnowveL
TAKE YOUR RESEARCH TO NEXT LEVEL

KNOWVEL JOURNALS · TAKE YOUR RESEARCH TO NEXT LEVEL
DATE: 06/07/2020

KNOWVEL JOURNALS
WWW.KNOWVEL.COM
INFO@KNOWVEL.COM


UMS
UNIVERSITI MALAYSIA SABAH
Certificate
OF PARTICIPATION
Presented to
Glennise Faye C. Mejica
In recognition of your contribution as
PRESENTER
In the 13th Virtual Conference on Seminar of Science and Technology 2020
Held on 6th to 7th October 2020
DR. MOHAMAD ZUL HILMEY MAKMUD
Chairman
13th Conference on Seminar Science and Technology 2020
PROF. DR. BABA MUSTA
Dean
Faculty of Science and Natural Resources
Universiti Malaysia Sabah
Eco Campus
Transforming Ideas into Reality
Transformation towards UNIVERSITY INDUSTRY 4.0
UMS KAMPUS RAHMAH
TERAS KECEMERLANGAN DAN KEUNGGULAN

FACULTY OF SCIENCE, MAEJO UNIVERSITY

Certificate of Appearance

This certificate is granted to

Glennise Faye C. Mejica

of the research paper entitled

"Development of natural dye based Dye-sensitized solar cell utilizing natural pigment from malabar spinach and red cabbage"

in The 1st International Conference on Science Technology & Innovation-Maejo University (1st ICSTI-MJU) at Faculty of Science, Maejo University, Thailand on March 19, 2021.

Asst. Prof. Dr. Tapana Cheunbarn

Dean of Faculty of Science, Maejo University

INTERNATIONAL CONFERENCE ON CHALLENGES AND PROGRESS IN BIOSCIENCES AND ENGINEERING – (ICCPBE 2021)

DU044(B)

October 28th & 29th 2021

CERTIFICATE

This is to certify that **Ms. Glennise Faye C.** of **School of Renewable Energy, Maejo University, Thailand** has presented a poster presentation entitled "Development of dye-sensitized solar cell under different natural dyes" in the **International Conference on Challenges and Progress in Biosciences and Engineering – (ICCPBE 2021)** organized by **Bharath Institute of Higher Education and Research (BIHER), India** and **MAHSA University, Malaysia** held on 28th and 29th October 2021.

Prof. Dr. S. Suresh Kumar
Pro Vice-Chancellor (Grants and Publications)
BIHER

Prof. Dr. Rusli Bin Nordin
Dean, FOMBN, MAHSA University

Dr. P. Velmurugan
Organizing Secretary
BIHER

Dr. V. Mohanavel
Organizing Secretary
BIHER

Dr. Paulraj Ponnaiah
Organizing Secretary, MAHSA University

Dr. Antony V Samrot
Organizing Secretary, MAHSA University

Dr. Remya R.R
Convenor
BIHER

Ms. Ketharin
Convenor
MAHSAUniversity

APPENDIX D

CERTIFICATE OF AWARDS

BEST PRESENTATION AWARD

THIS IS PROUDLY GIVEN TO

GLENNISE FAYE C. MEJICA

for the best presentation (1st position) at

THE INTERNATIONAL ONLINE CONFERENCE ON INNOVATIVE SCIENCE, ENGINEERING, AND TECHNOLOGY (IOCISET-2020) (JULY 03, 2020 - JULY 05, 2020)

on the topic ***"Extraction of Anthocyanin Pigments from Malabar Spinach Fruits as a Potential Photosensitizer for Dye-Sensitized Solar Cell"***

KnowveL

TAKE YOUR RESEARCH TO NEXT LEVEL

KNOWVEL JOURNALS — TAKE YOUR RESEARCH TO NEXT LEVEL

DATE: 13/07/2020

KNOWVEL JOURNALS

WWW.KNOWVEL.COM

INFO@KNOWVEL.COM

FACULTY OF SCIENCE, MAEJO UNIVERSITY

Certificate of a Presentation Award

This certificate is granted to

"Development of natural dye based Dye-sensitized solar cell utilizing natural pigment from malabar spinach and red cabbage"

by Glennise Faye C. Mejica , Yuwalee Unpaprom, Ubonwan Subhasaen, Thidarat Siriboon and, Rameshprabu Ramaraj

has been awarded

Bronze

in The 1st International Conference on Science Technology & Innovation-Maejo University (1st ICSTI-MJU) at Faculty of Science, Maejo University, Thailand on March 19, 2021.

T. Cheunbarn

Asst. Prof. Dr. Tapana Cheunbarn

Dean of Faculty of Science, Maejo University

INTERNATIONAL CONFERENCE ON CHALLENGES AND PROGRESS IN BIOSCIENCES AND ENGINEERING – (ICCPBE 2021)

October 28th & 29th 2021

DU044(B)

CERTIFICATE

This is to certify that **Ms. Glennise Faye C** of **Maejo University, Thailand** has secured the **First** place in the Poster presentation event in the **International Conference on Challenges and Progress in Biosciences and Engineering – (ICCPBE 2021)** organized by **Bharath Institute of Higher Education and Research (BIHER), India** and **MAHSA University, Malaysia** held on 28th and 29th October 2021.

Prof. Dr. S. Suresh Kumar
Pro Vice-Chancellor (Grants and Publications)
BIHER

Prof. Dr. Rusli Bin Nordin
Dean, FOMBN, MAHSA University

Dr. P. Velmurugan
Organizing Secretary
BIHER

Dr. V. Mohanavel
Organizing Secretary
BIHER

Dr. Paulraj Ponnaiah
Organizing Secretary,
MAHSA University

Dr. Antony V Samrot
Organizing Secretary, MAHSA University

Dr. Remya R.R
Convenor
BIHER

Ms. Ketharin
Convenor
MAHSAUniversity

APPENDIX E

CERTIFICATE OF MJU-TEP RESULTS

Certificate of MJU-TEP Results

This is to certify that

Miss Glennise Faye Mejica

took the Maejo University Test of English Proficiency (MJU-TEP) on

June 26th, 2020

The test results are as follows (see reverse side for more details):

1. Listening Comprehension Skill	25 / 30 marks
2. Semi-speaking Skill	23 / 25 marks
3. Semi-writing Skill	22 / 30 marks
4. Reading Comprehension Skill	27 / 35 marks
Total Score	**97 / 120 marks**

Given on July 2nd, 2020

(Dr. Sutkhet Sakunthong)

Acting Director, Maejo University Language Center

MJU-TEP Scores

of ***Miss Glennise Faye Mejica***

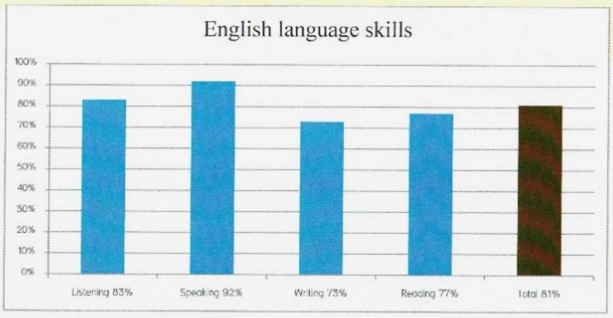

Meanings

1. Beginning users	0-20%	5. Competent users	61-70%
2. Very limited users	21-30%	6. Good users	71-80%
3. Limited users	31-40%	7. Very good users	81-90%
4. Modest users	41-60%	8. Expert users	91-100%

REFERENCES

Acikgoz, F. E. & Adiloglu, S. 2018. A Review on a New Exotic Vegetable for Turkey: Malabar Spinach (Basella alba L. or Basella rubra L.). **Journal of Horticulture**, 05(03).

Ahmadian, R. 2011. Estimating the impact of dye concentration on the photoelectrochemical performance of anthocyanin-sensitized solar cells: a power law model. **Journal of Photonics for Energy**, 1(1).

Alhamed, M., Issa, A. S. & Doubal, A. W. 2012. Studying of natural dyes properties as photo-sensitizer for dye sensitized solar cells (DSSC). **Journal of Electron Devices**, 16(

Amadi, L., Jenny, S. S., Ahmed, A., Brown, N., Yadav, S., Brown, D., Ghann, W., Gayrama, A., Jiru, M. & Uddin, J. 2015. Creation of Natural Dye Sensitized Solar Cell by Using Nanostructured Titanium Oxide. **Nanoscience and Nanoengineering**, 3(3), 25-32.

Anggraini, P. N., Lia Muliani, G. W., Retnaningsih, L. & Hidayat, J. 2016. Stability Optimization of TiO_2 Dye-Sensitized Solar Sub-modules in Z-Type Series Interconnection. **IEEE-ICSE2016**

Bagavathi, N. & Clara Dhanemozhi, A. 2019. Fabrication of Dye Sensitized Solar Cells by the Plasmonic Effect of Silver Nanoparticles and Basella Alba Dye. **Materials Today: Proceedings**, 8(271-278.

Calogero, G., Bartolotta, A., Di Marco, G., Di Carlo, A. & Bonaccorso, F. 2015. Vegetable-based dye-sensitized solar cells. **Chem Soc Rev**, 44(10), 3244-3294.

Carella, A., Borbone, F. & Centore, R. 2018. Research Progress on Photosensitizers for DSSC. **Front Chem**, 6(481.

Cherepy, N. J., Smestad, G. P., Gratzel, M. & Zhang, J. Z. 1997. Ultrafast Electron Injection: Implications for a Photoelectrochemical Cell Utilizing an Anthocyanin Dye-Sensitized TiO2 Nanocrystalline Electrode. **Journal of Physical Chemistry**.

Chien, C. Y., Hsu, B. D. 2013. Optimazation of the dye sensitized solar cell with anthocyanin as photosensitizer, Sol. Energy 98 pg. 203-211.

Costa, C., Ivanou, D., Pinto, J., Mendes, J. & Mendes, A. 2019. Impact of the architecture of dye sensitized solar cell-powered electrochromic devices on their photovoltaic performance and the ability to color change. **Solar Energy**, 182(22-28.

Dawoud, A. M. 2016. **Natural Pigments Extracted from Plant Leaves as Photosensitizers for Dye-sensitized Solar Cells.** Master

Degree of Science (M. Sc.) in Physics. Islamic University of Gaza.

Delgado-Vargas, F., Jimenez, A. R. & Paredes-Lopez, O. 2000. Natural pigments: carotenoids, anthocyanins, and betalains--characteristics, biosynthesis, processing, and stability. **Crit Rev Food Sci Nutr**, 40(3), 173-289.

Dinesh, V.P., Sriram kumar, R., Sukhananazerin, A., Mary Sneha, J., Manoj Kumar, P., Biji, P. 2019. Novel stainless steel based, eco-friendly dye-sensitized solar cells using electrospun porous ZnO nanofibers. Nano-Structures & Nano-Objects, 19.

Dong, Y., Cha, H., Zhang, J., Pastor, E., Tuladhar, P. S., McCulloch, I., Durrant, J. R. & Bakulin, A. A. 2019. The binding energy and dynamics of charge-transfer states in organic photovoltaics with low driving force for charge separation. **J Chem Phys**, 150(10), 104704.

Eli, D., Musa, G. P., Ezra, D. 2016. Chlorophyll and betalain as light-harvesting pigments for nanostructured TiO_2 based dye-sensitized solar cells. Journal of Energy and Natural Resources. 5:53–58.

García-Salinas, M. J. & Ariza, M. J. 2019. Optimizing a Simple Natural Dye Production Method for Dye-Sensitized Solar Cells: Examples for Betalain (Bougainvillea and Beetroot Extracts) and Anthocyanin Dyes. **Applied Sciences**, 9(12).

Giusti, M. & Wrolstad, R. E. 2001. Characterization and Measurement of Anthocyanins by UV-Visible Spectroscopy. **Current Protocols in Food Analytical Chemistry**.

Giusti, M.M., R.E Wrolstad, Acylated anthocyanins from edible sources and their applications in food systems, Biochem. Eng. J. 14(3) (2003) 217–225.

Gomesh, N., Arief, Z. M., Ramli, S., Irwanto, M., Irwan, Y. M., Mamat, M. R., Hashim, U. & Mariun, N. 2014. Performance Comparison between Dyes on Single Layered

TiO_2 Dye Sensitized Solar Cell. **Advanced Materials Research**, 1008-1009(78-81.

Faqih, P., Nurosyid, F., Kusumaningsih, T. 2020. Effect of acidic level (pH) of red dragon fruit (Hylocereus costaricencis) peels extract on DSSC efficiency, AIP Conference Proceedings 2237, 020014 https://doi.org/10.1063/5.0005686.

Hagfeldt, A., Boschloo, G., Sun, L., Kloo, L. & Pettersson, H. 2010. Dye-Sensitized Solar Cells **Chemical Reviews**, 110.

Hasoon, S. A., Al-Haddad, R. M. S., Shakir, O. T., Ibrahim, I. M. 2015. Natural dye-sensitized solar cell based on zinc oxide. International Journal of Scientific & Engineering Research. 6:137–142.

Hemalatha, K. V., Karthick, S. N., Justin Raj, C., Hong, N. Y., Kim, S. K. & Kim, H. J. 2012. Performance of Kerria japonica and Rosa chinensis flower dyes as sensitizers for dye-sensitized solar cells. **Spectrochim Acta A Mol Biomol Spectrosc**, 96(305-309.

Iftikhar, H., Sonai, G. G., Hashmi, S. G., Nogueira, A. F. & Lund, P. D. 2019. Progress on Electrolytes Development in Dye-Sensitized Solar Cells. **Materials (Basel)**, 12(12).

Jena, A., Mohanty, S. P., Kumar, P., Naduvath, J., Gondane, V., Lekha, P., Das, J., Narula, H. K., Mallick, S. & Bhargava, P. 2012. Dye Sensitized Solar Cells: A Review. **Transactions of the Indian Ceramic Society**, 71(1), 1-16.

Kabir, F., Bhuiyan, M. M. H., Manir, M. S., Rahaman, M. S., Khan, M. A. & Ikegami, T. 2019. Development of dye-sensitized solar cell based on combination of natural dyes extracted from Malabar spinach and red spinach. **Results in Physics**, 14.

Kay, A., Humphry-Baker, R., Graetzel (1994) J Phys Chem 98, 952–959.

Khammee P, Unpaprom Y, Whangchai K, Ramaraj R (2020) Comparative studies of the longan leaf pigment extraction as a photosensitizer for dye-sensitized solar cells' purpose. Biomass Conversion and Biorefinery.

Koo, B. K., D-Y. Lee, H-J. Kim, W-J. Lee, J-S. Song, H-J. Kim, J. 2006. Electroceram. 17, 79-82.

Khoo, H. E., Azlan, A., Tang, S. T. & Lim, S. M. 2017. Anthocyanidins and anthocyanins:

colored pigments as food, pharmaceutical ingredients, and the potential health benefits. **Food Nutr Res**, 61(1), 1361779.

Kumar, K. A., Subalakshmi, K. & Senthilselvan, J. 2016. Co-sensitization of natural dyes for improved efficiency in dye-sensitized solar cell application. p. In.

Kumara, N. T. R. N., Ekanayake, P., Lim, A., Liew, L. Y. C., Iskandar, M., Ming, L. C. & Senadeera, G. K. R. 2013. Layered co-sensitization for enhancement of conversion efficiency of natural dye sensitized solar cells. **Journal of Alloys and Compounds**, 581(186-191.

Lau, K. K. S. & Soroush, M. (2019). Overview of Dye-Sensitized Solar Cells. In **Dye-Sensitized Solar Cells** (pp. 1-49).

Lenzmann, F. O. & Kroon, J. M. 2007. Recent Advances in Dye-Sensitized Solar Cells. **Advances in OptoElectronics**, 2007(1-10).

Li, Y., M. Guo, M. Zhang, X. Wang, Hydrothermal synthesis and characterization of TiO_2 nanorod arrays on glass substrates, Mater. Res. Bull. 44 (2009)1232–1237.

Ludin, N. A., Al-Alwani Mahmoud, A. M., Bakar Mohamad, A., Kadhum, A. A. H., Sopian, K. & Abdul Karim, N. S. 2014. Review on the development of natural dye photosensitizer for dye-sensitized solar cells. **Renewable and Sustainable Energy Reviews**, 31(386-396.

Maabong, K., Muiva, C. M., Monowe, P., Sathiaraj, T. S., Hopkins, M., Nguyen, L., Malungwa, K., Thobega, M. 2015. Natural pigments as photosensitizers for dye-sensitized solar cells with TiO_2 thin films. International Journal of Renewable Energy Research. 5:54–60.

Matthews, D., Infelta, P. & Gratzel, M. 1996. Calculation of the Photocurrent-potential Characteristic for Regenerative, Semiconductor electrodes **Solar Energy Materials and Solar Cells**.

Marcano, E. DFT study of anthocyanidin and anthocyanin pigments for Dye-Sensitized Solar Cells: Electron injecting from the excited states and adsorption onto TiO_2 (anatase) surface, Phys. Sci. Rev. 2 (2019) 29–38.

Marques, A. D. S., Da Silva, V. A. S., Ribeiro, E. S. 2020. Dye-Sensitized Solar Cells: Components Screening for Glass substrate, Counter-Electrode, Photoanode and Electrolyte. Mat. Res. 23(5) https://doi.org/10.1590/1980-5373-mr-2020-0168.

Mazza, G. & Miniati, E. 1993. **Anthocyanins in fruits, vegetables, and grains**. Taylor & Francis Group.

Narayan, M. R. 2011. Fabrication and Characterization of Dye Sensitized Solar Cells using Locally Occuring Plant Dyes.

Ni, M., Leung, M. K. H., Leung, D. Y. C. 2008. Theoretical modelling of the electrode thickness effect on maximum power point of dye-sensitized solar cell. The Canadian Journal of Chemical Engineering, 86(1), 35-42.

Patel, Keyurkumar & Jaysukhlal. 2012. Studies on Electrochromic Thin Film Devices and Sensors 1-13.

Pawa,r K.S., Baviskar, P.K., Nadaf, A.B., Salunke-Gawali, S., Pathan, H. M. 2019. Layer-by-layer deposition of TiO_2–ZrO_2 electrode sensitized with pandan leaves: natural dye-sensitized solar cell. Mater Renew Sustain Energy 8:12

Prabavathy, N., Shalini, S., Balasundaraprabhu, R., Velauthapillai, D., Prasanna, S., Walke, P., and Muthukumarasamy, N. 2017. Effect of solvents in the extraction and stability of anthocyanin from the petals of Caesalpinia pulcherrima for natural dye sensitized solar cell applications, J. Mater. Sci. Mater. Electron. 28(13) 9882-9892

Ray-Yu Yang, P., Shou Lin, B. & George Kuo, P. 2008. Content and distribution of flavonoids among 91 edible plant species. **Asia Pacific Journal of Clinical Nutrition**.

Ritchie RJ (2006) Consistent sets of spectrophotometric chlorophyll equations for acetone, methanol and ethanol solvents. Photosynth Res 89:27–41.

Roslan, N., Ya'acob, M. E., Radzi, M. A. M., Hashimoto, Y., Jamaludin, D. & Chen, G. 2018. Dye Sensitized Solar Cell (DSSC) greenhouse shading: New insights for solar radiation manipulation. **Renewable and Sustainable Energy Reviews**, 92(171-186.

Roslan, N., Ya'acob, M. E., Jamaludin, D., Iskandar, A. N. & Othman, M. H. 2019. Dye sensitized solar cell field performance in tropical climatic condition: A case study. p. In **Applied Physics of Condensed Matter (Apcom 2019)**.

Sauer, M., J. Hofkens, and J. Enderlein 2011. Hanbook of Fluorescene Spectroscopy and

Imaging. Weinheim: WILEYVCH..

Shalini, S., Balasundara prabhu, R., Prasanna, S., Mallick, T. K. & Senthilarasu, S. 2015. Review on natural dye sensitized solar cells: Operation, materials and methods. **Renewable and Sustainable Energy Reviews**, 51(1306-1325.

Shalini, S., Balasundaraprabhu, R., Kumar, T. S., Prabavathy, N., Senthilarasu, S. & Prasanna, S. 2016. Status and outlook of sensitizers/dyes used in dye sensitized solar cells (DSSC): a review. **International Journal of Energy Research**, 40(10), 1303-1320.

Shamina, A. 2007. Food colours of plant origin. **CAB Reviews: Perspectives in Agriculture, Veterinary Science, Nutrition and Natural Resources**, 2(087).

Shi, Z., Lin, M. & Francis, F. J. 1992 Stability of Anthocyanins from Tradescania pallida. **Journal of Food Science**, 57(

Sladonja, B. 2013. **The Mediterranean Genetic Code - Grapevine and Olive**.

Smestad, G. P. & Gratzel, M. 1998. Demonstrating Electron Transfer and Nanotechnology: A Natural Dye-Sensitized Nanocrystalline Energy Converter Journal of Chemical Education.

Stadler, A. 2012. Transparent Conducting Oxides-An Up-To-Date Overview. **Materials (Basel, Switzerland)**, 5(4), 661-683.

Stasiak, N., Kukula-Koch, W. & Glowniak, K. 2014. Modern Industrial and Pharmacological Applications of Indigo Dye and its Derivatives. **Polish Pharmaceutical Society**, 71.

Taya, S. A., El-Agez, T. M., El-Ghamri, H. S., Abdel-Latif, M. S. 2013. Dye-sensitized solar cells using fresh and dried natural dyes. International Journal of Materials Science and Applications. 2:37–42.

Thomas, S., Deepak, T.G., Anjusree, G.S., Arun, T.A., Nair, S.V., Nair, A.S. 2014. A review on counter electrode materials in dye-sensitized solar cells. J. Mater. Chem. A, 2(13), 4474-4490.

Timberlake, C. F. & Henry, B. S. 1988. Anthocyanins as natural food colorants. **Prog Clin Biol Res**, 280(107-121.

Wang, H. & Hu, Y. H. 2012. Graphene as a counter electrode material for dye-sensitized solar cells. **Energy & Environmental Science**, 5(8).

Wei YS, Jin QQ, Ren TZ (2011) Expanded graphite/pencil-lead as counter electrode for dye-sensitized solar cells. Solid-State Electronics, 63(1), 76-82.

Wiriya-Alongkorn, W., Spreer, W., Ongprasert, S., Spohrer, K., Pankasemsuk, T. & Müller, J. 2013. Detecting drought stress in longan tree using thermal imaging. **Maejo International Journal of Science and Technology**.

World Population Review. 2019. [Online]. Available https://worldpopulationreview.com/.

Yano, A. & Cossu, M. 2019. Energy sustainable greenhouse crop cultivation using photovoltaic technologies. **Renewable and Sustainable Energy Reviews**, 109(116-137.

Zielewicz, W., Wróbel, B., Niedbała, G. 2020. Quantification of Chlorophyll and Carotene Pigments Content in Mountain Melick (Melica nutans L.) in Relation to Edaphic Variables. Forests, 11(11).

CURRICULUM VITAE

NAME	Glennise Faye C. Mejica
DATE OF BIRTH	13 April 1997
EDUCATION	Secondary: ST. JOSEPH SCHOOL– HIJAS DE JESUS San Miguel, Jordan, Guimaras Batch 2014 Tertiary: UNIVERSITY OF SAN AGUSTIN Gen. Luna St., Iloilo City Bachelor of Science in Chemical Engineering Batch 2019